



## Annex 32

# Economical heating and cooling systems for low energy houses

Final Report – Part 4

Editor:  
Carsten Wemhoener  
Operating Agent - Annex 32  
Institute of Energy in Building  
University of Applied Sciences North-  
Western Switzerland  
carsten.wemhoener@fhnw.ch

December 2011

Report no. HPT-AN32-4

**Published by**

Heat Pump Centre  
c/o RISE – Research Institutes of Sweden  
Box 857, SE-501 15 Borås  
Sweden  
Phone +46 10 16 53 42

**Website**

<https://heatpumpingtechnologies.org>

**Legal Notice**

Neither the Heat Pump Centre nor any person acting on its behalf:  
(a) makes any warranty or representation, express or implied, with respect to the information contained in this report; or  
(b) assumes liabilities with respect to the use of, or damages, resulting from, the use of this information.  
Reference herein to any specific commercial product, process, or service by trade name, trademark, manufacturer, or otherwise, does not necessarily constitute or imply its endorsement recommendation or favoring.  
The views and opinions of authors expressed herein do not necessarily state or reflect those of the Heat Pump Centre, or any of its employees. The information herein is presented in the authors' own words.

**© Heat Pump Centre**

All rights reserved. No part of this publication may be reproduced, stored in a retrieval system, or transmitted in any form or by any means, electronic, mechanical, photocopying, recording or otherwise, without prior permission of the Heat Pump Centre, Borås, Sweden.

**Production**

Heat Pump Centre, Borås, Sweden

**ISBN 978-91-89561-50-2**  
**Report No. HPT-AN32-4**

## Preface

This project was carried out within the Technology Collaboration Programme on Heat Pumping Technologies (HPT TCP), which is a Technology Collaboration Programme within the International Energy Agency, IEA.

### **The IEA**

The IEA was established in 1974 within the framework of the Organization for Economic Cooperation and Development (OECD) to implement an International Energy Programme. A basic aim of the IEA is to foster cooperation among the IEA participating countries to increase energy security through energy conservation, development of alternative energy sources, new energy technology and research and development (R&D). This is achieved, in part, through a programme of energy technology and R&D collaboration, currently within the framework of nearly 40 Technology Collaboration Programmes.

### **The Technology Collaboration Programme on Heat Pumping Technologies (HPT TCP)**

The Technology Collaboration Programme on Heat Pumping Technologies (HPT TCP) forms the legal basis for the implementing agreement for a programme of research, development, demonstration, and promotion of heat pumping technologies. Signatories of the TCP are either governments or organizations designated by their respective governments to conduct programmes in the field of energy conservation.

Under the TCP, collaborative tasks, or “Annexes”, in the field of heat pumps are undertaken. These tasks are conducted on a cost-sharing and/or task-sharing basis by the participating countries. An Annex is in general coordinated by one country which acts as the Operating Agent (manager). Annexes have specific topics and work plans and operate for a specified period, usually several years. The objectives vary from information exchange to the development and implementation of technology. This report presents the results of one Annex.

The Programme is governed by an Executive Committee, which monitors existing projects and identifies new areas where collaborative effort may be beneficial.

### **Disclaimer**

The HPT TCP is part of a network of autonomous collaborative partnerships focused on a wide range of energy technologies known as Technology Collaboration Programmes or TCPs. The TCPs are organized under the auspices of the International Energy Agency (IEA), but the TCPs are functionally and legally autonomous. Views, findings and publications of the HPT TCP do not necessarily represent the views or policies of the IEA Secretariat or its individual member countries.

### **The Heat Pump Centre**

A central role within the HPT TCP is played by the Heat Pump Centre (HPC).

Consistent with the overall objective of the HPT TCP, the HPC seeks to accelerate the implementation of heat pump technologies and thereby optimize the use of energy resources for the benefit of the environment. This is achieved by offering a worldwide information service to support all those who can play a part in the implementation of heat pumping technology including researchers, engineers, manufacturers, installers, equipment users, and energy policy makers in utilities, government offices and other organizations. Activities of the HPC include the production of a Magazine with an additional newsletter 3 times per year, the HPT TCP webpage, the organization of workshops, an inquiry service and a promotion programme. The HPC also publishes selected results from other Annexes, and this publication is one result of this activity.

For further information about the Technology Collaboration Programme on Heat Pumping Technologies (HPT TCP) and for inquiries on heat pump issues in general contact the Heat Pump Centre at the following address:

Heat Pump Centre  
c/o RISE - Research Institutes of Sweden  
Box 857, SE-501 15 BORÅS, Sweden  
Phone: +46 10 516 53 42  
Website: <https://heatpumpingtechnologies.org>



 Schweizerische Eidgenossenschaft  
Confédération suisse  
Confederazione Svizzera  
Confederaziun svizra  
Swiss Federal Office of Energy SFOE

## Prototype systems

New integrated heat pump systems for the application in low energy houses

**Worked out by**

**Carsten Wemhoener (Editor)**  
**Institute of Energy in Building**  
**University of Applied Sciences North-Western Switzerland**  
**E-Mail: [carsten.wemhoener@fhnw.ch](mailto:carsten.wemhoener@fhnw.ch)**

# Imprint

---

## IEA HPP Annex 32 " Economical heating and cooling systems for low energy houses"

The work presented here is a contribution to the Annex 32 in the Heat Pump Programme (HPP) Implementing Agreement of the International Energy Agency (IEA)

### Operating Agent (Switzerland):

Institute of Energy in Building, Univ. of Applied Sciences Northwestern Switzerland, Muttenz  
Carsten Wemhöner, [carsten.wemhoener@fhnw.ch](mailto:carsten.wemhoener@fhnw.ch)

### National team leaders in IEA HPP Annex 32

#### Austria:

Institute of thermal engineering (IWT), Graz Technical University, Austria  
Ao. Univ. Prof. Dr. René Rieberer, [rene.rieberer@tugraz.at](mailto:rene.rieberer@tugraz.at)

#### Canada:

Laboratoire des technologies de l'énergie (LTE), Hydro Québec, Shawinigan, Canada  
Vasile Minea, PhD, [minea.vasile@ireq.ca](mailto:minea.vasile@ireq.ca)

#### France:

Electricité de France, Research&Development, Department ENERBAT, Moret-sur-Loing, France  
Catherine Martinlagardette, [catherine.martinlagardette@edf.fr](mailto:catherine.martinlagardette@edf.fr)

#### Germany:

Fraunhofer Institute of Solar energy systems (FhG-ISE), Freiburg (Brsg.), Germany  
Marek Miara, [marek.miara@ise.fraunhofer.de](mailto:marek.miara@ise.fraunhofer.de)

#### Japan:

Graduate School of Engineering, Hokkaido University, Sapporo, Japan  
Prof. Dr. Eng. Katsunori Nagano, [nagano@eng.hokudai.ac.jp](mailto:nagano@eng.hokudai.ac.jp)

#### The Netherlands: Agentschap NL, Utrecht, Netherlands

Onno Kleefkens, [onno.kleefkens@agentschapnl.nl](mailto:onno.kleefkens@agentschapnl.nl)

#### Norway:

SINTEF Energy Research, Trondheim, Norway  
Maria Justo Alonso [maria.justo.alonso@sintef.no](mailto:maria.justo.alonso@sintef.no), Dr. Ing. Jørn Stene (2006-08) [jost@cowi.no](mailto:jost@cowi.no)

#### Sweden:

SP Technical Research Institute of Sweden, Borås, Sweden  
Svein Ruud, [svein.ruud@sp.se](mailto:svein.ruud@sp.se)

#### Switzerland:

Institute of Energy in Building, Univ. of Applied Sciences Northwestern Switzerland, Muttenz  
Prof. Dr. Thomas Afjei, [thomas.afjei@fhnw.ch](mailto:thomas.afjei@fhnw.ch)

#### USA:

Oak Ridge National Laboratory, Oak Ridge, Tennessee, United States of America  
Van D. Baxter, [baxtervd@ornl.gov](mailto:baxtervd@ornl.gov), Arun Vohra (retired 2008), Department of Energy, Washington DC

---

## IEA HPP Annex 32

IEA HPP Annex 32 is a corporate research project on technical building systems with heat pumps for the application in low energy houses.

The project is accomplished in the Heat Pump Programme (HPP) of the International Energy Agency (IEA).

Internet: <http://www.annex32.net>



## Summary

---

This report gives a summary of the system concepts and designs as well as lab-testing and simulation results of the prototype systems of integrated heat pumps developed in the frame of IEA HPP Annex 32 on "Economical heating and cooling systems for low energy buildings". Since the functionality of the building technology is extended in low energy houses due to mechanical ventilation needs and an additional comfort cooling, integrated heat pumps have advantages of internal heat recovery options, while the heat would be probably wasted in appliances with single functionality, e.g. in case of combined space cooling and water heating.

All developed prototypes have multiple integrated functions. The prototypes thereby mainly address two aspects not covered by many of the marketable heat pumps for the application in low energy houses to date: on the one hand, additional functionalities like a passive or active cooling function are integrated in the developments, and on the other hand, use of natural refrigerants with reduced global warming impact is considered by some of the prototype developments. All developed prototypes are adapted to the typical capacity range of residential low and ultra-low energy houses of 3-5 kW.

In Norway, feasibility studies of CO<sub>2</sub>-heat pump applications in low energy houses have been carried out, both for combined space heating and DHW and for DHW-only operation. Simulation results of a central CO<sub>2</sub> heat pump water heater for blocks of flat yielded a seasonal performance factor of 3.7 with a gray water heat source of 7 degrees and a DHW temperature of 65°C. This means about 75% primary energy saving compared to a direct electrical water heating and still about 25% primary energy saving compared to a solar water heater of a solar fraction of 50% and with direct electrical back-up heating which are common water heating layouts in Norway. The system is also economically advantageous. For combined space and water heating heat pumps simulation showed, that a CO<sub>2</sub> heat pump outperforms a conventional heat pump at a DHW share of 60%. With improved CO<sub>2</sub> technology (improved compressor and ejector) the break-even point is shifted to 50% DHW share.

In Austria a 5 kW CO<sub>2</sub>-B/W heat pump prototype has been built and lab-tested. System simulations for space heating, DHW, passive and active cooling in a typical low energy house yields an overall system performance of 3.2, in case of higher cooling loads in extreme summers, the performance increases. Further system improvements are seen in improved components (compressor efficiency for low capacities, ejector) as well as system integration of the buffer storage and control.

At the Oak Ridge National Laboratory, USA, an air-source and ground-source integrated heat pump covering all building services including humidification and dehumidification has been developed, lab-tested and simulated. Annual simulation in a residential NZEB for 5 climates of the US show energy saving potentials for 47-62% for the air-source and 52-65% for the ground source prototypes compared to DOE minimum requirement state-of-the-art technology. Economical evaluation yield simple payback times of 6-15 year for the ground source type and 4-8 year for the air-source prototype.

In Canada two field monitoring projects are equipped with solar PV/T systems for direct heating and as heat source for an air-source heat pump in the cold climate in Montreal region. A second ground source heat pump is used as back-up in one building. Systems simulations show that the buildings reach almost an annual net zero energy consumption. Moreover predictive control strategies can have advantages for the system control.

Some of the prototypes will be field monitored in the near futures in order to prove the functionality in real-world operation and analyse, if the promising results of simulations are reached under real boundary conditions, as well. Moreover, field testing will reveal further operational problems and optimisation potentials. However, due to the project time schedules, results of the field test could not be covered in the time frame of IEA HPP Annex 32.



# CONTENTS

---

IMPRINT .....	2
SUMMARY .....	3
CONTENTS .....	5
PREFACE .....	7
<b>1 INTRODUCTION .....</b>	<b>9</b>
<b>2 OVERVIEW OF INVESTIGATED PROTOTYPES .....</b>	<b>11</b>
2.1 SCOPE OF PROTOTYPE DEVELOPMENTS .....	11
2.2 OUTLINE OF NATIONAL PROTOTYPE PROJECTS .....	11
2.2.1 <i>System integration</i> .....	11
2.2.2 <i>Natural refrigerants</i> .....	11
<b>3 FEASIBILITY STUDY OF CO<sub>2</sub> HEAT PUMPS .....</b>	<b>13</b>
3.1 MAIN CHARACTERISTIC PROPERTIES OF CO <sub>2</sub> HEAT PUMP SYSTEMS .....	13
3.2 APPLICATIONS OF CO <sub>2</sub> HEAT PUMPS FOR DHW PRODUCTION .....	14
3.3 CO <sub>2</sub> HEAT PUMP WATER HEATER IN APARTMENT HOUSE .....	15
3.3.1 <i>Grey Water as Heat Source</i> .....	17
3.4 INTEGRATED CO <sub>2</sub> HEAT PUMPS IN LOW ENERGY HOUSES .....	18
<b>4 INTEGRATED CO<sub>2</sub> HEAT PUMP PROTOTYPE .....</b>	<b>21</b>
4.1 MOTIVATION .....	21
4.2 SYSTEM OUTLINE .....	21
4.2.1 <i>System 1: Reverse operating A/A HP with air-heating/-cooling</i> .....	22
4.2.2 <i>System 2: B/W HP with a hydraulic space heating/cooling system</i> .....	22
4.2.3 <i>System 3: Reverse operating B/W HP with hydraulic space heating/cooling</i> .....	23
4.2.4 <i>Results of the cycle simulation and conclusions for system layout</i> .....	24
4.3 DESIGN OF A PROTOTYPE UNIT .....	25
4.3.1 <i>System configuration of the prototype system</i> .....	25
4.3.2 <i>Bipartite gas cooler</i> .....	25
4.3.3 <i>Test rig</i> .....	27
4.3.4 <i>Results of prototype component testing</i> .....	29
4.4 SYSTEM EVALUATIONS WITH THE PROTOTYPE HEAT PUMP .....	31
4.4.1 <i>Heat pump model</i> .....	31
4.4.2 <i>Boundary conditions</i> .....	33
4.4.2.1 <i>Reference building</i> .....	33
4.4.2.2 <i>Climate, heat source, heat emission and DHW demand</i> .....	33
4.4.2.3 <i>Shading, system and room temperature control</i> .....	34
4.4.3 <i>Results of the system simulations</i> .....	38
4.5 CONCLUSIONS AND OUTLOOK .....	41
<b>5 INTEGRATED HEAT PUMP FOR NET ZERO ENERGY HOUSES .....</b>	<b>43</b>
5.1 MOTIVATION .....	43
5.2 SYSTEM CONCEPT .....	43
5.2.1 <i>Dehumidification and water heating mode</i> .....	45
5.2.2 <i>Space heating (cooling) and DHW</i> .....	45
5.3 PROTOTYPE TESTING .....	47
5.4 SYSTEM SIMULATION RESULTS OF THE PROTOTYPE SYSTEM .....	51

5.4.1	<i>Baseline system</i>	51
5.4.2	<i>GS- and AS-IHP</i>	52
5.4.3	<i>Heat pump model</i>	52
5.4.4	<i>Annual energy performance</i>	53
5.4.5	<i>Economic analysis</i>	56
5.5	PROPOSED CONCEPT DESIGN SPECIFICATIONS	57
5.5.1	<i>Refrigerant Compressor (C)</i>	58
5.5.2	<i>Indoor Fan (FI)</i>	58
5.5.3	<i>Outdoor Fan (FO)</i>	58
5.5.4	<i>Refrigerant-to-Water Heat Exchanger (HXRWI)</i>	58
5.5.5	<i>Water-to-Air Heat Exchanger (HXWA)</i>	58
5.5.6	<i>Indoor Refrigerant-to-Air Heat Exchanger (HXRAI)</i>	59
5.5.7	<i>Outdoor Refrigerant-to-Air Heat Exchanger (HXRAO)</i>	59
5.5.8	<i>Electrical Resistance Water Heating Elements</i>	59
5.5.9	<i>Domestic Water Pump (PI)</i>	59
5.5.10	<i>Hot Water Storage Tank (WT)</i>	59
5.5.11	<i>Other components</i>	59
5.5.12	<i>Components GS-IHP</i>	59
5.6	CONCLUSIONS AND OUTLOOK	60
5.6.1	<i>Conclusions</i>	60
5.6.2	<i>Recommendations</i>	60
5.6.3	<i>Field monitoring</i>	60
<b>6</b>	<b>PROPANE W-W HEAT PUMP FOR PASSIVE HOUSE</b>	<b>63</b>
6.1	MOTIVATION	63
6.2	DESCRIPTION OF THE PROTOTYPE	63
6.3	RESULTS OF PROTOTYPE COMPONENT TESTING	65
6.3.1	<i>Operating Modes – Operational Strategy</i>	65
6.3.2	<i>Instrumentation</i>	67
6.3.3	<i>Laboratory Testing</i>	67
6.4	HEAT PUMP FIELD TESTING IN A LOW ENERGY HOUSE	68
6.4.1	<i>Field Testing – Measurements and Discussion</i>	69
<b>7</b>	<b>BUILDING INTEGRATED PV/THERMAL</b>	<b>73</b>
7.1	MOTIVATION	73
7.2	BUILDING AND SYSTEM CONCEPT OF THE ECOTERRA™ HOME	73
7.3	SIMULATION AND FIELD MONITORING OF THE ECOTERRA HOUSE	75
7.3.1	<i>Energy balance</i>	75
7.3.2	<i>Field monitoring results</i>	76
7.4	BUILDING AND SYSTEM CONCEPT ALSTONVALE NZEH	77
7.5	SIMULATIONS OF THE ANZEK ENERGY SYSTEM	79
7.5.1	<i>Energy balance</i>	79
7.5.2	<i>Simulation of control strategies</i>	79
7.6	CONCLUSIONS	80
<b>8</b>	<b>CONCLUSIONS</b>	<b>83</b>
<b>9</b>	<b>ACKNOWLEDGEMENT</b>	<b>85</b>
<b>10</b>	<b>REFERENCES</b>	<b>87</b>

# PREFACE

---

## Introduction to IEA HPP Annex 32

Since the mid of the nineties low energy buildings with a significantly reduced energy consumption down to ultra-low energy standard (typical space heating energy need of 15 kWh/(m<sup>2</sup>a)) or even net zero energy consumption (on an annual basis by an integration of on-site renewable energy systems) have been realised.

These building concepts recently show strong market growth in different European countries. Many governments address the spread of low energy buildings as a major strategy to reach climate protection targets according to the Kyoto protocol. Heat pump markets are growing in many countries as well.

Low energy buildings have significantly different load characteristics compared to conventional existing buildings. This requires adapted system solutions to entirely use energy-efficiency potentials for the remaining energy needs.

Integrated heat pump solutions have favourable features for the use in low energy houses. The main advantages are the potential for internal heat recovery and simultaneous operation to cover different building needs at the same time as well as installation space and cost benefits. This leads to a significantly improved system performance in an adequate capacity range to reduce primary energy consumption and cut CO<sub>2</sub>-emissions and costs.

However, in many countries, no adequate system solutions are available on the market or energy performance of available and newly-introduced low energy house technology is not yet approved by field experience. Therefore, system development and field approval of functionality and real-world operational performance of the systems are needed. These are the main working areas of IEA HPP Annex 32.

## Main objectives of IEA HPP Annex 32

The main objectives of the IEA HPP Annex 32 are the further development and field monitoring of integrated heat pump systems for the use in low energy buildings, leading to the following objectives:

- To characterise the state-of-the-art in the different participating countries
- To assess and compare the energy performance of different system solutions for the residential low energy house sector
- To develop and lab-test new system solutions of integrated heat pumps in the low-energy-house capacity range including the use of natural refrigerants
- To accomplished field tests of new developments and marketable systems and to document best-practice examples
- To disseminate the results

## Results of the IEA HPP Annex 32

The results of IEA HPP Annex 32 comprise:

- Overview of market system solutions of integrated heat pumps for low energy houses
- Design recommendations of the standard system solutions
- New system developments as prototypes including lab-test and simulation results
- Documentation of field monitoring results of new and marketable systems
- Dissemination of results by a website, workshop presentation and reports



# 1 INTRODUCTION

Low energy houses have growing market shares in many countries. While the first efforts concentrated on the building envelope, adequate building technologies hold further energy saving potentials in these houses.

Heat pumps have several advantages for the application in low energy houses. In particular integrated solutions for different buildings services have efficiency benefits, e.g. by covering different building needs in simultaneous operation.

However, integrated heat pumps in the low capacity range required in low energy houses are still rare on the market. Moreover, market trends try to integrate further functionalities like a comfort cooling function or a link to the ventilation system, so trends go to higher integrated systems. While not very common in Europe, there are regions in Japan and the USA, where dehumidification is a major requirement of the building technology, and no integrated system solutions including a dehumidification exist, so far.

Last but not least most of the market available heat pumps are operated with HFC refrigerants, which have reduced Ozone Depletion Potential (ODP) values, but still have a considerable Global Warming Potential (GWP). Natural refrigerants like Carbon-Dioxide (CO<sub>2</sub>, R744), Propane (C<sub>3</sub>H<sub>8</sub>, R290), Ammonia (NH<sub>3</sub>, R717) and water (H<sub>2</sub>O, R718) have nearly no GWP and may even have advantages for the use in low energy houses. For instance, CO<sub>2</sub> reaches a high performance for DHW production and low energy houses are characterised by increasing fractions of energy needs for the DHW production due to strongly reduced space heating needs.

Tab. 1: Overview of characteristics of common HFC and natural refrigerants (BFE, 2008)

Refrigerant	GWP <sub>100a</sub> (CO <sub>2</sub> = 1)	Practical limit [kg/m <sup>3</sup> ]	Security information	Critical temperature [°C]	Temperture glide at 1 bar [K]	Boiling temperature at 1 bar [°C]
R134a	1200	0.25	-	101	0	-26
R407C	1520	0.31	-	87	7.4	-44
R404A	3260	0.48	-	73	0.7	-47
R410A	1720	0.44	-	72	<0.2	-51
R417A	1950	0.15	-	90	5.6	-43
R507A	3300	0.52	-	71	0	-47
R290 (C <sub>3</sub> H <sub>8</sub> )	3	0.008	flammable	97	0	-42
R717 (NH <sub>3</sub> )	0	0.00035	toxic	133	0	-33
R718 (H <sub>2</sub> O)	0	-	-	374	0	100
R723 (NH <sub>3</sub> &DME)	8	-	toxic	131	0	-37
R744 (CO <sub>2</sub> )	1	0.07	high pressure	31	0	-57*

Therefore, the main focus of the prototype developments in IEA HPP Annex 32 addresses the issues of system integration of extended functionality, mainly space heating, DHW and space cooling, but also dehumidification, as well as the use of natural refrigerants.



## 2 OVERVIEW OF INVESTIGATED PROTOTYPES

---

### 2.1 Scope of prototype developments

Focus of the multifunctional integrated heat pump concept and prototype developments in the frame of Annex 32 are the

- integration of a passive cooling or simultaneous active cooling and DHW function
- integration of a dehumidification function
- use of natural refrigerants with reduced global warming potential
- building integrated renewable system components as heat source for the heat pump

### 2.2 Outline of national prototype projects

#### 2.2.1 System integration

In the Canadian field test houses in the frame of the nationwide Equilibrium™ Initiative of the Canadian Mortgage and Housing Corporation uses building integrated PV/Thermal systems in combination with a heat pump to cover the space heating need of the building. While one system uses a ground source heat pump independent of the PV/T system, the other system uses the PV/T as a heat source. Simulation results show that the two housing concepts nearly achieve a net zero energy consumption.

The USA has developed a ground-source and air-source highly-integrated prototype of a multifunctional heat pump systems covering all building needs including the functions space heating (SH), DHW, V, space cooling (SC) including a humidification (H) and dehumidification (DH) function. A prototype has been constructed and lab-tested to evaluate component efficiencies in the manifold operation modes and to perform calibrated system simulations. Simulations yielded the assessment, if the target value of above 50% energy savings compared to marketable DOE minimum requirement technology is reached under different boundary conditions.

#### 2.2.2 Natural refrigerants

Austria has compared different system configurations and different refrigerant for the derivation of an optimised prototype integrated heat pump for low energy houses. The refrigerant CO<sub>2</sub> was chosen as best solutions for a ground-source integrated prototype for the functions space heating, DHW production and active space cooling also in simultaneous mode as well as a passive space cooling function. Lab-tests with the constructed prototype were carried out to evaluate component performance and derive parameters to calibrate a simulation model, with which system simulation for a low energy single family house have been performed.

Norway has performed several feasibility studies for the application of CO<sub>2</sub> heat pumps in low energy houses.

A CO<sub>2</sub> heat pump water heater for an apartment block of flats has been simulated with a water source and compared to different alternative configurations of advanced water heaters with conventional HFC refrigerants and to other systems for DHW heating.

An integrated CO<sub>2</sub> heat pump with tripartite gas cooler for both simultaneous and single operation of space and DHW heating has been compared to best market available HFC ground-source heat pumps depending on the DHW ratio on the total heating demand.

A propane W/W heat pump prototype including a simultaneous space heating and DHW function has been developed and lab-tested. The security measures due to the flammability of propane were designed according the EN 378:2008. The system is currently in field testing in a passive house in southern Norway.



### 3 FEASIBILITY STUDY OF CO<sub>2</sub> HEAT PUMPS

#### 3.1 Main Characteristic Properties of CO<sub>2</sub> Heat Pump Systems

Carbon dioxide (CO<sub>2</sub>, R744) is a non-toxic and non-flammable working fluid that neither contributes to ozone depletion nor global warming (ODP=0, GWP=0). CO<sub>2</sub> has excellent thermophysical properties, and by utilizing these properties by means of optimized component and system design for the heat pump unit, the DHW system and the heat distribution system, high energy efficiency can be achieved.

CO<sub>2</sub> has an particularly low critical temperature (31.1 °C) and high critical pressure (73.8 bars). As a consequence, the operating pressure in CO<sub>2</sub> heat pump systems will typically be 5 to 10 times higher than that of HFC, ammonia and propane heat pumps, i.e. 20 to 40 bars during evaporation and 80 to 130 bars during heat rejection. Due to the low critical temperature most CO<sub>2</sub> heat pumps operate in a so-called transcritical cycle with evaporation at subcritical pressure ( $p_e < 73.8$  bars) and heat rejection at supercritical pressure ( $p_{gc} > 73.8$  bar). Unlike a subcritical heat pump cycle, heat is not given off by means of condensation of the working fluid in a condenser but by cooling of high-pressure CO<sub>2</sub> gas in a heat exchanger (gas cooler). The temperature drop for the CO<sub>2</sub> gas during heat rejection is denoted the temperature glide. Fig. 2 shows a principle illustration of the transcritical CO<sub>2</sub> heat pump cycle in a Temperature-Enthalpy (T-h) diagram (1-2: Compression, 2-3: Heat rejection in a gas cooler, 3-4: Expansion/throttling, 4-1: Evaporation).

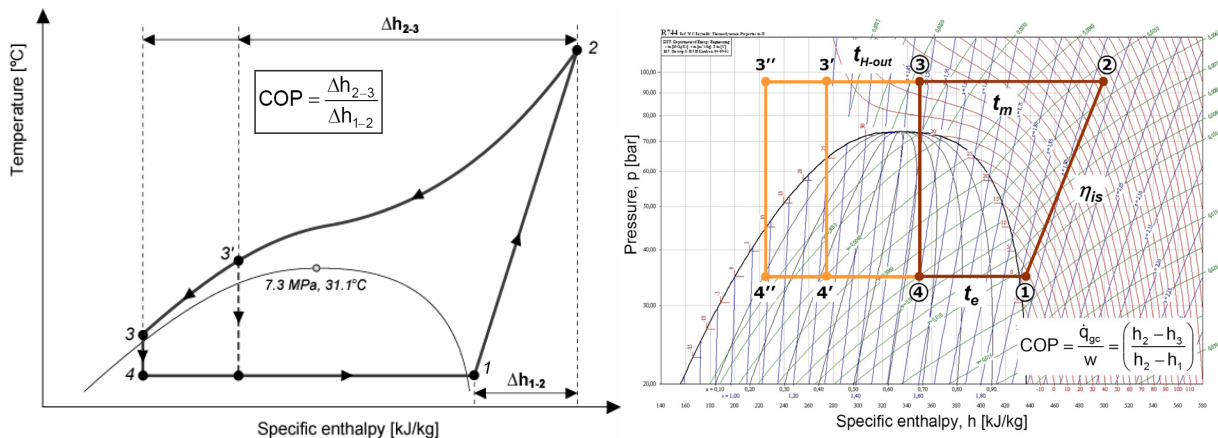


Fig. 1: Principle illustration of the transcritical CO<sub>2</sub> heat pump cycle in a temperature enthalpy T-h diagram (left) and pressure-enthalpy (p-h) diagram (right) at decreasing CO<sub>2</sub> outlet temperature from the gas cooler,  $t_{H-out}$  (3, 3' and 3'') (from Justo Alonso and Stene, 2010)

Fig. 1 illustrates a single-stage CO<sub>2</sub> heat pump cycle in a pressure-enthalpy (p-h) diagram. In the example, the evaporation temperature ( $t_e$ ) is 0 °C, and the high-pressure CO<sub>2</sub> gas at 95 bar is cooled down from 100 °C (2) to 40 °C (3) in the gas cooler. Due to the relatively high CO<sub>2</sub> outlet temperature from the gas cooler ( $t_{H-out}$ ), the COP is relatively low (COP=2.7). If the outlet CO<sub>2</sub> temperature can be reduced to e.g. 25 °C (3') or 10 °C (3'') by further heat rejection at a lower temperature level, the COP will increase by 25% (COP=3.4) and 55% (COP=4.2), respectively. The different COPs correspond to about 63%, 70% and 76% percentage energy saving compared to an electric heating system.

The main factors that determine the Coefficient of Performance (COP) for a single-stage CO<sub>2</sub> heat pump unit at varying operating conditions are the evaporation temperature ( $t_e$ ), the overall isentropic efficiency for the compressor ( $\eta_{is}$ ), the optimum gas cooler pressure ( $p_{gc}$ ), the CO<sub>2</sub> outlet temperature in the gas cooler ( $t_{H-out}$ ) and possible recovery of expansion en-

ergy ( $\Delta h_{2-3}$ ) by means of an ejector or expander.

Since the discharge gas temperature from the compressor in a single-stage CO<sub>2</sub> heat pump cycle is relatively high (> 80 °C), a CO<sub>2</sub> heat pump can meet high-temperature heating demands. However, in order to achieve a high COP for a CO<sub>2</sub> heat pump system, it is *essential that useful heat is rejected over a large temperature range*, resulting in a large enthalpy difference for the CO<sub>2</sub> in the gas cooler ( $h_2-h_3$ ) and a relatively low CO<sub>2</sub> temperature ( $t_{H-out}=t_3$ ) before the expansion/throttling valve. This in turn presupposes a relatively low inlet water temperature in the gas cooler, i.e. a low return temperature in the (hydraulic) heat distribution system and/or a low inlet water temperature from the DHW tank.

The power input to the compressor is more or less proportional to the gas cooler pressure ( $p_{gc}$ ), i.e. the higher the gas cooler pressure, the higher the power input. Consequently, CO<sub>2</sub> heat pumps should preferably be designed for a moderate optimum gas cooler pressure.

### 3.2 Applications of CO<sub>2</sub> heat pumps for DHW production

Heat pumps with carbon dioxide (CO<sub>2</sub>, R744) refrigerant are a new and promising technology for distinct applications, among others DHW heat pump water heaters (HPWH). CO<sub>2</sub> is a non-flammable and non-toxic gas with a global warming potential (GWP) = 1 when used as refrigerant, in contrast to common HFC refrigerants. Due to the low critical temperature of 31.1 °C, a so-called transcritical cycle is used for CO<sub>2</sub> heat pumps, where the heat is rejected by cooling down the superheated CO<sub>2</sub> in a single counter-flow gas cooler, see Fig. 2.

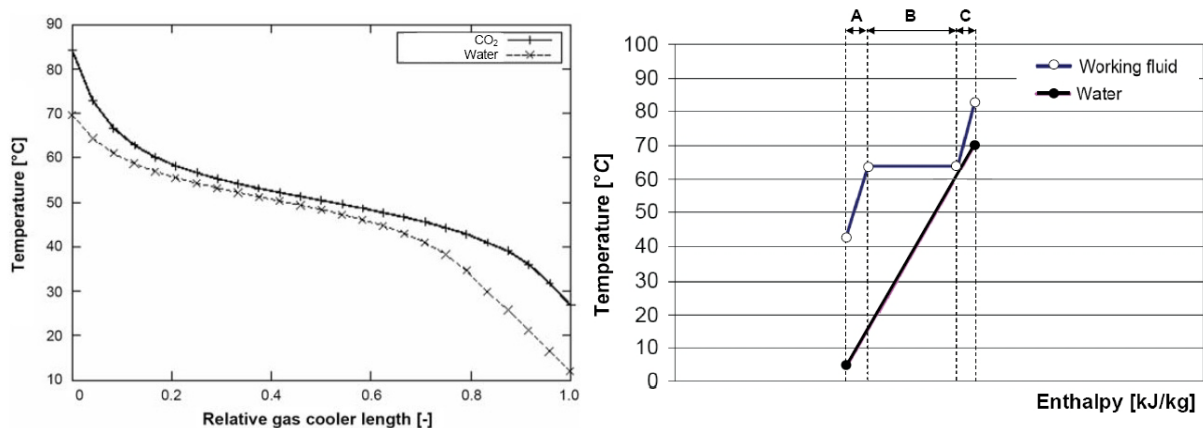


Fig. 2: Heating-up of DHW in counter-flow gas cooler with superheated CO<sub>2</sub>-refrigerant (left) and in a common desuperheater-condenser-subcooler configuration (right) (from Justo Alonso and Stene, 2010)

Common advanced designs of HPWH use up to four heat exchangers in order to best fit the temperatures of the heated DHW. In a desuperheater, the higher discharge temperatures of the refrigerant at the compressor outlet are used for reheating the DHW without increasing the condensation temperature. At the closest temperature spread (pinch point) the condensation of the refrigerant starts and a subcooling of the refrigerant for preheating the DHW has efficiency gains for the expansion process. Moreover, a suction gas heat exchanger can be used to transfer heat of the subcooled condensate to superheat the suction gas in order to increase desuperheating potential. Since the temperature fit reflects the exergy losses of the heat transfer, it becomes clear that the cooling down of the CO<sub>2</sub> refrigerant in a counter-flow heat exchanger has exergetic benefits compared to the condensation at nearly constant temperature of other refrigerant. Thus, a higher COP for the DHW application can be expected, although very high DHW outlet temperatures of 70°C and more can be reached.

### 3.3 CO<sub>2</sub> heat pump water heater in apartment house

The first study was accomplished for central HPWH for an apartment building. The apartment building for the study consists of 40 flats, and the DHW is used for washbasins, bathtubs, showers, washing-up and cleaning and also for the washing machine, dish-washer in order to save electricity for these appliances.

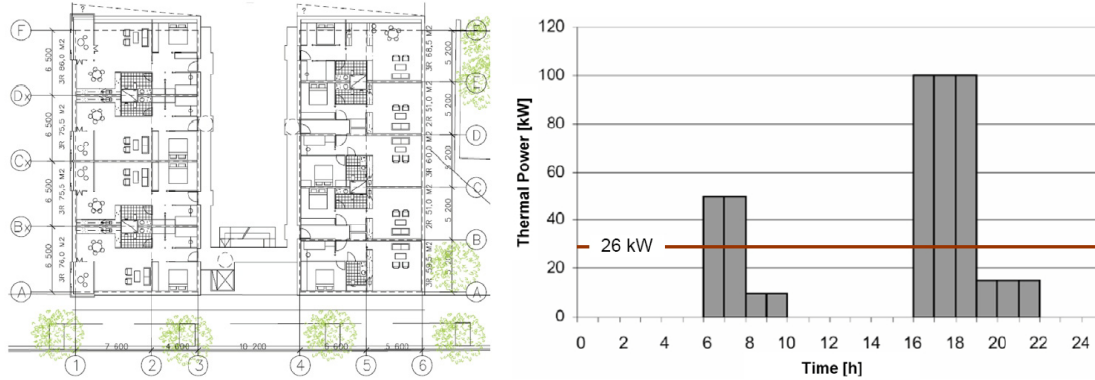


Fig. 3: Sketch of the apartment building (left) and tapping pattern for one day (right) (Hjerkinn, 2007)

The DHW energy demand was estimated to 170'000 kWh/a, i.e. about 12 kW/24 h, which makes-up a DHW energy of 4'220 kWh/(a-flat). The required heating capacity of the heat pump was estimated to 26 kW, which was evaluated assuming an operation time for the heat pump of 18 h per the 24 h of the day at city water and tapping temperatures of 5 °C and 45 °C respectively and a storage covering instantaneous demands. The storage volume with maximum and minimum storage temperature of 55 °C and 70 °C respectively was calculated to  $V = 3800$  l according to the equation

$$V = \left( \frac{Q - \dot{Q} \cdot t}{a} \right) = \frac{300\text{kWh} - 26\text{kW} \cdot 2.8\text{h}}{0.06\text{kWh/l}} \approx 3800\text{l}$$

eq. 1

with a peak DHW energy demand  $Q = 300$  kWh during  $t = 2.8$  hours and an accumulation factor of the DHW storage of  $a = 0.06$  kWh/l. The following different heat pump configurations have been considered in the study

- System 1 - Heat pump with condenser and desuperheater
- System 2 - Heat pump with condenser, desuperheater and subcooler
- System 3 - Heat pump with condenser, desuperheater and suction gas heat exchanger
- System 4 - Heat pump with CO<sub>2</sub> refrigerant and single gas cooler

Parameter variations have been simulated for the evaporation temperature (-10 to +10 °C), the water inlet temperatures (5-30 °C) and DHW outlet temperatures (60-85 °C) with the objective to find the maximum COP for the system.

Fig. 4 shows the simulations results on COP for the parameter variations and the system variants in function of the evaporation temperature. The CO<sub>2</sub>-HPWH achieved 20% higher COP than the state-of-the-art units with R134a and R290 (propane) due to a high compressor efficiency and the excellent temperature fit in the gas cooler. The state-of-the-art heat pump system configuration 2 and 3 nearly achieved the same COP, while system 1 has a 15% lower COP due to higher condensation temperatures and poorer temperature fit in the heat exchangers.

Due to the simulation results a CO<sub>2</sub>-HPWH will be installed with a design heating capacity of 26 kW at 12 °C cold water inlet temperature 70 °C DHW temperature and 3 K temperature difference in the gas cooler at an isentropic/volumetric compressor efficiency of 0.7/0.75.

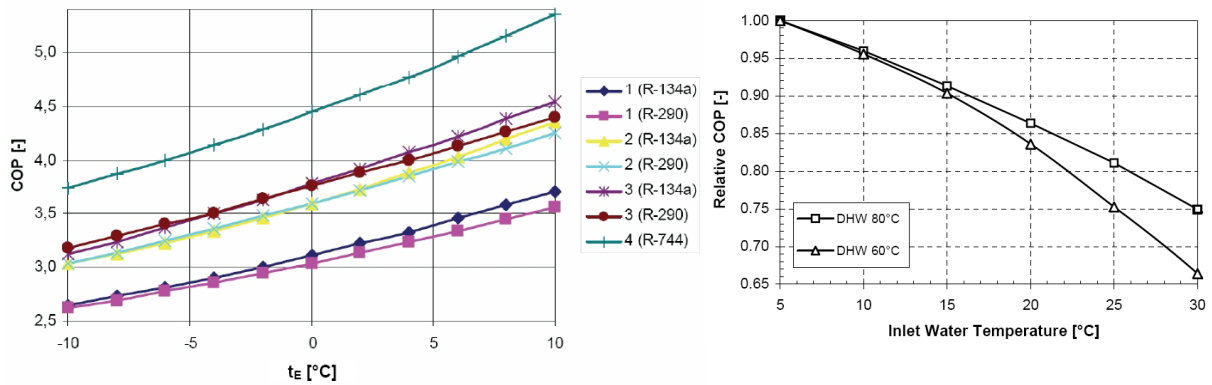


Fig. 4: Simulation results of the parameter variations (left) and impact of the inlet water temperature on the COP of a CO<sub>2</sub> HPWH (right) (from Hjerkin, 2007)

The inlet water temperature has a substantial impact on the COP of the CO<sub>2</sub>-HPWH, which is shown in Fig. 4 due to the change in enthalpy difference of the CO<sub>2</sub> refrigerant, see figure Fig. 2. A variation of the inlet temperature from 5 °C via 15 °C to 25 °C reduces the COP by 10% and 25%. Therefore, the DHW tanks shall use small diameter storage tanks in serial connection to keep stratification as well as efficient diffusers at the tank inlet to minimize mixing. Therefore, the system configuration depicted in Fig. 5 was chosen.

During the tapping, cold water is flowing to the bottom of tank 4 while the same amount is extracted from the top of tank 1. The heat pump is usually running during the tapping. An inverter controlled pump circulates the city water to the gas cooler, where it is heated to the set-point temperature (T1) before entering the top of DHW tank 1. After the tapping, the heat pump runs until the temperature T2 in tank 4 reaches the set-point temperature (70 °C). During operation the gas pressure is continuously optimised in order to maximise the COP.

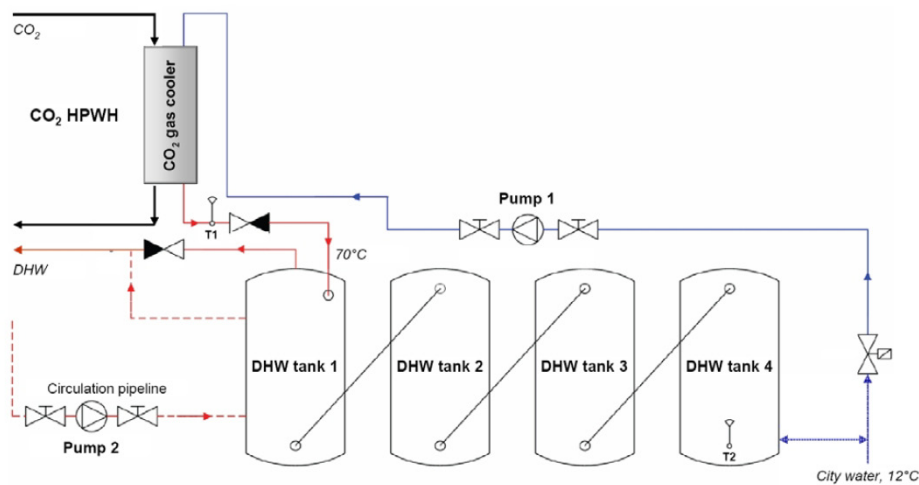


Fig. 5: System configuration for the 26 kW CO<sub>2</sub> - HPWH for the apartment building (from Hjerkin, 2007)

System simulation with an advanced simulation programme CSIM (Skaugen, 2002) developed at NTNU for the optimisation of CO<sub>2</sub> heat pumps delivered a COP of the system of 3.8 at 7 °C ground water heat source. This corresponds to an energy saving of 70-75% compared to an electrical immersion heater and to 20-25% compared to a common Nordic solar heating system layout with electrical back-up heater. The maximum permissible investment cost was evaluated under the boundary conditions of a conservative average COP of 3.5, and an electricity price of 0.1 €/kWh and an interest rate of 6% to 125'000 € or 4'800 €/kW with the reference system of an electrical immersion heater.

Thus, the CO<sub>2</sub> HPWH will be a very economic system solution.

### 3.3.1 Grey Water as Heat Source

In traditional grey water heat pump systems the inlet city water at e.g. 10 °C is preheated by the grey water at e.g. 30 °C and reheated by the heat pump condenser to approx. 35-40 °C. Electric immersion heaters are used to reheat the DHW to the required temperature, e.g. 60 °C. Since the outlet DHW temperature from the grey water heat recovery system is only 35-40 °C, the system covers less than 50 to 60 % of the total DHW heating demand. The remaining 40-50 % is covered by electric immersion heaters in the storage tanks. A much more energy efficient alternative is to use a CO<sub>2</sub> water-to-water heat pump water heater.

Fig. 6 shows a principle example of two heat exchangers and CO<sub>2</sub> heat pump configurations. In *System A* the grey water is used for preheating of DHW from 5 to 15 °C before it is utilized as a heat source for a CO<sub>2</sub> heat pump, which reheats the DHW from 15 to 70 °C. In this system configuration the evaporator must be equipped with an automatic cleaning system. In *System B* the CO<sub>2</sub> evaporator is separated from the grey water by means of a heat exchanger with an automatic cleaning system. The grey water is only used as a heat source for the CO<sub>2</sub> heat pump, which heats the DHW from 5 to 70 °C. The total heating capacity for the systems will be practically the same since the CO<sub>2</sub> heat pump in System B operates with a higher evaporation temperature (3.5 vs. 0.5 °C) and has a lower gas cooler inlet water temperature (5 vs. 15 °C). *System B is the recommended configuration for CO<sub>2</sub> heat pump water heaters* since it achieves the highest COP and a standard water-to-water CO<sub>2</sub> heat pump water heater can be used.

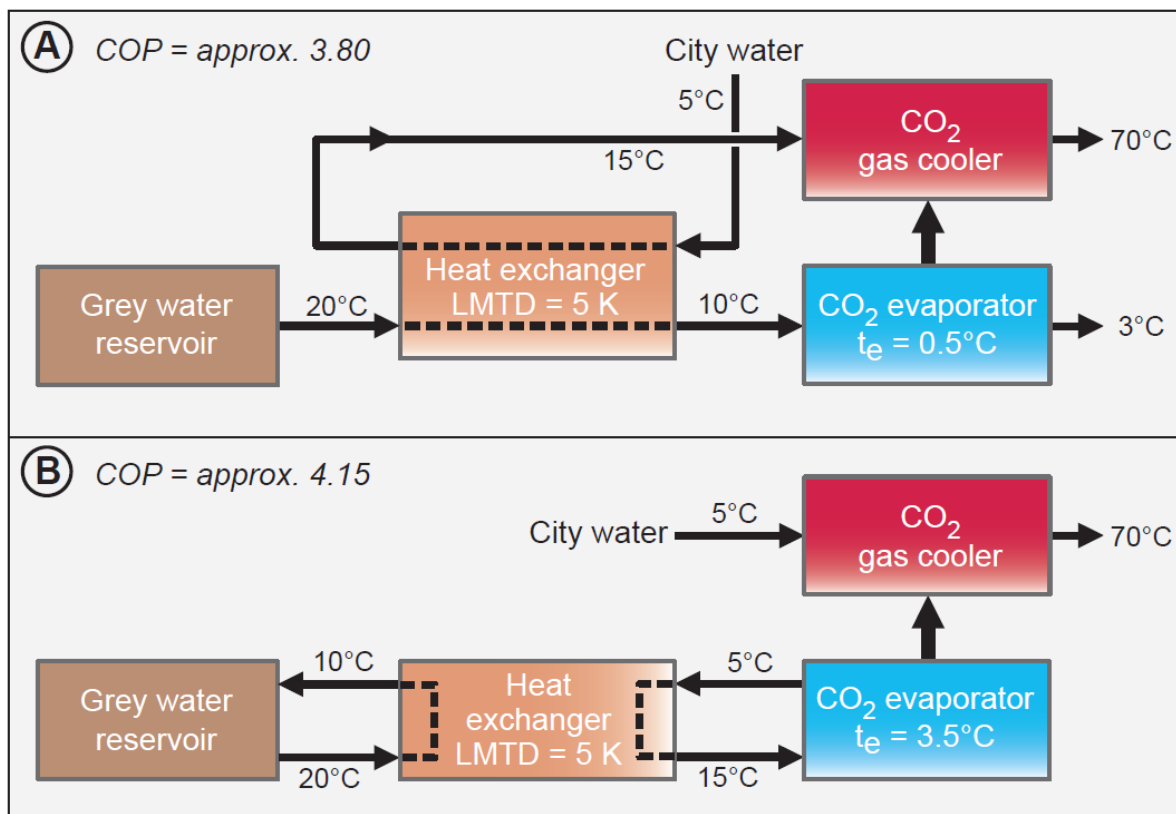


Fig. 6: Different types of connection of a grey water heat source to the CO<sub>2</sub> heat pump (Justo Alonso and Stene, 2010)

### 3.4 Integrated CO<sub>2</sub> heat pumps in low energy houses

Due to the higher fractions of more than 50% DHW energy of the total heat energy need, CO<sub>2</sub> heat pumps may have overall efficiency benefits for system layouts, where the heat pump works for space heating and DHW both in single and simultaneous operation mode. Therefore, a 6.5 kW prototype of an integrated B/W CO<sub>2</sub> heat pump depicted in Fig. 7 has been lab-tested.

In order to achieve a high COP of a CO<sub>2</sub> heat pump the rejection of useful heat over a large temperature range is essential, resulting in a large enthalpy difference for the CO<sub>2</sub> in the gas cooler. Testing of various system configurations in Stene (2004) and Stene (2006) led to the configuration of a tripartite gas cooler, where the incoming cold water for the DHW supply is preheated in the gas cooler A in Fig. 7, the low-temperature space heating emission is connected to the gas cooler B and the DHW is reheated in the gas cooler C. This configuration guarantees the best temperature fit to the CO<sub>2</sub> cycle, see Fig. 2.

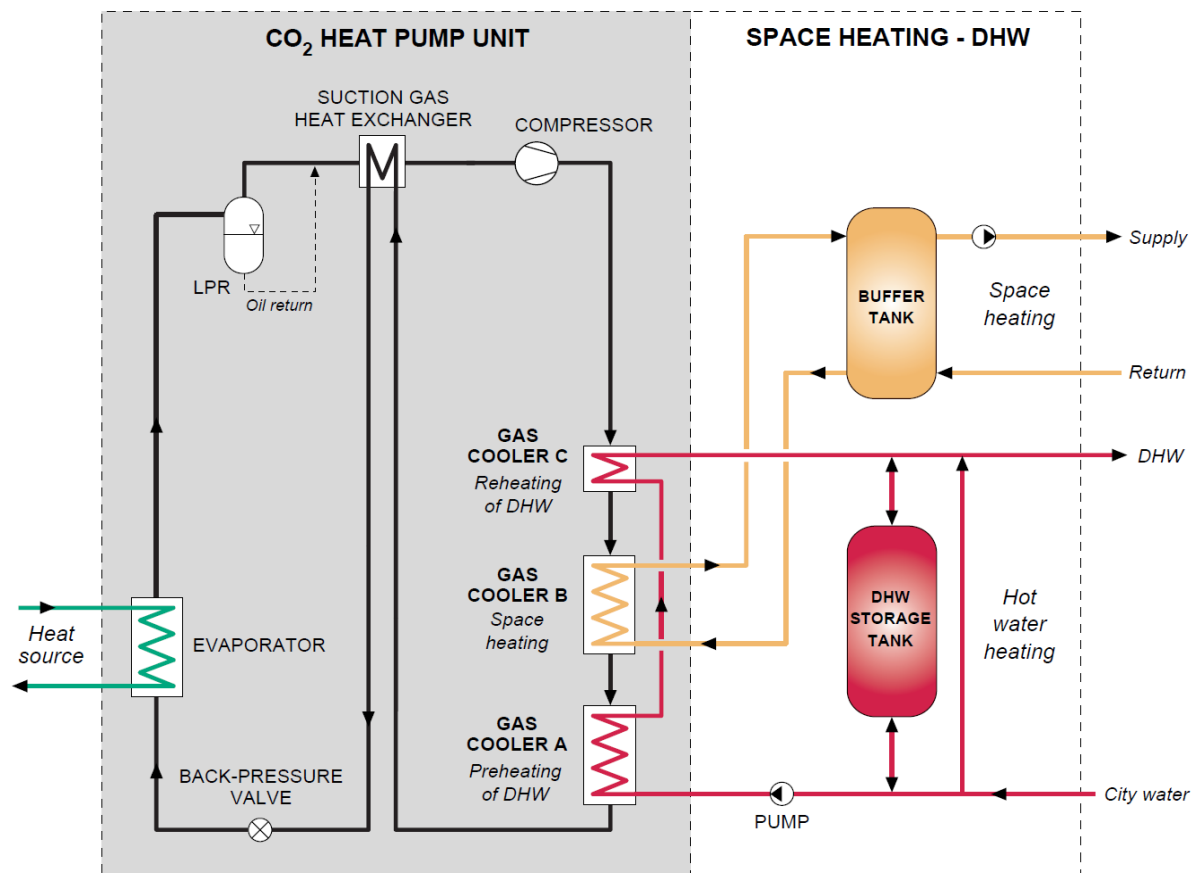


Fig. 7: Layout of the prototype B/W CO<sub>2</sub> heat pumps and comparison of a prototype and improved CO<sub>2</sub> heat pump to state-of-the art (Justo Alonso and Stene, 2010)

The prototype CO<sub>2</sub> heat pump unit was equipped with a hermetic rolling piston compressor, a tripartite counter-flow tube-in-tube gas cooler and a counter-flow tube-in-tube suction gas heat exchanger. An expansion valve (back-pressure valve) and a low-pressure liquid receiver (LPR) were used to control the pressure in the tripartite gas cooler. Gas cooler units A and C were connected to an unvented single-shell DHW storage tank and an inverter controlled pump by means of a closed water loop. Gas cooler unit B was connected to a low-temperature hydronic heat distribution system with a large insulated buffer tank.

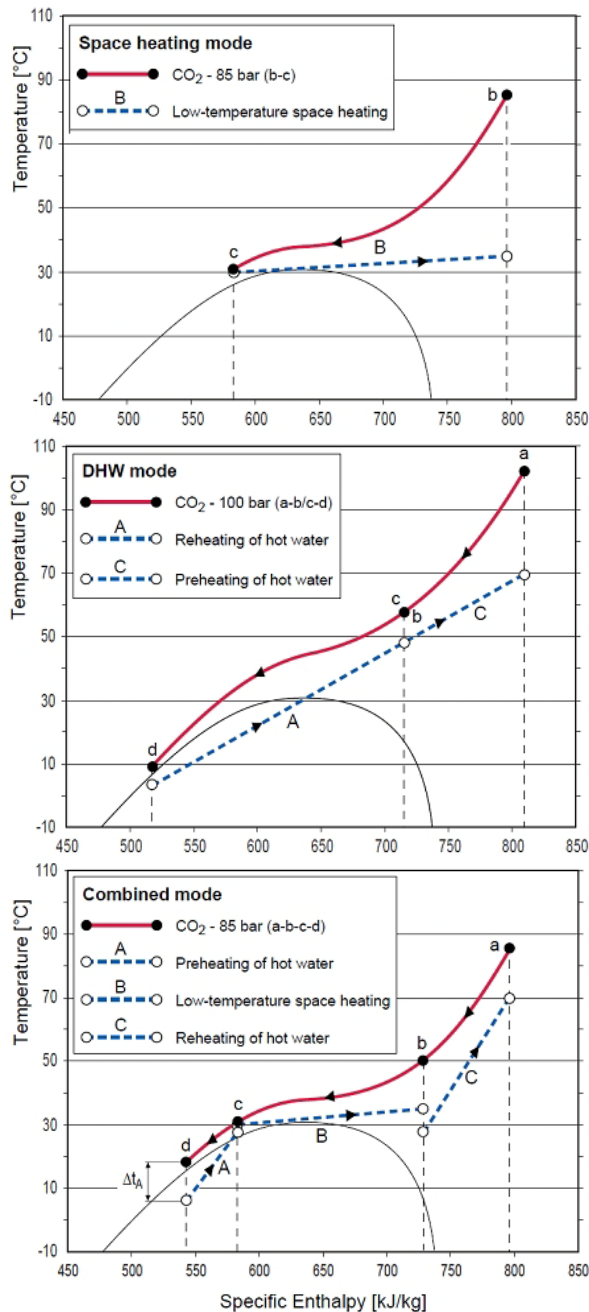


Fig. 8: CO<sub>2</sub> cycle in different operation modes (Stene, 2004)

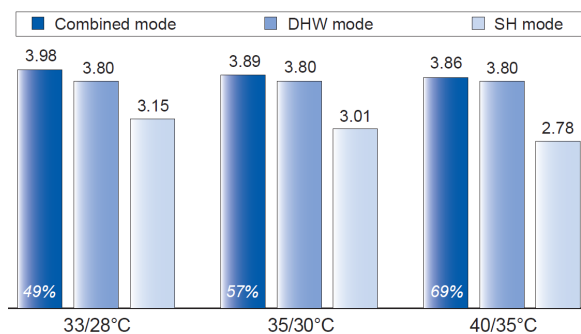


Fig. 9: Measured maximum COP at 60 °C DHW temperature and various SH supply/return temperatures (Stene, 2004)

The integrated CO<sub>2</sub> heat pump unit was tested in three different operating modes: 1) Simultaneous space heating and DHW heating (Combined mode), 2) Hot water heating (DHW mode) and 3) Space heating (SH mode). During tapping of DHW, hot water was delivered at the tapping site, while cold city water entered the bottom of the DHW tank. During charging of the DHW tank in the Combined and DHW modes, the cold city water from the bottom of the DHW tank was pumped through gas cooler units A and C, heated to the set-point temperature, and returned at the top of the tank.

The CO<sub>2</sub> system was tested at 40/35 °C, 35/30 °C or 33/28 °C supply/return temperature in the space heating system, and 60 °C, 70 °C or 80 °C in the DHW system (Stene, 2004/2008-3). The heat rejection processes in the three different operating modes are illustrated in temperature-enthalpy diagrams in Fig. 8. In the example, the supply/return temperatures for the floor heating system are 35/30 °C, while the city water temperature and the set-point for the DHW are 6.5 and 70 °C, respectively. In the Combined mode, the so-called DHW heating capacity ratio is approx. 45%, which means that 45% of the total heating capacity of the tripartite gas cooler is used for hot water heating.

Fig. 9 shows, as an example, the measured COP at optimum gas cooler pressure ( $p_{gc-opt}$ ), 60 °C DHW temperature and various supply/return temperatures for the space heating system for the 6.5 kW prototype brine-to-water CO<sub>2</sub> heat pump with a tripartite gas cooler (Stene, 2004).

The numbers at the bottom of the combined mode bars display the DHW heating capacity ratio. The measured COP in the combined heating mode was 2-10% higher than that of DHW heating mode due to the moderate optimum gas cooler pressure (85-95 bar) and the relatively low CO<sub>2</sub>-outlet temperature from the tripartite gas cooler. This is due to an excellent temperature fit between the CO<sub>2</sub> and the water.

The measured COP in the SH mode was 20-30 % lower than that of the Combined mode. This was a result of the poor temperature fit between the CO<sub>2</sub> and the water, and the fact that the CO<sub>2</sub> outlet temperature from the gas cooler was limited by the relatively high return temperature in the space heating system. *The higher the return temperature, the lower are the COP in SH heating mode and combined heating mode.*

The Seasonal Performance Factor (SPF) for the prototype CO<sub>2</sub> heat pump unit and a state-of-the-art high-efficiency brine-to-water heat pump unit with HFC or propane as working fluid has been calculated. It was assumed constant inlet brine temperature for the evaporator (0 °C) as well as constant temperature levels in the space heating system (35/30 °C) and the DHW system (10/60 °C) (Stene, 2008-3). An improved CO<sub>2</sub> heat pump unit with 10% higher COP than the prototype system was also investigated. The COP can be increased by e.g. using a more energy efficient compressor, optimizing the design and operation of the tripartite gas cooler or replacing the expansion valve by an ejector. Fig. 10 left shows measured COPs for the heat pump systems.

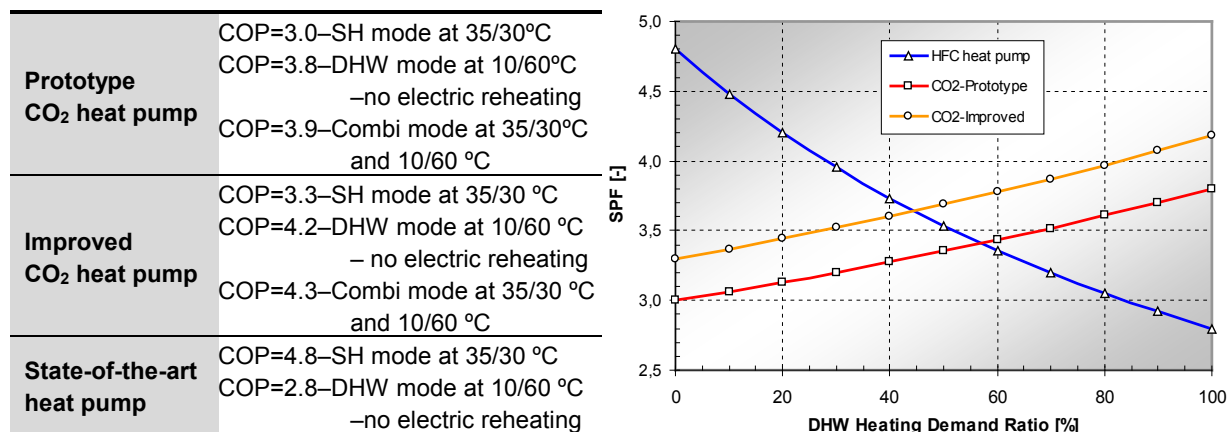


Fig. 10: SPF of CO<sub>2</sub> and HFC heat pump variants (left) and dependent on DHW share (right) (Justo Alonso and Stene, 2010)

The CO<sub>2</sub> (R744) heat pump units achieve the highest COP during operation in DHW heating mode and Combined heating mode, whereas the state-of-the-art heat pump unit operating in a standard (subcritical) heat pump cycle achieves the highest COP in SH heating mode.

Fig. 10 right shows the calculated SPFs for the three residential heat pump systems during monovalent operation presented as a function of the annual *DHW heating demand ratio*. The latter is defined as the ratio of the annual DHW heating demand and the total annual heating demand of the residence. The calculated SPF values neither include thermodynamic losses in the DHW tank caused by mixing of hot and cold water nor internal conductive heat transfer. At low DHW heating demand ratios, the state-of-the-art heat pump is more efficient than the CO<sub>2</sub> systems due to their relatively poor COP during operation in SH heating mode. At increasing DHW heating demand ratios, the SPFs of the CO<sub>2</sub> systems are gradually improved, since an increasing part of the heating demand is covered by operation in combined heating mode and DHW heating mode. The SPF for the state-of-the-art heat pump drops quite rapidly with increasing DHW heating demand, since the COP during operation in DHW heating mode is about 35% lower than that of SH heating mode. At the actual operating conditions, the break-even for the CO<sub>2</sub> systems occurs at a DHW heating demand ratio around 45-55%. In existing houses where the DHW heating demand ratio typically ranges from 10 to 30%, a state-of-the-art high-efficiency heat pump system will in general be more energy efficient than an integrated single-stage CO<sub>2</sub> heat pump system. However, in ultra-low-energy houses and passive houses, where the DHW heating demand ratio ranges from typically 50%, an integrated CO<sub>2</sub> heat pump system with a tripartite gas cooler will outperform the most energy efficient heat pump systems on the market.

At 70% DHW heating demand ratio, the COP for the improved CO<sub>2</sub> heat pump is about 3.9. This corresponds to a net energy saving of ≈75% compared with a direct electric system.

## 4 INTEGRATED CO<sub>2</sub> HEAT PUMP PROTOTYPE

### 4.1 Motivation

Austria has a strong growing market of low energy and passive houses. Between 2006 and 2008, the number of passive houses has more than doubled from 1670 to 4150 built houses (according to [www.ig-passivhaus.at](http://www.ig-passivhaus.at)). Multifunctional integrated heat pump solutions are expected to have a better performance and advantages in low energy houses due to internal heat recovery for other functions and due to simultaneous operation to cover several building needs at the same time. Moreover, most of available heat pumps on the market use HFC refrigerants which have a global warming impact. Natural refrigerants, on the other hand, have negligible global warming impact down to 1 (CO<sub>2</sub>-equivalent) of CO<sub>2</sub> itself.

Therefore, the national Austrian project at the Institute of Thermal Engineering (IWT) of Graz University of Technology (TU Graz) is dedicated to the development of an integrated heat pump in the capacity range of 3-5 kW, preferentially using a natural refrigerant, e.g. CO<sub>2</sub> (R744) or propane (R290). The project comprises the steps (Heinz and Rieberer, 2010) of

- a system assessment (3 system layouts)
- a cycle analysis to identify the best refrigerant for the system layout (3 refrigerants)
- construction and lab-testing of a prototype
- detailed simulations of the chosen system and its dynamic interaction with the heating system and the building (Dynamic simulations in TRNSYS (2007))

### 4.2 System outline

As first step, three system layouts for further investigations have been defined, which are depicted in Fig. 11 and described in the following.

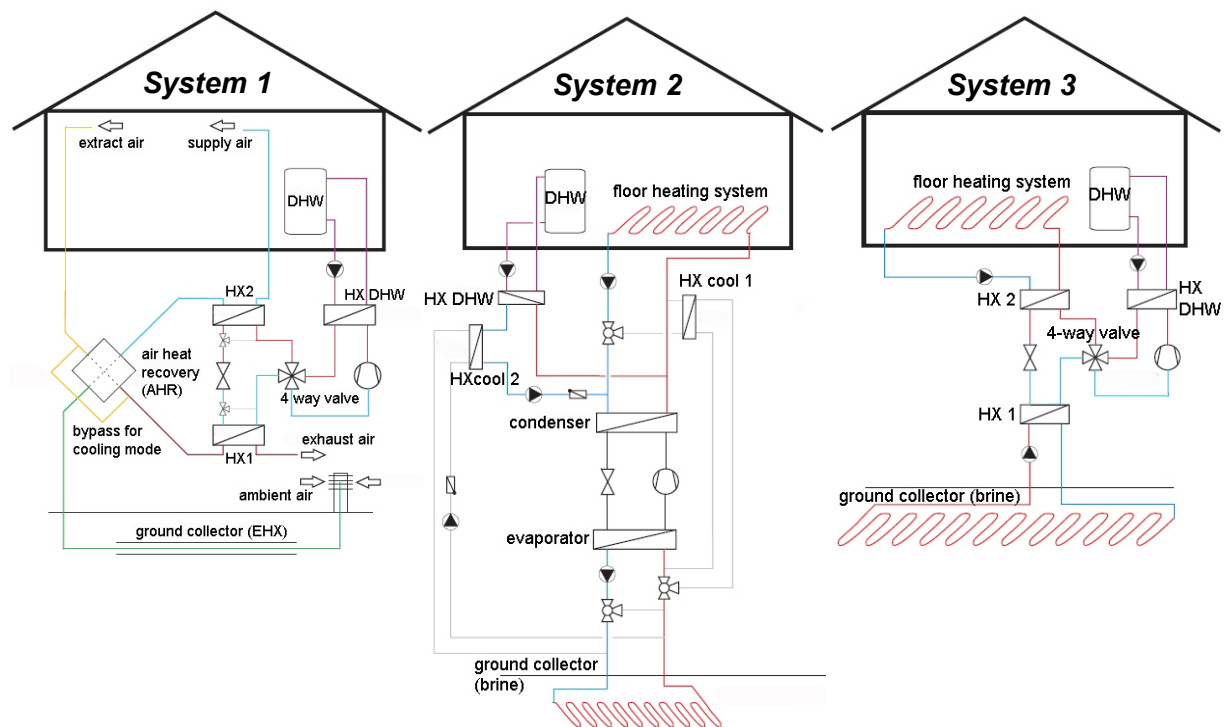


Fig. 11: Systems configurations investigated in the Austrian project

#### 4.2.1 System 1: Reverse operating A/A HP with air-heating/-cooling

This system is a fresh air heating system with controlled ventilation. The heating of the building is done solely via the hygienically necessary air exchange rate of 0.4 1/h. As the supply air temperature is limited due to comfort criteria, the heating capacity is limited to about 10-12 W/m<sup>2</sup> reducing the applicability to passive houses. If higher heating or cooling capacities are required, the air flow rate and thus the air exchange rate would have to be (further) increased, as otherwise unacceptable high (or low) air supply temperatures would be required. Due to the increased air exchange the ventilation losses of the building would be increased. Additionally, the increased air exchange would cause a very dry indoor air at low ambient temperatures due to the low absolute humidity of the supply air.

##### Heating mode

In heating mode the ambient air is pre-heated via a ground-to-air heat exchanger (EHX) that consists of pipes, buried in the ground in a depth of about 1.5 m. The EHX should ensure an air temperature higher than 0 °C at the outlet, in order to prevent a freezing of condensate on the exhaust air side of the ventilation heat recovery heat exchanger (AHR). The AHR is a cross flow heat exchanger in which heat is transferred from the extracted air from the room to the fresh air coming from the EHX. The AHR is assumed to achieve a heat recovery rate of 70%. After the AHR the air is reheated to the temperature necessary to cover the heating demand by the condenser of the heat pump situated in the supply air duct (HX<sub>2</sub>) or by an electrical heater (not shown in Fig. 11 left) in times of DHW production. The extracted air flow is used for the heat recovery in the AHR and serves after the AHR as heat source for the heat pump evaporator situated in the exhaust air duct (HX<sub>1</sub>). The second condenser for the preparation of DHW (HX<sub>DHW</sub>) is only flown through by fresh water in the DHW mode. Thus, it is assumed that no condensation takes place in this heat exchanger in the heating mode. The heat exchanger HX<sub>DHW</sub> acts as the condenser for charging a DHW tank. HX<sub>2</sub> is bypassed and the re-heating of the supply air is done by an electrical heater, which is installed in the supply air duct. HX<sub>1</sub> acts as the evaporator of the heat pump. A simultaneous heating and DHW preparation is possible, if HX<sub>DHW</sub> is used as a desuperheater and HX<sub>2</sub> as the condenser of the heat pump, which, however, was not investigated within the project.

##### Cooling mode

In the cooling mode the air heat recovery is by-passed, as the air coming from the EHX is normally colder than the extracted air. The air-exchange rate has to be increased to 1/h in order to be able to achieve a suitable cooling capacity with acceptable supply air temperatures. The heat pump process is reversed by the 4-way-valve, i.e. HX<sub>2</sub> in the supply air duct acts as the evaporator, cooling down the air from the outlet EHX to the temperature necessary to cover the cooling demand (see Fig. 11 left). HX<sub>1</sub> in the exhaust air duct is operated as the condenser.

In the reverse mode the refrigerant flows through these heat exchangers in the reverse direction, therefore the heat exchangers are operated in parallel flow instead of counter flow. This is a disadvantage, as the process has to be operated with higher condensation and lower evaporation temperatures than in counterflow operation.

In case of a simultaneous demand for DHW the condensation of the refrigerant is done in the second condenser for the preparation of DHW (HX<sub>DHW</sub>) and HX<sub>1</sub> is bypassed. This is done in order to prevent a reheating of cold refrigerant by air with a higher temperature.

#### 4.2.2 System 2: B/W HP with a hydraulic space heating/cooling system

In this system a hydraulic floor heating system is used both to heat and to cool the building. Controlled ventilation is not used in this investigation, the air exchange is done solely by window ventilation, assuming an air exchange rate of 0.4 1/h. Using a hydraulic heating system much higher heating and cooling capacities can be achieved compared to an air heating system enabling the use in buildings which have higher heat loads than passive houses. A

sketch of the system design is shown in Fig. 11 centre. The heat pump consists of a non-reversible refrigerant cycle. A ground collector (brine) is used as the heat source for the heat pump and partially also as the heat sink in the cooling mode.

#### Heating mode

In the heating mode the condenser of the heat pump is used to heat the water flowing through the floor heating system to the supply temperature necessary to cover the heating demand. The evaporator of the heat pump extracts heat from the brine cycle of the ground collector.

For the preparation of hot water a DHW tank is used, which is charged by a heat exchanger ( $HX_{DHW}$ ) that is not connected to the refrigerant cycle, but which is indirectly charged by the heating loop. Alternatively, a second condenser for the DHW preparation can be used to increase the efficiency of the heat pump (lower condensing temperature) and to enable a combined operation (simultaneous heating and preparation of DHW).

#### Cooling mode

In the cooling mode the floor heating system is used to cool the living space. With this system three different cooling modes are possible:

##### a) Active cooling with simultaneous DHW preparation

The heat collected in the floor heating system is transferred to the brine cycle and the evaporator via the heat exchanger  $HX_{cool1}$ . The condenser heat is used to charge the DHW tank. Thus both the warm and the cold side of the heat pump are utilized.

##### b) Active cooling

If the DHW tank is already entirely charged, the condenser heat can alternatively be transferred to the brine cycle by an additional heat exchanger  $HX_{cool2}$ . This also requires an additional pump in the brine cycle. For buildings with a small cooling demand, like it is usually the case in residential buildings in Austria, it is thinkable to omit active cooling (without DHW preparation), i.e. no  $HX_{cool2}$  and second connection to the brine cycle are required.

##### c) Passive cooling

As the brine loop is connected to the floor heating system by  $HX_{cool1}$ , it is also possible to perform passive cooling with the ground heat exchanger acting as the heat sink, i.e. without operation of the heat pump.

### **4.2.3 System 3: Reverse operating B/W HP with hydraulic space heating/cooling**

System 3 is quite the same as System 2 except for using a reversible heat pump cycle. This has the advantage that  $HX_{cool1}$ ,  $HX_{cool2}$  and the additional pump in the brine cycle (see Fig. 11 middle) are not necessary, which saves costs and increases the efficiency due to avoiding the temperature differences in  $HX_{cool1}$  and  $HX_{cool2}$  in cooling mode. On the other hand, the refrigerant cycle is more complex and passive cooling is not possible.

#### Heating mode

The condenser of the heat pump is used to heat the heating water to the supply temperature necessary to cover the heating demand. The evaporator of the heat pump extracts heat from the brine cycle of the ground collector. For the preparation of DHW a tank is used, which is charged by a second condenser ( $HX_{DHW}$ ). A combined operation mode with simultaneous heating and DHW preparation is possible, if  $HX_{DHW}$  is used as desuperheater and  $HX_2$  as condenser of the heat pump, but this was not investigated.

#### Cooling mode

The heat pump cycle is reversed via the 4-way valve. Thus, both  $HX_2$  used as the evaporator in this mode and  $HX_1$  are operated in parallel flow, as the flow direction of the refrigerant is reversed. Thus, the process has to be operated with higher condensation (and possibly lower evaporation) temperatures than in counterflow configuration.

Two cooling modes are possible:

In simultaneous active cooling with DHW preparation, the heat exchanger  $HX_{DHW}$  is used as condenser to charge the DHW tank. Thus, both the warm and the cold side of the heat pump are utilized.

If the DHW tank is entirely charged, the simultaneous operation is not possible, thus in active cooling-only the condenser heat is rejected to the ground via the heat exchanger  $HX_1$ . In system 3, passive cooling is not possible.

#### **4.2.4 Results of the cycle simulation and conclusions for system layout**

Summarising, the following decisions were taken based on the results of the cycle simulations, which are detailed in the country report (Heinz and Rieberer, 2010).

##### **4.2.4.1 System choice**

All three system concepts have been analysed in detail by means of simulations of the refrigerant cycle.

In a national workshop with planners and heat pump manufacturers the system concepts and the simulation results were presented and discussed. The choice was made for a system quite similar to system 2 (see chap. 4.2.2) mainly due to the following reasons:

- The system to be developed shall be suitable for a broad range of low energy buildings with different heating demands. System 1 (fresh air heating system) can only be applied in buildings that have a heating demand of  $< 15 \text{ kWh}/(\text{m}^2\cdot\text{a})$ .
- Air heating systems are hardly used in residential buildings in Austria, where mainly hydraulic heating systems are installed. Therefore, it is expected, that user acceptance for an integrated heat pump in combination with a hydraulic heating system will be far higher on the Austrian market.
- In general the cooling demand of residential buildings in the Austrian climate can be kept at a minimum. If only small cooling loads occur, it should be possible to cover these with passive cooling, without using the heat pump. A reversible refrigerant cycle, as it is used in System 3, is therefore not considered as necessary. However, if passive cooling is not sufficient, System 2 also offers the possibility of active cooling.

##### **4.2.4.2 Refrigerant choice**

The results of the simulations of the refrigerant cycles (Heinz and Rieberer 2008) with different refrigerants (R134a, R290, R744) led to the following conclusions concerning the refrigerant choice for the system to be further investigated:

- With the refrigerant R290 the highest seasonal performance factor ( $\text{SPF}=3.6$ ) can be expected with the used assumptions. However, as R290 is flammable, there are relatively strict safety regulations concerning the refrigerant content in the cycle and/or the necessary air volume in the room of installation acc. to EN 378 (2008).
- With R744 ( $\text{CO}_2$ ) and R134a approximately the same SPF can be expected ( $\text{SPF}=3.3$ ). While  $\text{CO}_2$  enables higher efficiencies for the preparation of DHW, R134a is advantageous in the heating mode.
- With regard to the decreasing heating energy demands of low energy buildings and the therefore rising fraction of the energy demand for DHW and due to the fact that  $\text{CO}_2$  is a natural refrigerant,  $\text{CO}_2$  will be used for the further investigations in the project.

## 4.3 Design of a prototype unit

### 4.3.1 System configuration of the prototype system

A schematic view of the system layout of the prototype brine-to-water heat pump with the refrigerant  $\text{CO}_2$  is shown in Fig. 12.

A central buffer storage, which is charged by the heat pump, serves as hydraulic decoupling between the heating system (red lines, 2) and the heat pump (black lines, 1). The DHW (green lines, 3) is produced by the external heat exchanger  $\text{HX}_{\text{DHW}}$ . The control of the operation should as far as possible guarantee low return temperatures of the heating water to reach low inlet temperatures to the gas cooler ( $\text{GC}_1$ ) of the heat pump. In order to preserve the stratification the return of the heating system is charged to the storage by a stratification device. The gas cooler is divided into two parts: In  $\text{GC}_1$  (red lines, 2) the water is drawn from the bottom of the storage and heated to the required temperature level of 30-35°C of the floor heating system and is charged to the middle of the storage. In the upper part (violet lines, 4) the preheated water is reheated to the DHW temperature of about 50-55°C and charged to the upper part of the storage. With this configuration the operation modes space heating-only, (only  $\text{GC}_1$  in operation), DHW-only and simultaneous space heating and DHW operation ( $\text{GC}_1$  and  $\text{GC}_2$  in operation) can be realised. In simultaneous operation the amount of DHW for the reheating in  $\text{GC}_2$  is controlled by a thermostatic valve.

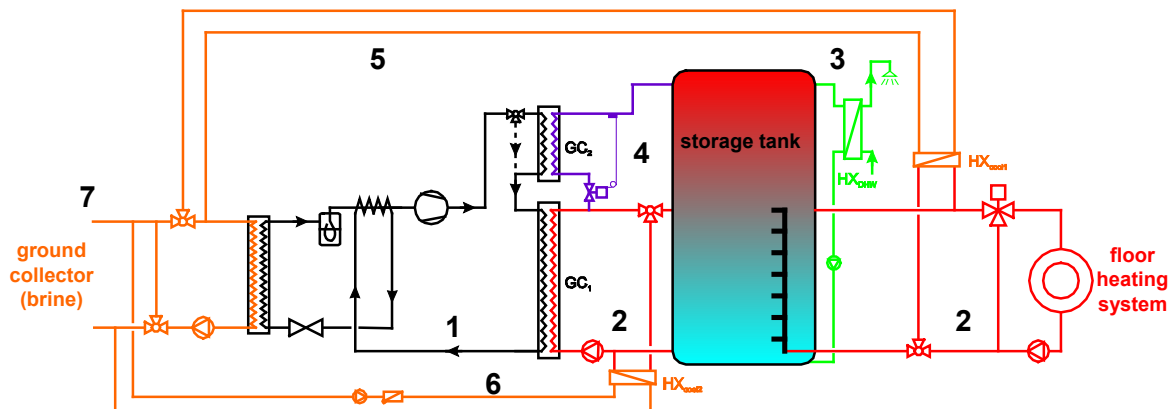


Fig. 12: System layout of the Austria prototype system

The cooling operation can be realised by an external hydraulic (orange lines, 5 and 6). For a passive cooling option a short cut between the source and the sink can be made by the heat exchanger  $\text{HX}_{\text{cool1}}$  (orange lines, 5). As emission system in the room the floor heating is used in the cooling operation, as well. For the active cooling operation the condenser heat of  $\text{GC}_1$  can be rejected by  $\text{HX}_{\text{cool2}}$  into the ground, in simultaneous cooling- and DHW operation the condenser heat is used for the DHW production.

### 4.3.2 Bipartite gas cooler

The heat pump is equipped with only two gas coolers. In the system that was used for the comparison of refrigerants as well as the system investigated in chap. 3.4 a tripartite gas cooler is used, whereby two are used to pre- and reheat the DHW and one is used for space heating. Reasons for using a tripartite gas cooler are

- to provide enough heat exchange surface for the DHW preparation mode, as the surface of the gas cooler for the reheating of DHW is quite small and the gas cooler for heating cannot be used in this mode.
- to ensure that the  $\text{CO}_2$  can be cooled down to a quite low temperature by the cold water entering the first gas cooler.

The first reason does not apply in the prototype layout including the buffer storage, where both gas coolers are flown through by the same fluid (heating water), thus providing enough

heat exchange surface for the operation mode, in which the heating water is heated to about 55°C (for the instantaneous DHW preparation).

The CO<sub>2</sub> temperature at the outlet of the last gas cooler in the current system with two gas coolers tends to be higher and therefore the COP of the heat pump is lower. However, this applies only to the combined heating and DHW mode.

The COP as a function of the ambient temperature in this mode under the assumed conditions for both systems with tripartite and bipartite gas cooler is shown in Fig. 13. It can be seen that the advantage of the tripartite gas cooler decreases with an increasing ambient temperature. This is due to the decreasing return temperature of the floor heating system, which is the limiting factor for the CO<sub>2</sub> temperature at the outlet of the gas cooler in case of the bipartite gas cooler.

In the system with the buffer storage tank the inlet temperature into gas cooler 1 is depending on the current temperature at the bottom of the buffer tank, which itself depends on the connected heating and DHW preparation system and the current mode of operation.

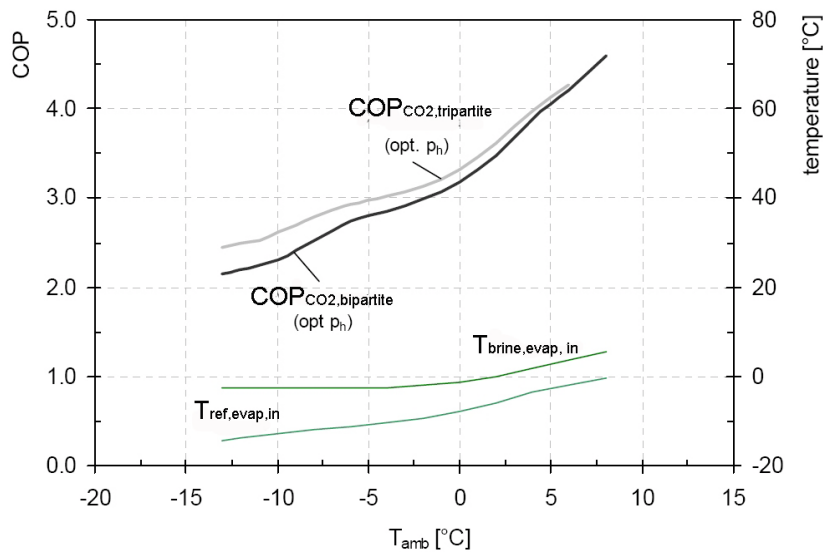


Fig. 13: Comparison of bipartite and tripartite gas cooler

After a DHW draw-off the temperature will be near to the cold water temperature (15°C). After some time with no draw-off the temperature will be equal to the return temperature from the floor heating system, which was assumed for the calculation shown in Fig. 13. In practise the average temperature at the bottom of the tank will be lower than this temperature, depending on the relation of the energy demand for DHW and the space heating energy demand. Due to the following reasons it is expected that the SPF will be approximately the same as with a tripartite gas cooler:

- For the system with the tripartite gas cooler a cold water inlet temperature of 15°C was assumed in the simulations. In practise it can be expected that this temperature will average to higher values, due to the heat transfer processes from warmer to colder water layers in a DHW tank. This would decrease the COP difference compared to a system with a bipartite gas cooler.
- In the DHW mode the average water inlet temperature into the gas cooler will be slightly higher in the current system with buffer storage due to the mixing of water coming from the heat exchanger for the preparation of DHW ( $\text{HX}_{\text{DHW}}$ ) and the return water from the heating system. However, the temperature of the water, which is used for the preparation of DHW, can be chosen lower than the DHW temperature in a system with a DHW tank, where a temperature of >60°C is needed in order to avoid problems with legionella bacteria.
- The losses due to start-stop operation are reduced due to the buffer storage, which enables a compensation of the mismatch between the capacity provided by the heat pump

and the capacity requirement of the heating system. In case of a speed controlled compressor, where the capacity of the heat pump can be adjusted to the actual heating demand, this is not absolutely necessary. However, speed control does only work in a certain range and thus the number of start-stop cycles of the heat pump will be reduced in any case.

### 4.3.3 Test rig

A schematic view and a photograph of the test rig is given in Fig. 14. The system was designed to fulfil the following purposes:

- Provide the possibility of creating the necessary thermodynamic conditions (inlet temperatures and mass flow rates etc.) at the heat exchangers of the heat pump in order to simulate different load conditions and operation modes.
- Measurement equipment with an appropriate accuracy, in order to be able to analyse the heat pump cycle in detail in different operating conditions. The following data is measured:
  - Refrigerant pressure and temperature at the inlet and outlet of every component of the heat pump cycle
  - Refrigerant mass flow rate
  - Electricity consumption of the compressor
  - Brine and water inlet and outlet temperatures of every heat exchanger
  - Brine and water flow rates
- Automatic adjustment of different operating conditions via electronic controllers

The test rig consists of the following cycles:

- The refrigerant cycle (black loop in Fig. 14)
- The brine cycle (orange loop in Fig. 14)
- The heating cycle (red loop in Fig. 14)
- The hot water cycle for the preparation of DHW (blue loop in Fig. 14)

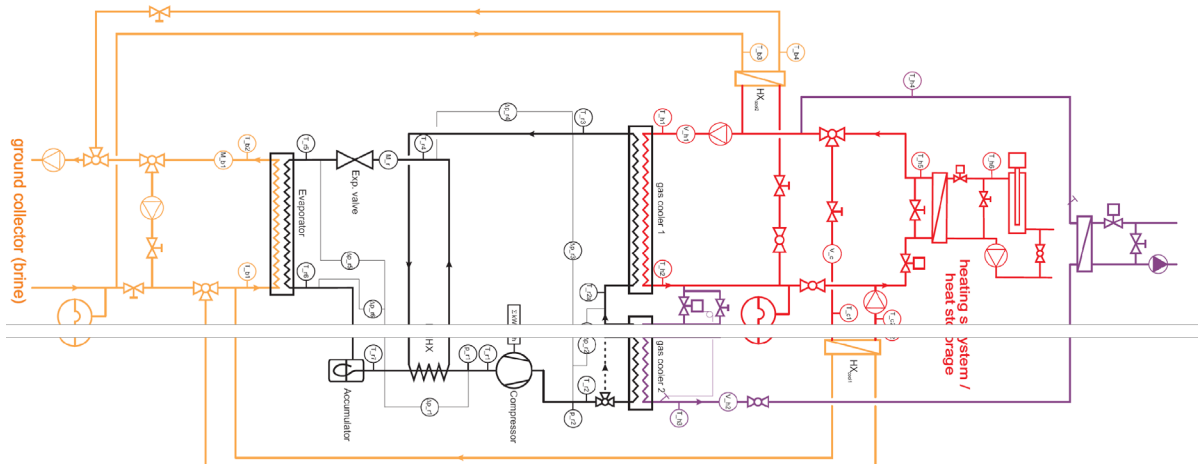
The cooling cycle, the heating cycle and the hot water cycle for the preparation of DHW characterise the periphery facilities connected to the refrigerant cycle.

The layout of the refrigerant cycle used in this system is shown in black colour in Fig. 14, including the measurement equipment that has been installed in the laboratory prototype.

The compressor in the laboratory prototype is a speed controlled hermetic compressor with a swept volume of 4 cm<sup>3</sup>. The bipartite gas cooler and the internal heat exchanger (IHX) are tube-in-tube heat exchangers, which were tailor-made in the workshop of the institute. The evaporator and the accumulator are compact components from the car industry. The expansion device is an electronic expansion valve.

The measured data obtained with the test rig was used to validate a detailed steady state model of the heat pump cycle that was developed within the project.

As can be seen, the heat pump test rig does not contain a buffer storage. This is due to the principal purpose of the rig to analyse the refrigerant cycle in different operating modes by providing the appropriate conditions at the evaporator and the gas coolers of the refrigerant cycle. The behaviour of the system including a storage tank will be analysed in detail in the dynamic system simulation (see chap. 4.4).



**Legend:**

- $T$  – temperature measurement
- $p$  – pressure measurement
- $\Delta p$  - pressure difference measurement
- $V$  – volume flow measurement
- $M$  – mass flow measurement
- $kWh$  – electricity consumption measurement
- IHX – internal heat exchanger
- $r$  – refrigerant
- $h$  – water
- $b$  - brine

Fig. 14: Schematic and photograph of the test rig

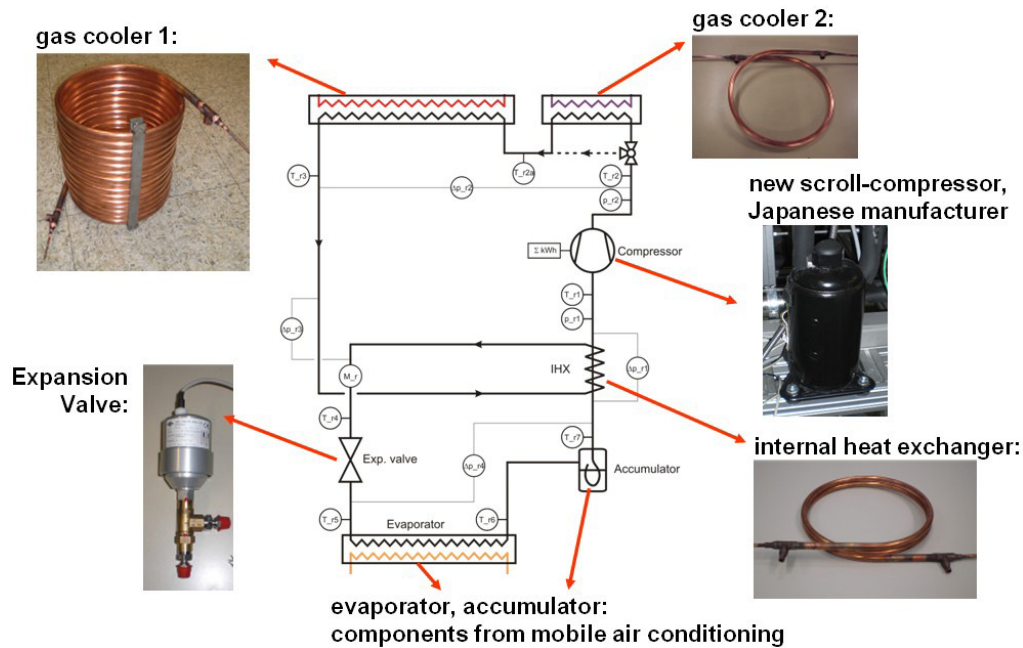


Fig. 15: Components of the refrigerant cycle

### 4.3.4 Results of prototype component testing

The laboratory prototype was used to conduct an extensive experimental analysis of the heat pump cycle in different modes of operation. The obtained data was used to validate a steady state simulation model of the heat pump cycle. In the following exemplary measurement results, which were obtained in different modes of operation, are presented.

As a first step the performance of the used compressor was measured in order to develop a compressor performance map, which is used as a basis for the simulation model of the heat pump system. A test matrix with 40 different operating conditions was established using varying suction pressures, discharge pressures and compressor speeds. Based on the refrigerant mass flow rate, the power consumption of the compressor, suction and discharge temperature and pressure, the overall isentropic efficiency, the volumetric efficiency and the heat loss of the compressor were evaluated. The results show that there is only a small dependency of the isentropic and the volumetric efficiency on the compressor speed and the suction pressure. The overall isentropic efficiency (thermal capacity/electricity consumption of the compressor) varies between 0.66 and 0.52 and the volumetric efficiency between 0.94 and 0.82 for pressure ratios between 1.7 and 3.3. The isentropic efficiency seems quite low, but it has to be considered that this is a small compressor with a relatively low capacity.

For the complete heat pump cycle a test matrix with about 100 different operating conditions was established. One of the objectives was to obtain enough data for different operating conditions of the individual components in order to validate a simulation model of the heat pump system.

#### Heating mode:

In the heating mode water is heated via gas cooler 1 from the temperature  $T_{h1}$  to  $T_{h2}$ . Gas cooler 2 is bypassed (see Fig. 16 a). As the water outlet temperature  $T_{h2}$  is relatively low, the heat pump cycle is mostly operated with sub-critical pressures in the heating mode. In the shown example the water outlet temperature  $T_{h2}$  is about 30°C and the high pressure is about 69 bar (compare the data in the upper left corner of Fig. 16 b). The water inlet temperature into the gas cooler, which in this system is dependent on the temperature at the bottom of the storage tank, is assumed with 20°C in this example.

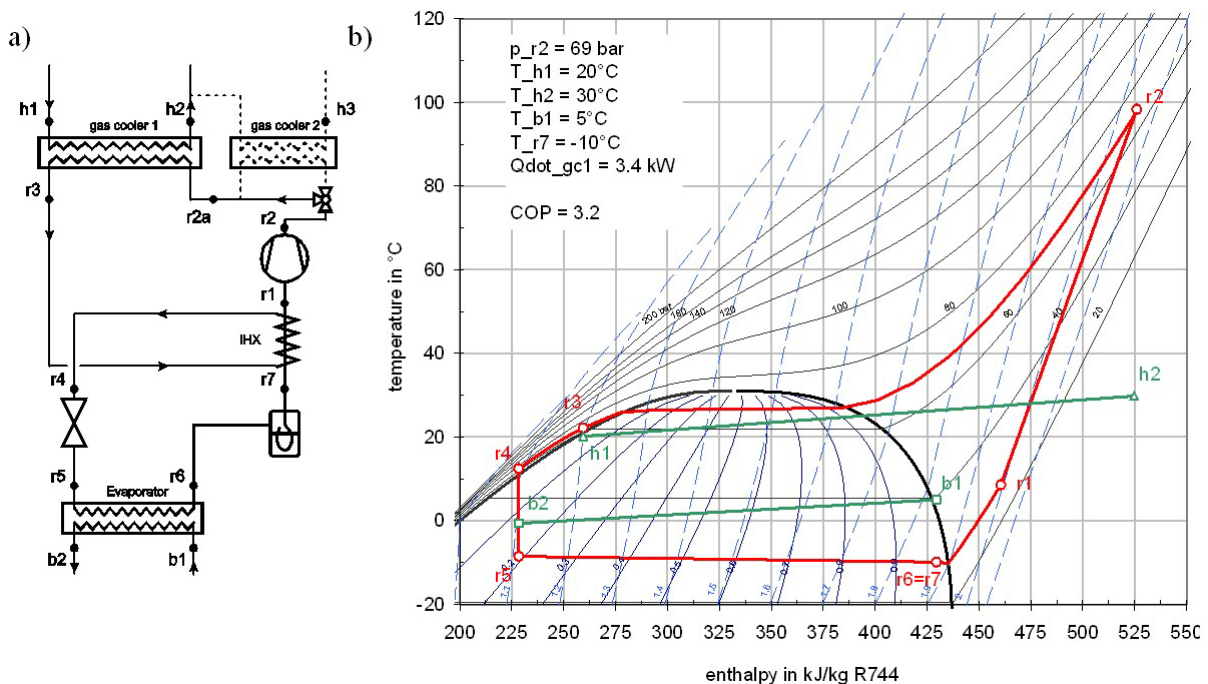


Fig. 16: Process in heating mode (left) and corresponding process in the T-h diagram (right)

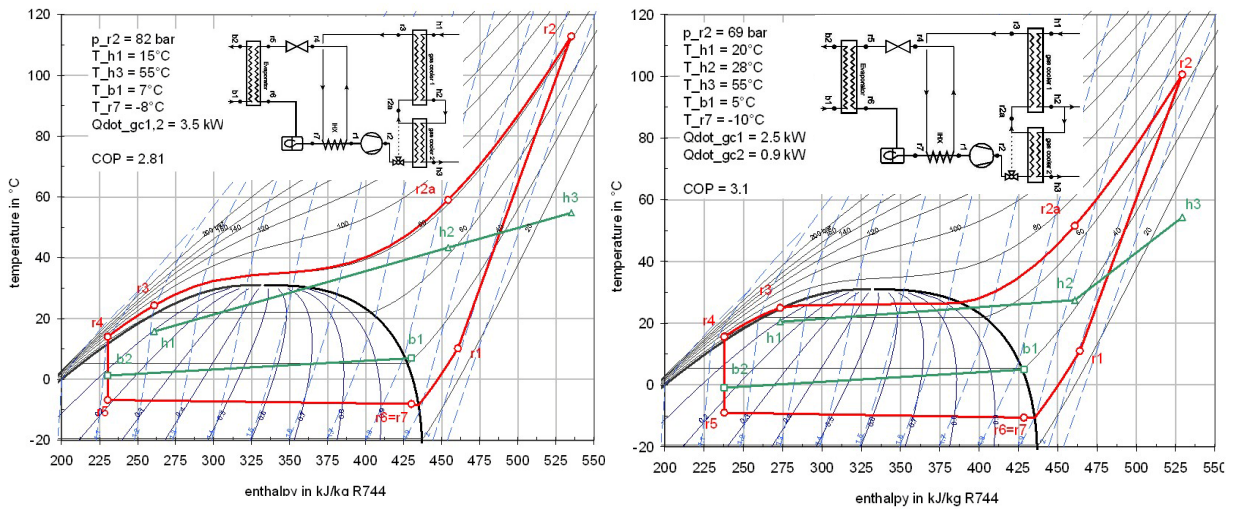


Fig. 17: Test of the DHW-only mode (left) and the combined SH/DHW mode (right)

In practise the water inlet temperature can vary in a range of the return temperature of the floor heating system to the return temperature of the DHW heat exchanger. As can be seen in Fig. 16 and also in the following figures, the temperature difference between the heat source and the evaporation temperature ( $T_{b1}$  and  $T_{r6}$ ) is with about 15 K relatively high. This is due to the used evaporator, which is under-dimensioned for this application. An evaporator with a larger heat transfer area would help to decrease the temperature difference and therefore to increase the COP of the cycle at a given brine temperature. Another possibility for improvement is the brine mass flow rate, which was limited to about 500 kg/h in the test rig. A higher flow rate would help to increase the evaporation temperature (see chap. 4.4.1).

#### DHW mode:

In the DHW mode the water flows through the two gas coolers in series (compare Fig. 17 left). In gas cooler 1 it is pre-heated from the temperature  $T_{h1}$  to  $T_{h2}$  and re-heated in gas cooler 2 to the temperature  $T_{h3}$ , which is typically about 55-60 °C. In this mode the heat pump cycle is generally operated at super-critical pressures. Fig. 17 left shows a heat pump process of an exemplary measurement in the DHW mode.

#### Combined heating and DHW mode:

In the combined heating and DHW mode water is pre-heated in gas cooler 1 to the required temperature for the floor heating system. A part of the water mass flow is re-heated in gas cooler 2 to a temperature of 55-60 °C (see Fig. 17 right). Thus, both the heating of water for the floor heating system and for DHW preparation is accomplished simultaneously. The simultaneous operation has the advantage that water for DHW can be prepared at lower high-pressures compared to the DHW mode (compare Fig. 17 left and right), which results in a higher COP.

#### Combined cooling and DHW mode

In this mode the evaporator of the heat pump is used to cool the building via the floor heating system. This is done through a bypass system and the heat exchanger  $HX_{cool1}$  (compare Fig. 12). At the same time water for the DHW preparation is heated via gas cooler 1 and gas cooler 2. The heat pump process in this mode will therefore be similar to the DHW mode, but with a tendency to higher evaporation temperatures. As both the hot and the cold side of the heat pump are used, relatively high COP values are possible (compare chap. 4.4.3.2).

## 4.4 System evaluations with the prototype heat pump

In order to analyse the performance of the integrated heat pump in a system in the course of a whole year, dynamic system simulations in the simulation environment TRNSYS (SEL, 2005) were carried out. The whole system consisting of the heat pump and its control, a buffer storage tank, a hydronic floor heating system, a brine ground collector and the building were set up in a simulation.

### 4.4.1 Heat pump model

In addition to the model used for the refrigerant cycle analysis a second, more detailed model was developed within the software KULI (2009). This model enables a quick analysis of different operating conditions of the heat pump cycle. The main characteristics of the heat pump model are a modular structure with different component models to build up a system. The measured performance map of the used compressor as described in chap. 4.3.4 is used as an input for the model. A tube-in-tube heat exchanger model calculates the heat transfer coefficients and the pressure losses based on the geometrical data of the heat exchangers and the local properties and flow conditions of the refrigerant, water or brine. The model provides the possibility to run a large number of simulations in quite a short time, so the necessary number of measurements is reduced. By using the model performance maps of the heat pump cycle for the different operation modes in the relevant range of operating conditions can be generated, which are further on used to run yearly simulations in TRNSYS (SEL, 2005). In order to obtain reliable results, the measured data from the laboratory prototype was used to adapt and validate the model. The parameters of each heat exchanger were adapted in a way to fit the measured data as close as possible. Fig. 37 left shows a comparison of 77 cycle measurements and simulation results of the COP of the heat pump. Most of the simulation results are in a range of  $\pm 5\%$  of the measured results. The original geometric data of the heat exchangers had to be adapted only slightly to achieve this degree of agreement. Exemplarily a comparison of a measured and a simulated process is shown in the p-h diagram in Fig. 18 right.

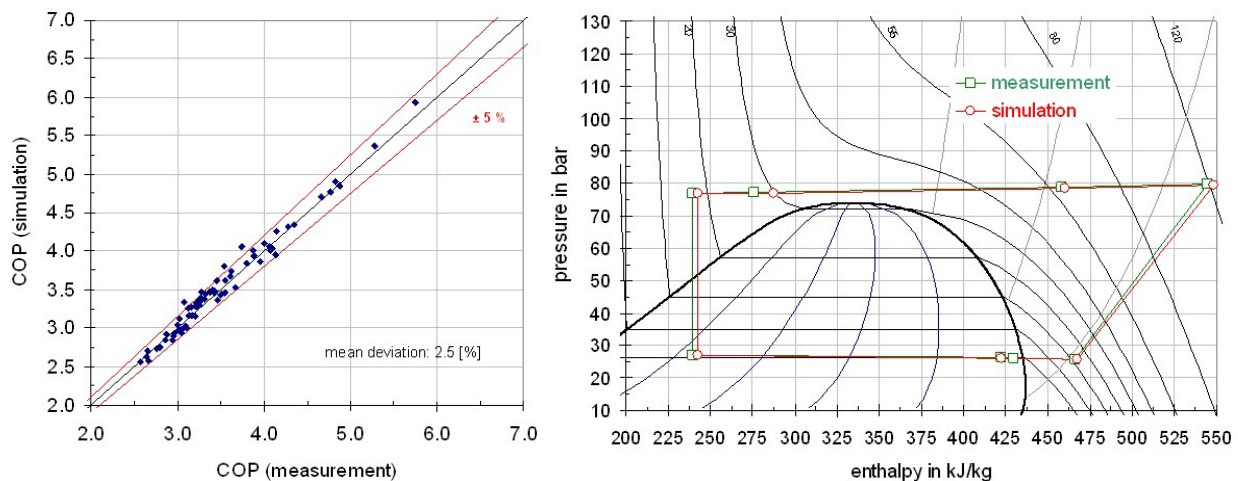


Fig. 18: Comparison of simulated and measured COP (left) and cycle simulation (right)

Furthermore, the model can be used to quickly determine the optimum high pressure level for the respective operation conditions without the necessity of extensive measurements.

The performance maps of the heat pump for the different operation modes were integrated in a TRNSYS model. This model enables a considerably faster simulation compared to the detailed steady state model. For each operation mode a performance map with a number of independent parameters was established, which shall cover all different operating conditions

that can occur during a year. For example for the DHW mode a performance map dependent on the water inlet temperature  $T_{h1}$ , the brine inlet temperature  $T_{b1}$  and the compressor speed  $n$  and a constant water outlet temperature  $T_{h3}$  of 55 °C was generated. Fig. 19 shows the set of parameters used for each operation mode. For each combination of these parameters simulations with the detailed model were performed. Additionally, simulations with different high pressures were done for each operation point.

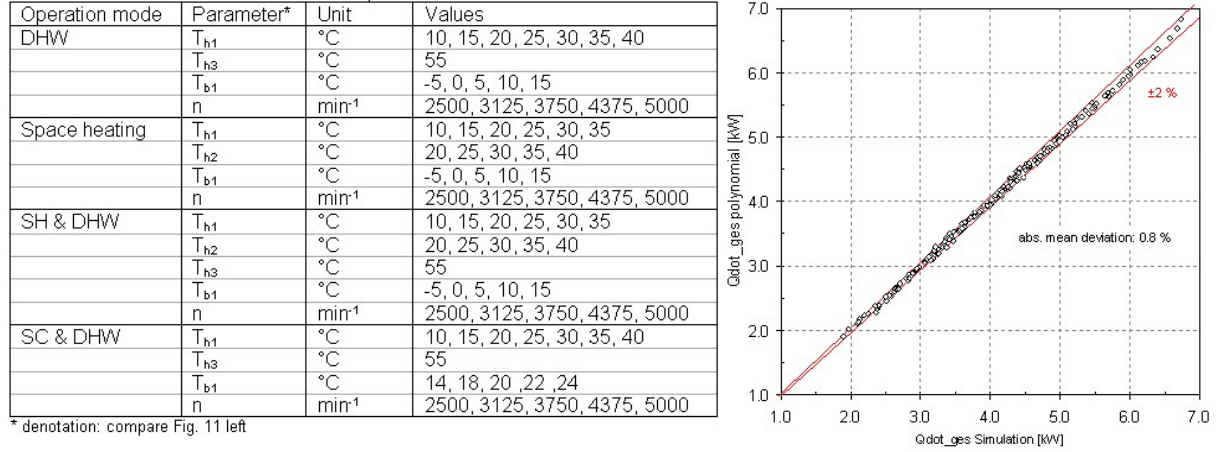


Fig. 19: Operation points for the heat pump performance map (left) and validation (right)

The simulations were evaluated for the optimum high pressure of each operation point. The results were used to generate equations for each operation mode, that enable a calculation of the thermal capacity of the gas coolers (total capacity  $\dot{Q}_{tot}$  and capacity of gas cooler 1  $\dot{Q}_{GC1}$ ), of the evaporator  $\dot{Q}_{evap}$  and the electricity consumption of the compressor  $P_{comp}$  dependent on the respective parameters. The generation of these equations was done via a linear regression in the software EES (Klein, 2007). As an example the form of the resulting polynomial for  $\dot{Q}_{tot}$  for the DHW mode is shown in eq. 2.

$$\begin{aligned}
 \dot{Q}_{tot} = & a_0 + a_1 * T_{h1} + a_2 * T_{h1}^2 + a_3 * T_{h1}^3 + a_4 * T_{b1} + a_5 * T_{b1}^2 \\
 & + a_6 * T_{b1}^3 + a_7 * n + a_8 * n^2 + a_9 * n^3 + a_{10} * T_{h1} * T_{b1} + a_{11} * T_{h1} * T_{b1}^2 \\
 & + a_{12} * T_{h1} * n + a_{13} * T_{h1} * n^2 + a_{14} * T_{h1}^2 * T_{b1} + a_{15} * T_{h1}^2 * T_{b1}^2 \\
 & + a_{16} * T_{h1}^2 * n + a_{17} * T_{h1}^2 * n^2 + a_{18} * T_{b1} * n + a_{19} * T_{b1} * n^2 \\
 & + a_{20} * T_{b1}^2 * n + a_{21} * T_{b1}^2 * n^2
 \end{aligned}$$

eq. 2

With the generated equations the results of the detailed simulations can be reproduced accurately for all operation modes. Fig. 19 right shows a comparison of the values calculated with the polynomial and the simulated data. The accuracy is better than  $\pm 2\%$  in most cases. During the analysis it turned out that the evaporator of the laboratory prototype is underdimensioned. In a simulation the effect of a larger evaporator (100% larger heat transfer area) and a higher brine mass flow was analysed. The results show, that the COP of the cycle can be improved significantly by these measures. For the simulations of the heat pump cycle that were used for the generation of the performance maps described above a doubled heat transfer area and a brine flow rate of 1000 kg/h were assumed accordingly.

## 4.4.2 Boundary conditions

### 4.4.2.1 Reference building

As a boundary condition for the dynamic simulation of the system a low energy building with a living space area of 140 m<sup>2</sup> (ground floor area 10m x 7m) is used, based on a building model used as a reference building in IEA SHC Task 32 “Advanced storage concepts for solar and low energy buildings” (see Fig. 20). This model was slightly modified, e.g. the wall constructions were changed to achieve a higher heat demand of the building than in the original version (40 instead of 30 kWh/(m<sup>2</sup>a)). A detailed description of the building and the used assumptions concerning the user behaviour is given in Heimrath and Haller (2007).

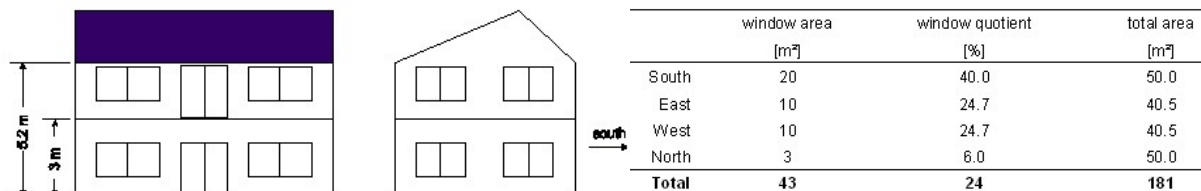


Fig. 20: Reference building used for the simulations (left) and window areas (right)

The wall constructions used in this work are given in Tab. 2.

Tab. 2: Wall constructions used for the system simulations

assembly	layer	layer thickness [m]	density [kg/m <sup>3</sup> ]	conduct. [W/mK]	capacity [kJ/kgK]	U - Value construction [W/m <sup>2</sup> K]
external wall	plaster inside	0.015	1200	0.600	1.00	0.200
	Mertl brick	0.210	1380	0.700	1.00	
	EPS	0.180	17	0.040	0.70	
	plaster outside	0.003	1800	0.700	1.00	
	<b>Σ</b>	<b>0.408</b>				
ground floor	wood	0.015	600	0.150	2.50	0.185
	plaster floor (floor heating)	0.070	2000	1.400	1.00	
	XPS	0.180	38	0.037	1.45	
	concrete	0.300	2000	1.330	1.08	
	<b>Σ</b>	<b>0.565</b>				
roof ceiling	gypsumboard	0.025	900	0.211	1.00	0.127
	plywood	0.015	300	0.081	2.50	
	rockwool	0.260	60	0.036	1.03	
	plywood	0.015	300	0.081	2.50	
	<b>Σ</b>	<b>0.315</b>				
<b>intermediate ceiling</b>	wood	0.015	600	0.150	2.50	0.607
	plaster floor (floor heating)	0.055	2000	1.400	1.00	
	EPS	0.04	17	0.040	0.70	
	concrete	0.2	2000	1.330	1.08	
	plaster inside	0.005	1800	0.700	1.00	
	<b>Σ</b>	<b>0.315</b>				
internal wall	plaster inside	0.01	1200	0.600	1.00	0.932
	brick	0.200	650	0.230	0.92	
	plaster insided	0.01	1200	0.600	1.00	
	<b>Σ</b>	<b>0.220</b>				

### 4.4.2.2 Climate, heat source, heat emission and DHW demand

An average climate of the city of Graz was used for the simulations (design outdoor temperature  $T_{OD} = -12$  °C, heating degree days  $HGT_{20/12}$ : 3500 Kd/a) (Meteonorm, 2005). These assumptions result in a heat load of the building of 6.1 kW ( $T_{OD} = -12$  °C,  $T_{ID} = 20$  °C) and a heating demand of 40 kWh/m<sup>2</sup>a.

A brine ground collector is used as the heat source of the heat pump. The collector was dimensioned according to Vaillant (2002), resulting in the data provided in Fig. 21 bottom. The seasonal evolution of the undisturbed ground temperature is calculated with the TRNSYS Type 501, which is based on a model developed by Kasuda et al. (1965).

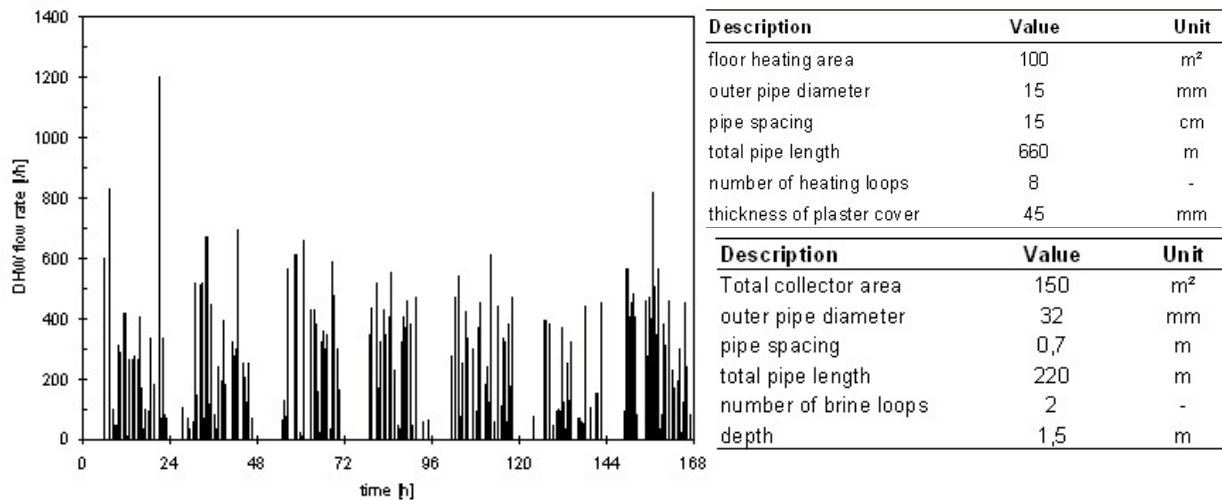


Fig. 21: DHW profile (left) and design of the floor heating (top) and ground collector (bottom)

The calculation of the dynamic evolution of the temperatures in the earth layers adjacent to the ground collector is done under consideration of the heat transfer processes and the thermal capacities in the ground. The assumed thermal properties of the ground are: density 1800 kg/m<sup>3</sup>, thermal conductivity 2.5 W/mK, thermal capacity 1.26 kJ/(kgK). The brine mass flow through the collector is set to 1000 kg/h. The electricity consumption of the brine pump is assumed to be 75 W at this flow rate.

The hydronic floor heating system is integrated as a so-called “active layer” into the plaster floor of the ground floor plate and the intermediate ceiling, with an area of 50 m<sup>2</sup> both on the ground floor and the 1<sup>st</sup> floor. The dimensioning of the floor heating system was done according to Gabotherm (2006) with a flow/return temperature at the design ambient temperature (-12 °C) of 32/28 °C. The most important data of the floor heating system is shown in Fig. 21 top.

For the domestic hot water energy need a statistically generated demand profile that considers the evolution of the demand over the year, different weekdays, during the day and also times of absence (e.g. holidays) is used. Different studies, ranging from telephone surveys to detailed measurements, were used as a basis (Jordan and Vajen, 2001). The profile consists of a dataset, in which a DHW flow rate is assigned to each time step (step size three minutes) of the simulated year. A DHW need of 200 l/d (4 persons with 50 l/(d-person)) with a DHW temperature of 45°C is used in the simulations. As an example Fig. 21 shows the evolution of the DHW need for one week of the generated DHW profile. For the evolution of the cold water temperature in the course of the year a time-dependent sine-function according to Heimrath and Haller (2007) is used.

#### 4.4.2.3 Shading, system and room temperature control

An overheating due to solar gains through the windows shall be reduced by the usage of an external blind shading (Heimrath and Haller, 2007). The control of the shading is done depending on the incident solar irradiation on the horizontal and on the room temperature. The following points must be fulfilled to activate the shading (off-values for hysteresis in parenthesis).

- Total global irradiation on the horizontal is above 300 (200) W/m<sup>2</sup>
- Room temperature must be above 23.8 (22.8) °C
- 24 hours average of the ambient temperature must be above 12 °C

The control of the room temperature is done both in the heating and in the cooling case via a hysteresis control by switching the heat pump (see Fig. 22) on and off. In the heating case

the pump is switched on, when the temperature falls below  $T_{\text{set,h,lo}}$  (21 °C in the base case) and is switched off, when the temperature reaches  $T_{\text{set,h,hi}}$  (22 °C in the base case). The flow rate through the floor heating system is 900 kg/h when the pump is switched on. The control of the flow temperature into the heating system is done depending on the ambient temperature according to a heating curve (radiator exponent 1.1, design flow/return temperature 32/28 °C at  $T_{\text{amb}}=-12$  °C) and the mixing valve HM (see Fig. 22). In the cooling case the pump is switched on when the temperature  $T_{\text{set,c,hi}}$  (25 °C in the base case) is exceeded and is switched off when the temperature  $T_{\text{set,c,lo}}$  is reached (24 °C in the base case). The mass flow rate through the floor heating system is assumed to be the same as in the heating operation. The mixing valve HM sets the flow temperature to constantly 20 °C independently on the ambient temperature.

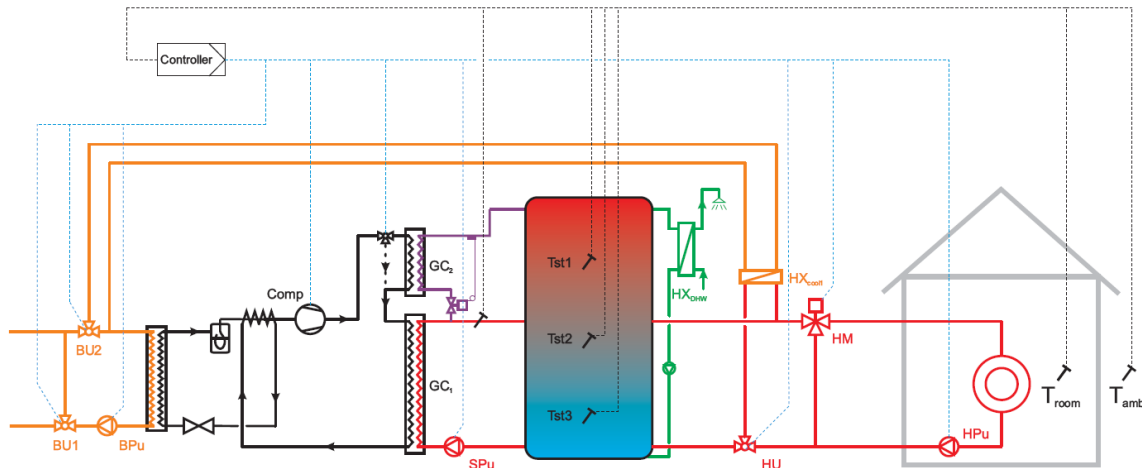


Fig. 22: Sketch of sensors and actors for the system control

The control of the system (heat pump and heating system) is done via a controller, which is integrated into the heat pump model in the simulation. The controller provides the functions of selection of the operation mode, room temperature control and control of the flow temperature dependent on the ambient temperature and charging of the buffer storage. Fig. 22 shows a sketch of the control system configuration. The charging of the buffer storage and the selection of the operation mode is done according to the temperatures measured in the buffer store at the locations  $T_{\text{ST1}}$ ,  $T_{\text{ST2}}$  and  $T_{\text{ST3}}$ . Operation modes are determined according to Fig. 23 left.

The decision which mode shall be used for the current time step is made according to the mode in the last time step and the temperatures in the buffer storage. Fig. 23 shows an overview of the used control logic. The variable “heating\_season” provides the information if the current time step is within the heating season or not. This decision is made depending on the 24-hours-average of the ambient temperature, which has to be lower than 12 °C in order to fulfil the heating criterion.

The charging of the buffer store is done via a hysteresis control. For example mode 1 (DHW preparation) is started when  $T_{\text{ST1}}$  falls below  $T_{\text{set,ST1a}}$  (see Fig. 22). The charging is stopped when  $T_{\text{set,ST1b}}$  is exceeded.

Mode 4 (cooling and DHW preparation) is only started, when the room temperature  $T_{\text{room}}$  exceeds the value  $T_{\text{set,c,hi}}$ , as the heat pump can only be operated when a cooling demand is available (no de-coupling of the heat pump from the floor heating system via the buffer storage as in the heating mode). In mode 5 the heat pump is off, cooling is done solely via the ground collector.

As the heat pump is hydraulically de-coupled from the heating system via the buffer storage, and the charging of the buffer is done only because of the temperatures in the storage, no information about the current heat load is available to the control. Despite of that the heat pump shall be operated with a compressor speed as low as possible for efficiency reasons.

In mode 2 and 3 the control of the compressor speed is done depending on the ambient temperature. The used dependency is shown in Fig. 23. In the DHW mode the compressor is always operated with the minimum speed of 2500 min<sup>-1</sup>, as the DHW draw-offs are – unlike the heating load – not continuous and the available storage volume is large enough to cover large draw-offs (see Fig. 21).

In mode 4 (cooling & DHW) also the minimum compressor speed is used, as the thermal power of the evaporator should normally be higher than the necessary cooling load of the building with the relatively high brine inlet temperatures into the heat pump in this mode.

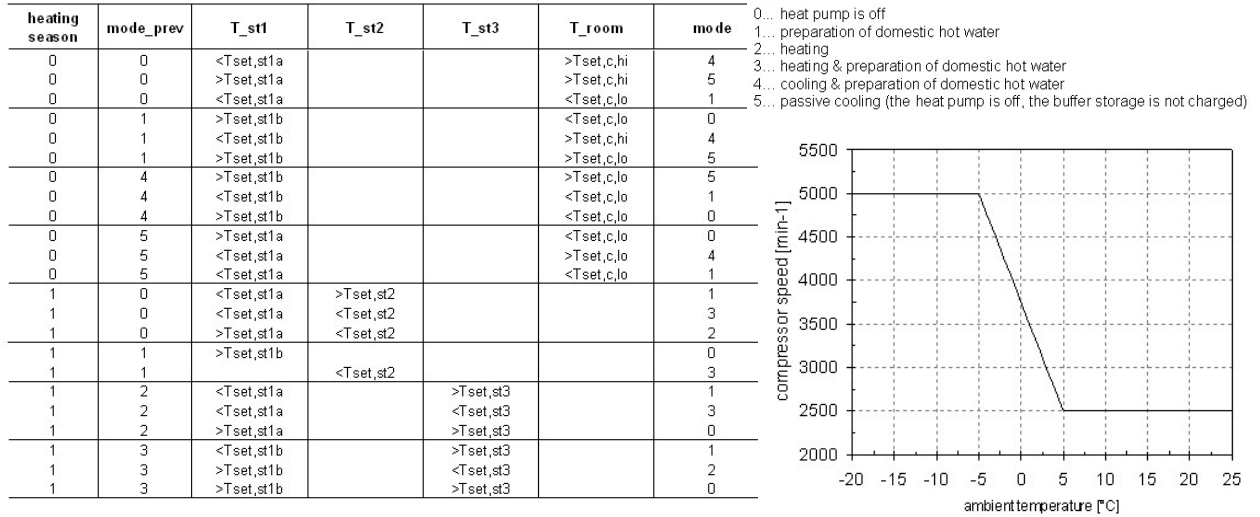


Fig. 23: Operation mode control and compressor control

Description	Value	Unit	Comment
<b>Heat pump</b>			
<i>compressor speed</i>			
heating mode	$f(T_{amb})$	min <sup>-1</sup>	compare Figure 4.5
cooling mode	2500	min <sup>-1</sup>	
T <sub>h2</sub>	T <sub>flow,th</sub> +1	°C	water outlet temperatur at gas cooler 2
<b>Buffer storage</b>			
volume	0.7	m <sup>3</sup>	
<i>relative heights of the connections</i>			
h <sub>HPin</sub>	0	-	
h <sub>GC1</sub>	0.7	-	
h <sub>GC2</sub>	1	-	
h <sub>hf</sub>	h <sub>GC1</sub> -0.05	-	
h <sub>hr</sub>	0.15	-	
h <sub>wf</sub>	1	-	
h <sub>wr</sub>	0	-	
<i>relative heights of the temp. sensors</i>			
h <sub>st1</sub>	(1+h <sub>GC1</sub> )/2	-	
h <sub>st2</sub>	h <sub>GC1</sub> -0.1	-	
h <sub>st3</sub>	0.2	-	
<i>switch points for the charging of the buffer storage</i>			
T <sub>set,st1a</sub>	48	°C	
T <sub>set,st1b</sub>	54	°C	
T <sub>set,st2</sub>	T <sub>flow,th</sub> -1	°C	
T <sub>set,st3</sub>	T <sub>flow,th</sub>	°C	
<b>Cooling mode</b>			
T <sub>cool</sub>	20	°C	flow temperatur into floor heating system
U <sub>A</sub> _HX <sub>cool1</sub>	3000	W/K	heat transfer value of HX <sub>cool1</sub>
T <sub>set,c,hi</sub>	25	°C	upper switch point for room temperatur control
T <sub>set,c,lo</sub>	24	°C	lower switch point for room temperatur control
<b>Heating mode</b>			
T <sub>flow,th</sub>	$f(T_{amb})$	°C	flow temperatur floor heating system (dependant on T <sub>amb</sub> )
T <sub>set,h,hi</sub>	22	°C	upper switch point for room temperatur control
T <sub>set,h,lo</sub>	21	°C	lower switch point for room temperatur control

Fig. 24: Assumptions for the control of components for the base case

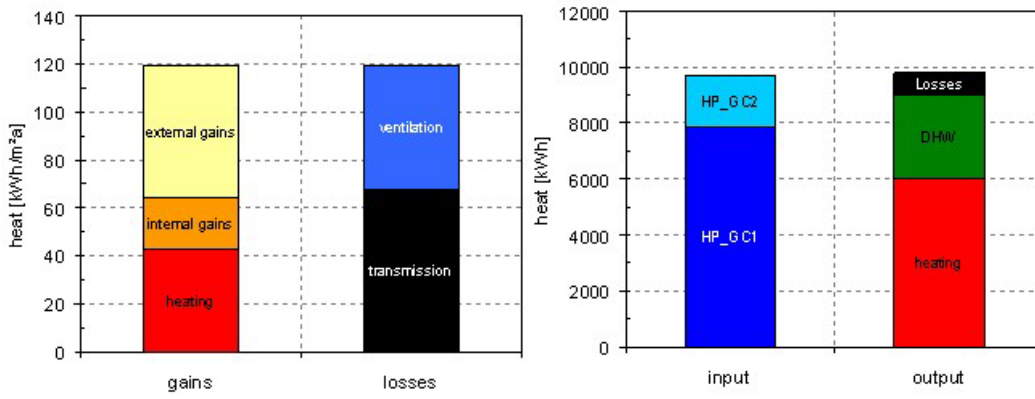


Fig. 25: Heat balance of losses and gains (left) as well as in- and output (right)

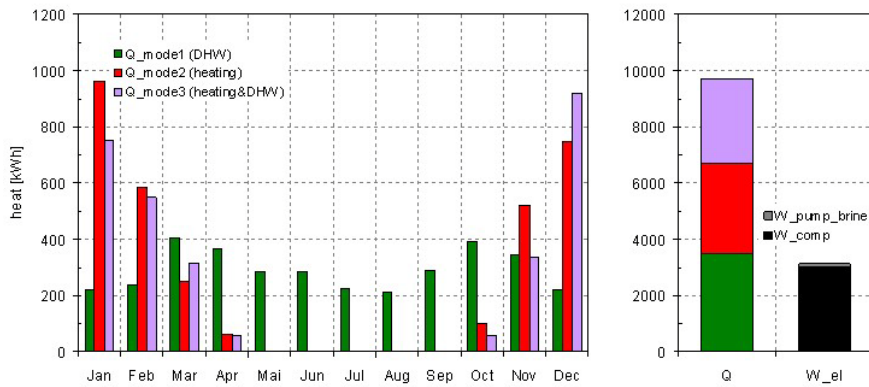


Fig. 26: Heat energy for the different operation modes (left) and electricity (right)

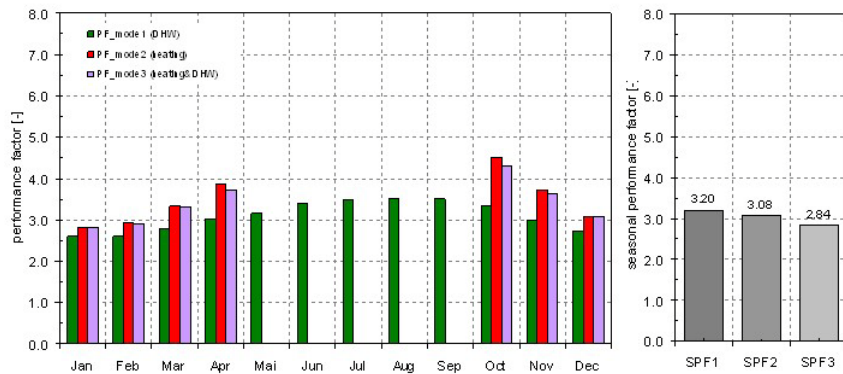


Fig. 27: Performance factors for the different operation modes (left) and seasonal (right)

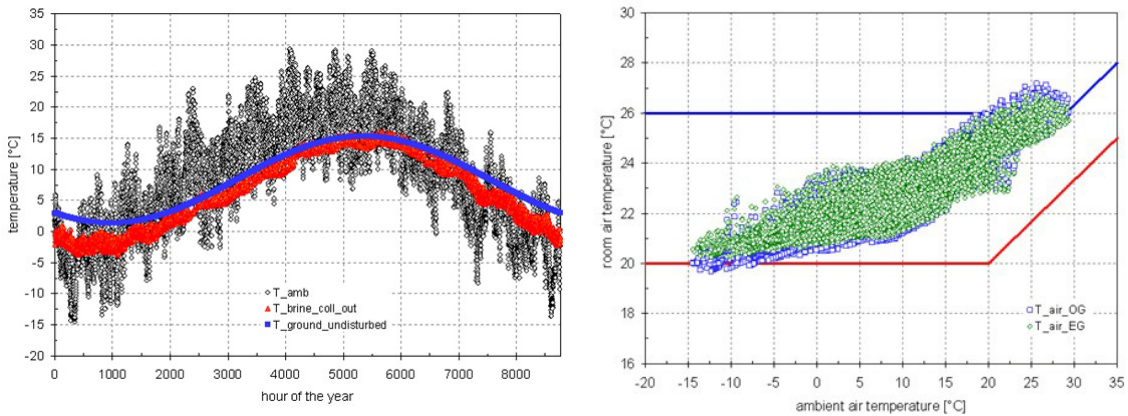


Fig. 28: Ambient and ground temperatures (left) and indoor temperatures (right)

#### 4.4.3 Results of the system simulations

Three seasonal performance factors (SPF) are evaluated. For  $SPF_1$  the heat rejected from the two gas coolers and the evaporator heat in the active cooling mode (mode 4) is divided by the compressors electricity consumption.  $SPF_2$  additionally includes the brine pump electricity. In  $SPF_3$  the delivered energy for floor heating  $Q_{heat}$ , for DHW  $Q_{DHW}$  and for active and passive cooling  $Q_{cool,act}$  and  $Q_{cool,pass}$  are considered, while storage losses - unlike in  $SPF_{1/2}$  - are not considered as delivered energy.

##### 4.4.3.1 Base case without cooling

In this case it is assumed that the building is neither cooled actively (heat pump) nor passively (ground). Fig. 25 shows the annual heat balance of the building. With the used assumptions and the average climate of Graz the heat demand of the building is  $40 \text{ kWh}/(\text{m}^2\text{a})$ . Due to the relatively large windows the solar gains amount to  $55 \text{ kWh}/(\text{m}^2\text{a})$ . The annual heat balance of the buffer store is depicted in Fig. 25. The heat input is provided from the gas coolers  $GC_1$  and  $GC_2$ , whereby approximately 20% are supplied by  $GC_2$ . The heat losses of the storage amount to  $750 \text{ kWh}$  ( $\approx 8\%$ ) of the annual heat input. Fig. 26 shows the monthly and annually heat provided by the heat pump in the different operation modes. About the same amounts of heat are provided in the different modes over the year. An overview of the results for the performance factors of the heat pump are shown in Fig. 27. On the left the monthly performance factors in the different operation modes in the course of the year are depicted. On the right the SPF-values are shown. As expected the performance in the simultaneous heating & DHW mode (mode3) are not much lower than in the heating mode (mode2). The differences in the individual months are on one hand due the heat source (see Fig. 28 left) and in the heating (and simultaneous) mode due to the dependency of the necessary flow temperature for the floor heating system on the ambient temperature. The room air temperatures on the ground floor and the first floor of the building (hourly average values) are shown in Fig. 28 right. The upper and lower limits indicated by the red and blue line in the figure represent the comfort limits for the operative temperature according to DIN 1946-2 (1994). The temperatures required for the heating case can be maintained for almost the whole year except for a few hours, where the heating capacity of the heat pump is a bit too low. Without cooling the room temperatures exceed the range for more than 150 h during the summer months due to the large windows and despite the used shading.

##### 4.4.3.2 Base case with cooling

The annual heat balance of the building with cooling function of the heat pump (mode 4 und 5, see Fig. 23) is shown in Fig. 29 left. The cooling demand of the building is  $\approx 8 \text{ kWh}/(\text{m}^2\text{a})$ . The annual heat balance of the buffer store (see Fig. 29 right) is almost the same as in the case with no cooling. The operative temperatures on the ground floor and the first floor are shown in Fig. 32 right. With the cooling function in operation the limits are not exceeded. Fig. 30 shows the heat provided by the heat pump in the different operation modes at the different months and annually. During the winter months the values for the modes 1 to 3 are quite similar to the case without cooling. During the summer both active and passive cooling is performed, whereby the main part of the cooling load is covered by passive cooling with the ground collector. The value of  $590 \text{ kWh}$  for mode 4 also includes the heat provided for DHW in this mode. The fraction of the cooling energy for the floor heating system in this mode amounts to  $250 \text{ kWh}$ . An overview of the results of the SPF is shown in Fig. 31. The values for mode 4 are relatively high due to the simultaneous use of the hot and the cold side of the heat pump. In the passive cooling mode the values are even higher (values were divided by 10 for the diagram), as here the heat pump is off and only the brine pump is accounted for as operating power. In total the SPFs are higher compared to the case with no cooling, due to the cooling demand which is considered as additional useful energy, which can be seen by comparing  $SPF_2$  to  $SPF_3$ . Fig. 32 left shows the ground temperature in the depth of the ground collector, the brine outlet temperature of the collector for the operation modes where heat is extracted (mode 1-3) and for the passive cooling mode.

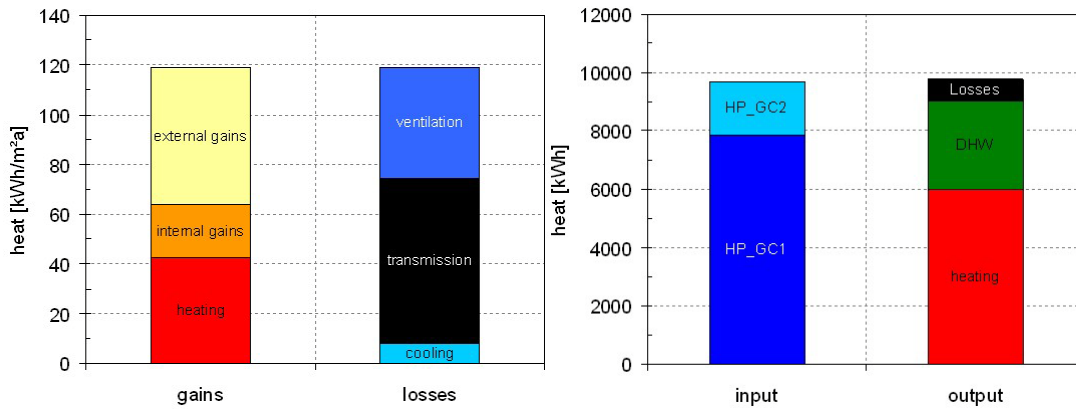


Fig. 29: Heat balance of losses and gains (left) as well as in- and output (right)

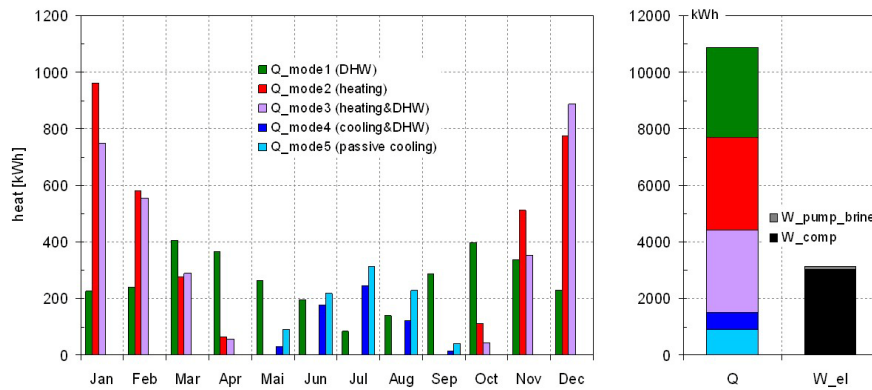


Fig. 30: Heat energy for the different operation modes (left) and electricity (right)

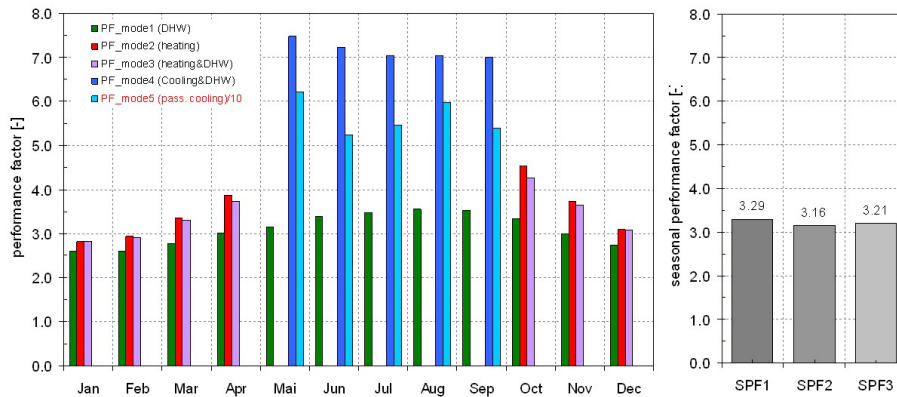


Fig. 31: Performance factors for the different operation modes (left) and seasonal (right)

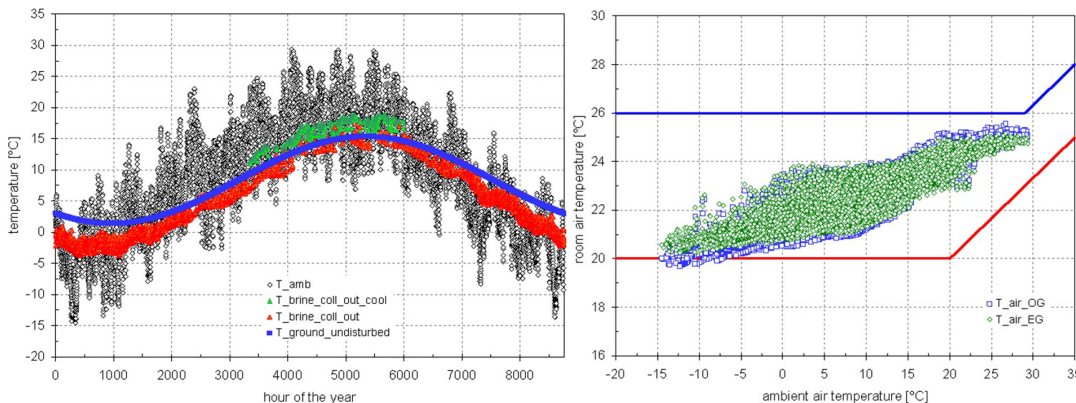


Fig. 32: Ambient and ground temperatures (left) and indoor temperatures (right)

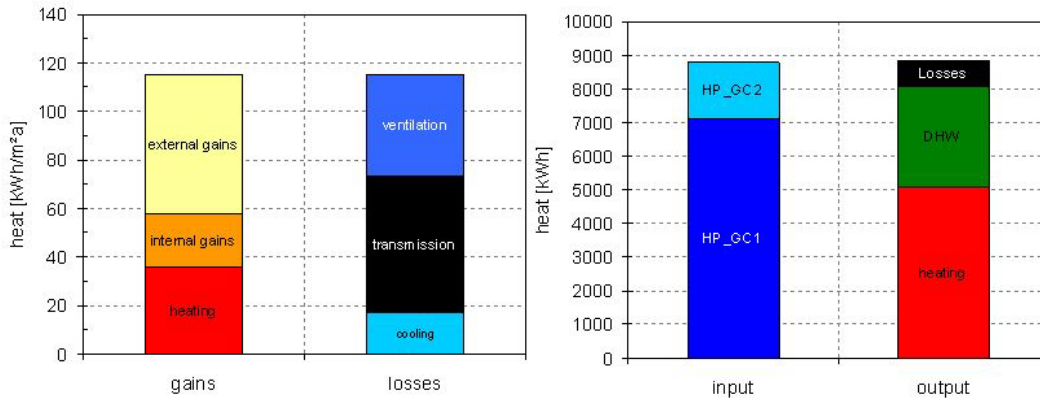


Fig. 33: Heat balance of losses and gains (left) as well as in- and output (right)

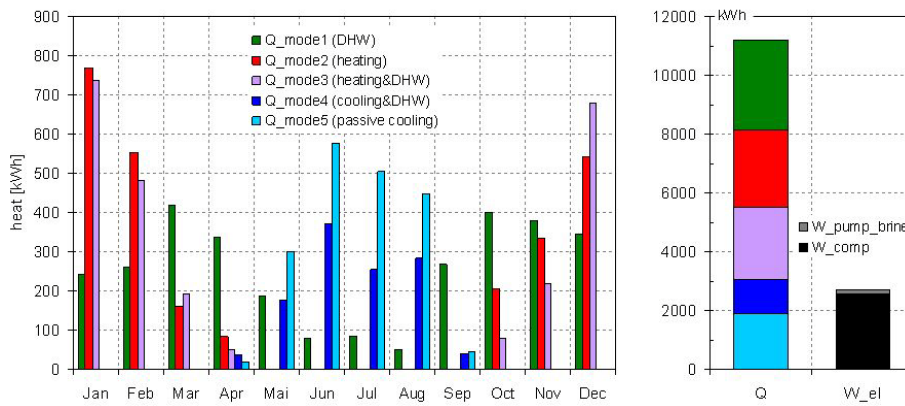


Fig. 34: Heat energy for the different operation modes (left) and electricity (right)

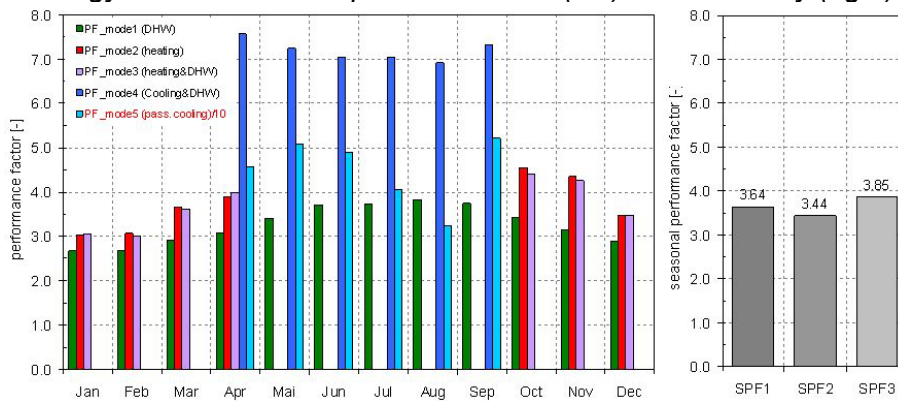


Fig. 35: Performance factors for the different operation modes (left) and seasonal (right)

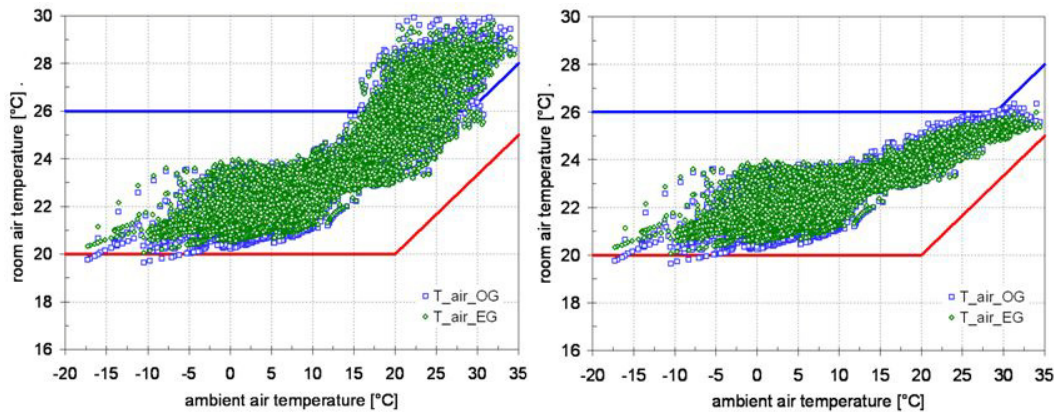


Fig. 36: Indoor temperatures without (left) and with cooling operation (right)

#### 4.4.3.3 Base case with cooling Graz 2003

In order to analyze the performance of the system under warmer climatic conditions, a simulation with a climate data set of the very hot summer 2003 in Graz was performed.

The resulting annual heat balance of the building is shown in Fig. 33 left. The cooling demand is 17 kWh/(m<sup>2</sup>a) and the heating demand 36 kWh/(m<sup>2</sup>a). The annual heat balance of the buffer store is shown in Fig. 33 right.

Fig. 36 right shows the air temperatures in the rooms on the ground floor and the first floor. On the left the temperatures with no cooling of the building are shown. The temperatures are too high for more than 1600 hours during the summer due to the large window areas and despite of the used shading. On the right of Fig. 36 the temperatures with an activated cooling function of the heat pump are shown. Here the temperatures can be kept within the comfort limits.

Fig. 34 shows the heat provided by the heat pump in the different modes of operation at individual months and annually. During the summer both active and passive cooling is performed, whereby the main part of the cooling load is covered passively by the ground collector. The value of 1165 kWh for mode 4 shown in the figure also includes the heat provided for DHW in this mode. The fraction of the cooling energy provided to the floor heating system in this mode amounts to 500 kWh. This means that about 80% of the total cooling demand is covered by passive cooling.

An overview of the results for the performance factors of the heat pump are shown in Fig. 35. With this climate data set the resulting SPF<sub>3</sub> are higher than with the average climate of Graz. This has the following reasons:

- The used climate is warmer than the average climate of Graz (HDD<sub>20/12</sub> 3270 instead of 3500, annual average of ambient temperature 10.6 °C instead of 8.4 °C). Therefore, also the heat source temperatures are slightly higher.
- The cooling demand is much higher, which increases the SPF, as the COP in the cooling modes is relatively high.

Due to the relatively high amount of cooling energy provided passively the SPF<sub>3</sub> is 3.85.

## 4.5 Conclusions and outlook

The analysed system is a promising possibility for the future heat supply of low energy buildings. In order to increase the attractiveness of the system, it would be desirable to increase the efficiency of the refrigerant cycle or the seasonal performance factor, respectively.

Especially the efficiency of hermetic compressors with low capacities, as they are used for heat pumps for low energy buildings, is relatively low. The isentropic efficiency of the compressor directly affects the COP of the heat pump cycle and is therefore very important. Research focused on the improvement of small compressors should be aimed for.

Also the use of an ejector for the recovery of expansion work could improve the efficiency of the heat pump cycle. Investigations for the refrigerant R744 show a potential for the improvement of the COP of 10-20% (Mauthner, 2008).

Optimisations are also still possible concerning the system integration of the heat pump. For example it could be considered to only use the buffer storage for the preparation of DHW, while the heating system is directly connected to the gas cooler of the heat pump. It could be analyzed, whether the system efficiency can be improved by thus reducing the storage losses and by avoiding a heat input from the DHW section of the tank into the space heating section.

The costs of the system at the moment cannot be estimated due to a lack of data concerning the costs of the components of the refrigerant cycle. However, it is assumed that – given a sufficient number of produced units – the price of the system could settle on the level of conventional systems.



## 5 INTEGRATED HEAT PUMP FOR NET ZERO ENERGY HOUSES

### 5.1 Motivation

The project of the United States is dedicated to the development of a highly-integrated heat pump (IHP) for Net Zero Energy House (NZEH) application as a co-operation of the space conditioning program of US governmental Department of Energy (DOE) and the Oak Ridge National Laboratory (ORNL). A motivation for the technology development is the strategic goal of the DOE to have market available net zero energy technology by the year 2020. In so far, the development is intended for future implementation and not for today's markets.

In a detailed scoping study by Baxter (2005) considering various system layout options, the IHP proved to be the most promising system for NZEH, covering the functionality for all building services of space heating (SH), water heating (DHW), ventilation (V), space cooling (SC), humidification (H) and dehumidification (DH). An integrated concept incorporating a heat pump has the advantage of simultaneous production of different building need, e.g. simultaneous SC and DHW in summer operation, while in stand-alone systems, the heat may be wasted. Thereby, higher investment costs of more energy-efficient components like variable speed controlled fans are justified, since they are used for multiple functions.

### 5.2 System concept

The integrated heat pump concept can be realised as air-source and ground-source heat pump. Fig. 40 left shows the basic layout of the air-source and Fig. 40 right of the ground-source IHP. Both layouts are similar, but for the air-source system the ground coil loop including the pump and the heat exchanger are replaced by an outdoor refrigerant-to-air heat exchanger and a variable speed fan.

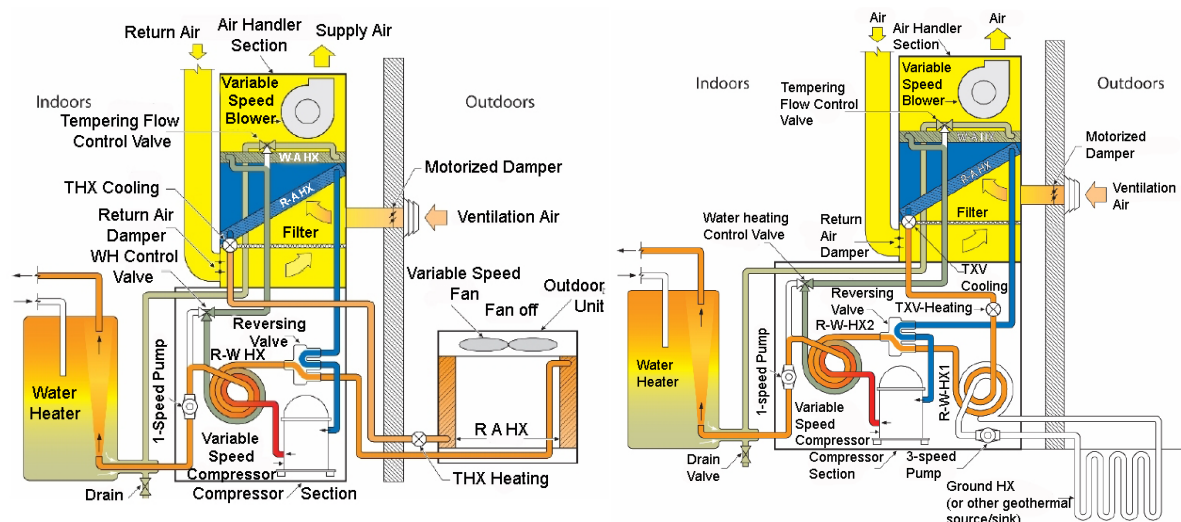


Fig. 37: Air-source IHP (left) and ground-source IHP (right) in dedicated dehumidification and water heating mode (Murphy et al., 2007a)

Fig. 38 left shows the principle of the ground source IHP. Three loops are interacting, one refrigerant, one DHW and one ground heat exchanger. Electrical energy consuming components are one variable speed compressor (C), one variable speed indoor blower (FI) and two pumps – one single speed pump (PI) for the DHW loop and one multiple-speed pump (PO) for the ground heat exchanger loop (GC). Four internal heat exchangers (HX) are included to meet the space conditioning and water heating loads: One refrigerant-to-air (fan coil, HXRAI), one water-to-air (tempering, HXWA), and two refrigerant-to-water (domestic hot water interface, HXRWI, and ground coil interface, HXRWO).

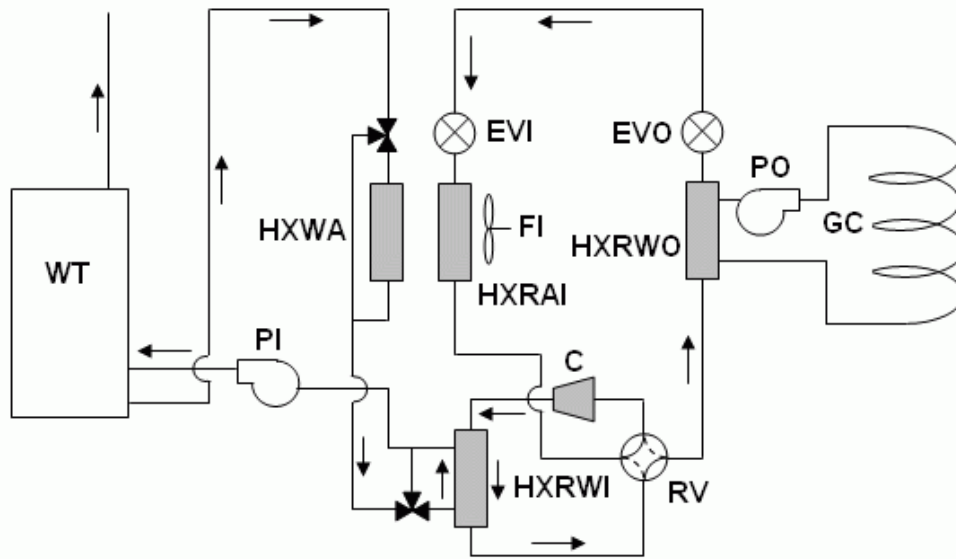


Fig. 38: Ground-source IHP principle shown in simultaneous space cooling/DHW mode

Further components shown are the reversing valve (RV) a refrigerant expansion valve (EV) and depicted as separate indoor (EVI) and outdoor (EVO) expansion valves, which could also be replaced by a single, bi-directional EV. Outdoor ventilation air is drawn through a duct with flow control damper (see Fig. 37), mixed with recirculating indoor air and distributed to the space via the blower, FI. The heat exchanger HXWA (see Fig. 38) uses hot water that is generated by heat recovery in the space cooling and dehumidification modes and stored in the hot water tank (WT), to temper the circulating air stream, as needed, in order to meet space neutral temperature requirements. Modulation of compressor speed and indoor fan speed can be used to control both supply air humidity and temperature as required. With this arrangement, water heating and air tempering is accomplished simultaneously. In detail, the available primary system operating modes corresponding to the loads are:

- space cooling (AC)
- space cooling with enhanced dehumidification (ACEAD)
- space cooling plus water heating (ACWH)
- space cooling with enhanced space dehumidification plus water heating (ACEADWH)
- space heating (AH)
- space heating plus water heating (AHWH)
- water heating (WH)
- dehumidification (AD)
- dehumidification plus water heating (ADWH)
- ventilation (AV)
- ventilation with ventilation air dehumidification (AVVAD)
- ventilation plus water heating (AVWH) and
- outdoor coil defrosting (OCD) (only air-source)

Tab. 3 gives the position or operation state, respectively, of the above described single components of the system concept depending on the operation mode for the AS-IHP and GS-IHP (in blue). Detail on the single operation modes and the control of the components are documented in Murphy et al. (2007a, b). Exemplary, two combined operation modes are described in the following.

Tab. 3: Mode/component matrix of operation of components depending on the mode

Mode	Component										
	C	RV	FO (PO)	FI	air return damper	air ventilation damper	P (PI)	water heating valve	water tempering valve	air resistance element	water resistance element
AC	on	cool	on	on	open	open					
ACEAD	on	cool	on	on	open	open					
ACWH	on	cool		on	open	open	on	open	() bypass		either
ACEADWH	on	cool		on	open	open	on	open	() bypass		either
AH	on	heat	on	on	open	open				either	
AHWH	on	heat	on	on	open either	open either	on	open	() bypass	either	either
WH	on	heat	on		() closed	() closed	on	open	() bypass		either
AD	on	cool	on	on	open	open	on	() bypass	open		
ADWH	on	cool	on ()	on	open	open	on	open	open		either
AV	on ()			on	open	open					
AVVAD	on	cool	on	on	() closed	open	on	() bypass	open		
AVWH (AS-only)	on		on	on	open	open	on	open			either
OCD (AS-only)	on	cool		on	open					either	

Legend: blue – ground-source IHP, black – air-source IHP, () – empty field

### 5.2.1 Dehumidification and water heating mode

When (1) the space relative humidity exceeds the thermostat humidity set point and (2) the lower water storage tank temperature is below its set point, both dehumidification and water heating loads are indicated. In the absence of other indicated loads, as shown in Fig. 37 left, the reversing valve is situated in the cooling position, the return and ventilation air dampers are open, and the heat pump system cools the circulated air and removes moisture from it in proportion to the dehumidification load by varying the compressor, indoor fan, and outdoor fan speeds. In this case, the air moisture removal rate is enhanced by reducing the indoor fan speed relative to the compressor speed. Both water circuit valves are open and the water pump is activated to permit flow through both the refrigerant-to-water HX and the water-to-air HX in the indoor unit. Heat is rejected to the water from the discharge refrigerant and (a smaller amount) rejected by the water to the dehumidified air in the indoor unit to provide re-heat to maintain the thermostat air temperature set point. Water-pump speed may be increased to maximum to provide sufficient water flow for both functions. Refrigerant discharge heat in excess of that which can be absorbed in the refrigerant-to-water HX is rejected by natural convection through the outdoor refrigerant-to-air HX. If the dehumidification load requirement is met before the water heating load requirement, the control system transitions to the water heating mode. If the water heating load requirement is met before the dehumidification load requirement, the control system transitions to the dehumidification mode.

When (1) the lower water storage tank temperature is below its set point and (2) the upper water storage tank temperature is below its set point, a critical water heating load is indicated. In this situation, the control system activates the upper electrical resistance element to minimize the chance of running out of hot water.

### 5.2.2 Space heating (cooling) and DHW

When (1) the space air temperature is below the thermostat heating (cooling) temperature set point and (2) the lower water storage temperature is below its set point, both space heating (cooling) and water heating loads are indicated.

In the absence of other indicated loads the reversing valve is situated in the heating (cooling) position, the return and ventilation air dampers are open, the water valve to the refrigerant-to-water HX circuit is open, the water pump is activated, and the heat pump system provides space heating (cooling) in proportion to the space heating (cooling) load by varying the compressor, indoor fan, and outdoor fan speeds (outdoor fan only activated in heating mode). In this space cooling and DHW mode, the outdoor fan is not active, so that most of the combined heat removed from the indoor air and energy input to the refrigerant from the compressor is transferred to the circulating water (in the refrigerant-to-water HX). The remainder of the heat is rejected by natural convection processes in the refrigerant line set and the

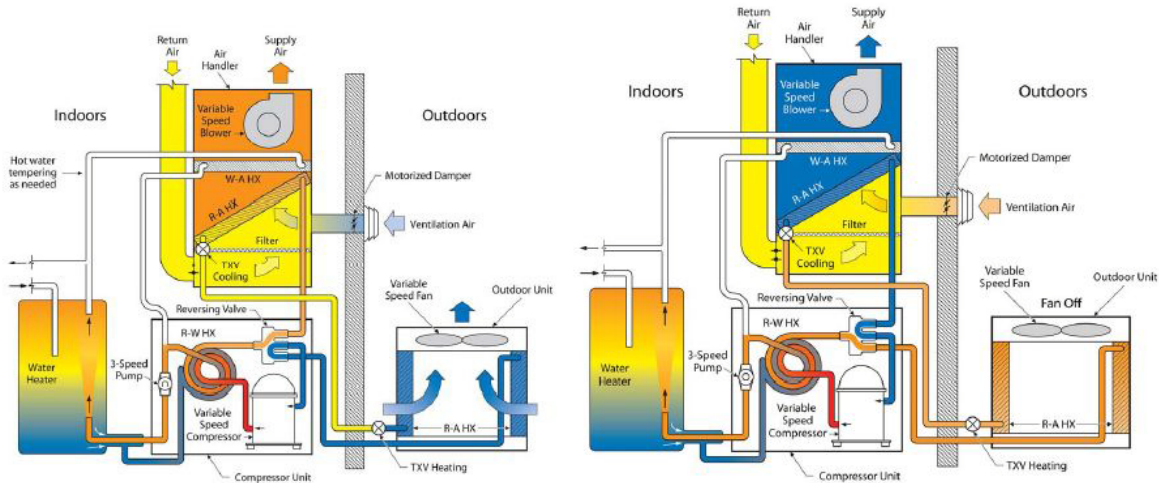


Fig. 39: AS-IHP in combined SH/DHW mode (left) and combined SC/DHW mode (right)

outdoor refrigerant-to-air HX. If the water heating load requirement is met before the space cooling load requirement, the control system transitions to the space cooling mode.

If the space cooling load requirement is met before the water heating mode requirement, the control system transitions to the water heating mode. Critical water heating load is handled as in combined dehumidification and DHW mode.

In space heating/DHW mode the heat rejected from the refrigerant is shared by the space heating (indoor refrigerant-to-air HX) and water (refrigerant-to-water HX) heating loads. The distribution of heat between these two loads depends primarily upon the indoor fan speed, which is controlled to meet the space heating load. As indoor fan speed increases, so does the proportion of rejected heat supplied to the indoor air. The compressor speed is to be set as a prescribed function of outdoor ambient in this mode between minimum and maximum water heating (cooling) speeds with the indoor fan speed providing the control to meet the space heating load. If the space heating requirement exceeds the capacity of the heat pump, the electrical resistance air heaters in the indoor unit are activated to provide supplemental heat, and the water pump is locked out (terminating water heating by the heat pump). In this circumstance, the lower electric resistance heating element in the storage tank is activated to provide water heating. If the water heating load requirement is met before the space heating load requirement, the control system transitions to the space heating mode. If the space heating load requirement is met before the water heating mode requirement, the control system transitions to the water heating mode.

At outdoor temperatures below a specified minimum for space heating operation, the compressor is locked out and both the total air heating load and the total water heating load are met using their respective electrical resistance heating elements. Critical water load are handled in the same way as in case of dehumidification/DHW operation.

### 5.3 Prototype testing

Based on a prototype, lab-testing for different operation modes and test conditions have been carried out. The test rig is depicted in Fig. 40.

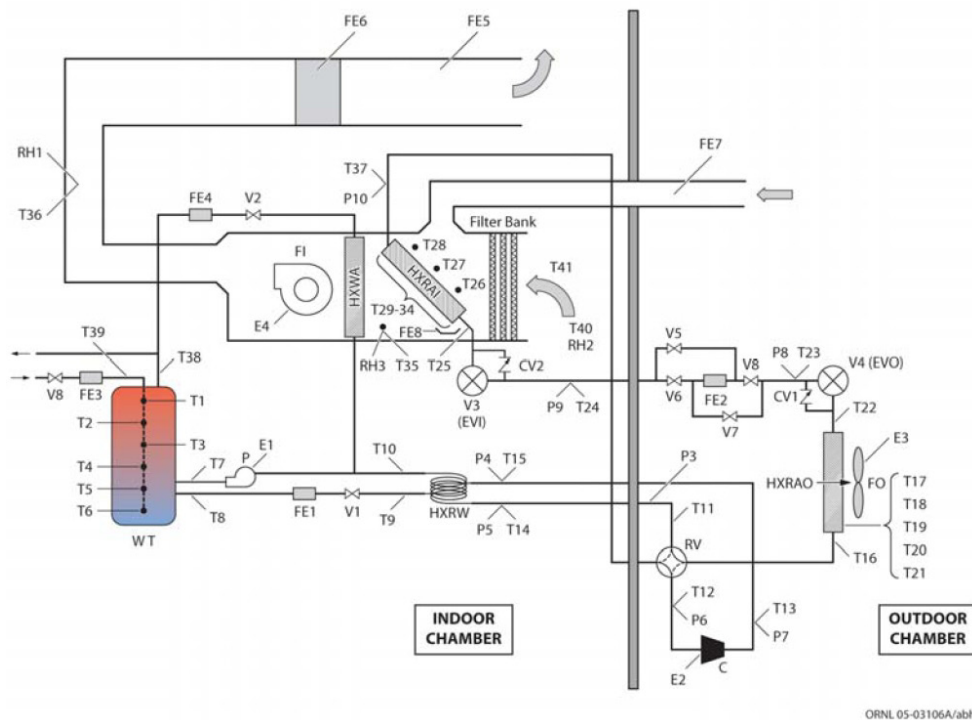


Fig. 40: Instrumentation location diagram of the test rig (T=temperature; P=pressure; FE=flowmeter; E=Power; RH=humidity)

Initial steady-state tests were conducted in cooling mode to determine the most suitable indoor airflow, compressor speed and refrigerant charge at the 35°C ambient design condition. Following these, four tests were conducted at the four outdoor dry bulb temperature (DBT) conditions prescribed for rating variable speed cooling systems in the US. An additional test took place with indoor airflow reduced by 30% to determine the amount of improved dehumidification. The SHR decreased by 10%. Tab. 4 shows the results from these tests.

Tab. 4: Steady-state space cooling performance

Outdoor DBT [°C]	Outdoor fan airflow [m <sup>3</sup> /s]	Indoor DBT/WB [°C]	Indoor Airflow [m <sup>3</sup> /s]	Compressor Speed [Hz]	Cooling capacity [W]	COP or EER [W/W]	SHR
35.0	0.535	26.7/19.4	0.230	79	4363	3.52	0.743
30.6	0.469	26.7/19.4	0.165	58	3147	4.34	0.749
27.8	0.401	26.7/19.4	0.115	36	2115	5.45	0.739
19.4	0.394	26.7/19.4	0.114	36	2185	6.92	0.727
27.8	0.388	26.7/19.4	0.080	36	1961	4.98	0.665

A number of simultaneous space cooling and water heating tests were conducted, as well. For these tests, fixed water temperatures into the tank were maintained. The performance of the IHP in this limited test series illustrates the efficiency advantage of recovering normally rejected heat to provide water heating, with an overall COP (SC and DHW ) of almost 10. Test results are shown in Tab. 5. The indoor return air conditions were 26.7 °C dry bulb temperature (DB)/19.4 °C wet bulb temperature (WB).

Tab. 5: Steady-state space cooling and water heating performance

<b>COP: Space cooling</b>	4.94	5.03	5.05	4.99
<b>COP: Space cooling + water heating</b>	9.45	9.71	9.71	9.62
<b>Water Heating Only COP</b>	4.52	4.68	4.66	4.63
<b>Heat to water [W]</b>	1603	2914	2784	2851
<b>Cooling to space [W]</b>	2071	3124	3013	3072
<b>Sensible heat ratio (SHR)</b>	0.739	0.732	0.775	0.775
<b>Avg. Tank temperature [°C]</b>	28.8	21.7	21.2	22.0
<b>Avg. Compressor power [W]</b>	372.8	569.4	541.3	558.2
<b>Avg. pump power [W]</b>	30.4	28.5	30.6	31.0
<b>Avg. indoor fan power [W]</b>	18.5	26.1	27.3	28.4

Dynamic water heating tests (water heated from starting cold condition to fully heated) were conducted, too. One of the major design considerations with the IHP (and with all water-heating heat pumps) is to accomplish water heating using the compressor without exceeding the compressor discharge pressure maximum imposed by the manufacturer. Example results of this analysis are shown in Fig. 41 right. The envelopes cover acceptable compressor discharge and suction pressures for the R22 variable-speed compressor used in the lab test IHP. The blue envelope covers acceptable conditions for the minimum and maximum compressor speeds - 30 Hz and 100 Hz. The red region contains acceptable compressor conditions in the range 45-90 Hz. It can be seen that compressor discharge and suction pressures remain within the acceptable operating envelope as the tank heats up. Tests were also run to examine the dehumidification performance of the IHP. By design, the IHP dehumidifies the return indoor air then reheats the air by passing hot water from the water tank through the reheat coil. The design point is that with 49 °C inlet water to the tempering coil, there would be sufficient reheating of the air leaving the indoor coil to establish space-neutral conditions.

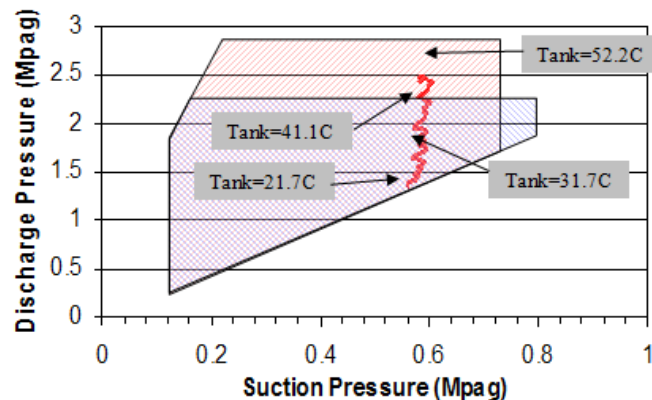


Fig. 41: Tank water heat-up process (red line) superimposed on compressor discharge/suction pressure map

The measurements were used to calibrate the parameters of the DOE/ORNL Mark VI Heat Pump Design Model (Rice and Jackson 2002). The measured refrigerant and indoor air flows were used with a data reduction program to calculate the delivered capacities of system HXs, the heat losses and gains and pressure losses in the connecting lines and to deduce the airflows across the outdoor coil at various fan speeds from the condenser energy balance. The performance map for the lab prototype compressor was adjusted for the effects of inverter efficiency, and reduced speeds based on the measured power and mass flow data. This adjusted compressor map was put into the HPDM and initial predictions of the conducted lab tests. HPDM predictions were compared to the actual lab results and, through an iterative process, the HPDM predictions were calibrated to the range of space cooling and water heating tests performed.

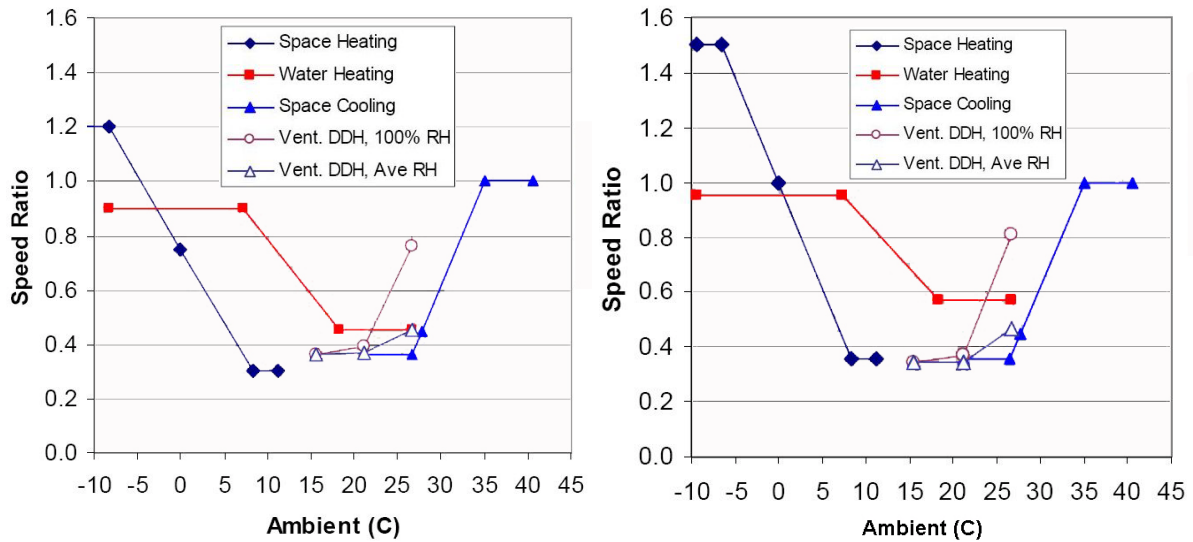


Fig. 42: Target GS-(left) and AS-IHP (right) compressor speed for different operation modes (Vent. – Ventilation, DDH – Dedicated Dehumidification, RH – relative humidity)

Using the calibrated HPDM, IHP design optimization and control assessments were conducted to establish target optimized compressor and fan speed control relationships based on the laboratory R-22 compressor, air-moving, and heat exchanger components. Subsequently a suitable compressor map for a state-of-the-art R-410A variable-speed rotary compressor was obtained and put into the calibrated HPDM. Revised target performance ranges were then established for both the air-source and ground-source IHPs using this preferred HFC refrigerant R-410A. Fig. 42 show the target compressor speed ranges for load tracking control for the air-source and ground-source IHPs, respectively.

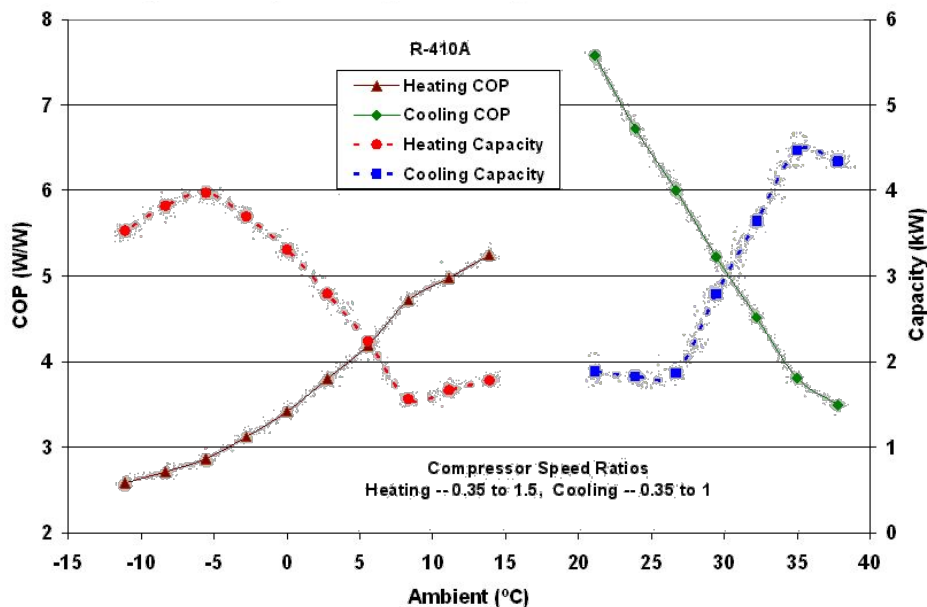


Fig. 43: Target AS-IHP performance vs. equivalent ambients in SH and SC modes

In Fig. 43 target performance of the AS-IHP and in Fig. 44 of the GS-IHP are shown for space heating and cooling for the assumed load tracking behavior. The respective COPs are shown by the solid lines, and the delivered capacities are given by the dotted lines. The points where the trend lines change slope are where the minimum and maximum compressor speeds are reached and the system reverts to ambient trends similar to a single-speed unit, but at minimum and maximum speeds.

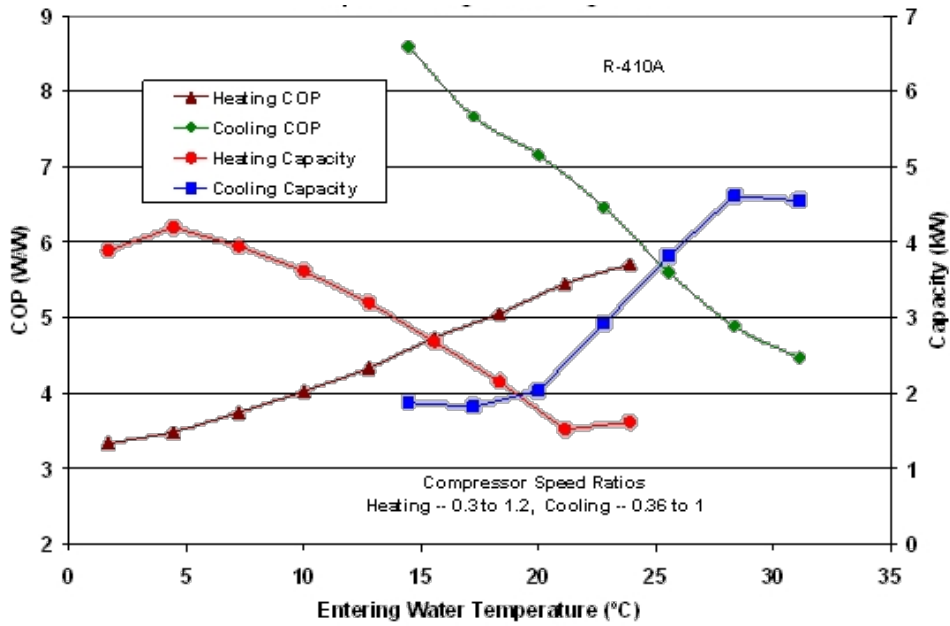


Fig. 44: Target GS-IHP performance vs. equivalent ambients in SH and SC modes

It can be seen from Fig. 43 that the AS-IHP design cooling capacity at 35°C is just over 4.4 kW (1.25 tons). Similarly at the maximum overspeed operation in heating mode, a heating capacity of about 4.0 kW is reached at about -7°C ambient. Typically a single-speed heat pump has about the same heating capacity at 8.3°C as the design cooling capacity and then drops with ambient to a much lower capacity at -7°C, having a similar capacity to the variable-speed system shown here only at the design speed of 79 Hz (speed ratio of 1.0) at 0°C ambient. GS-IHP performance in Fig. 43 is given as a function of equivalent ambient temperature entering water temperature (EWT). The design cooling capacity of 4.4 kW is reached at about 27-28°C EWT. A maximum heating capacity of about 4.2 kW is reached at about 4-5°C EWT. The relationship between EWT and ambient air temperatures is shown (for the Atlanta location) in Fig. 41 right. On average, the heating EWT exceeds the ambient air temperature by about 10°C and is about 6.7°C less than the ambient temperature during the cooling season.

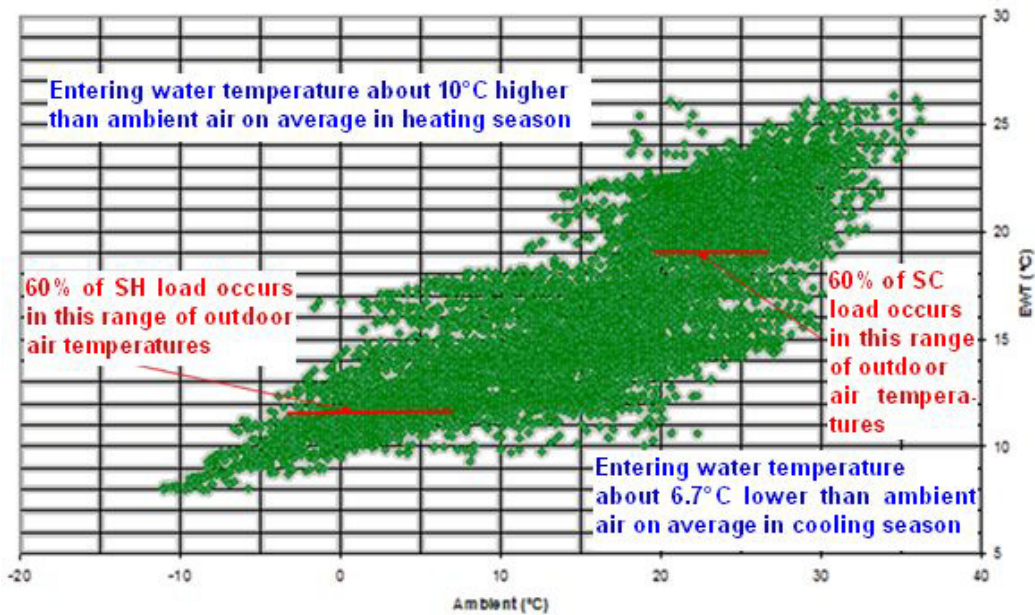


Fig. 45: Correlation of the entering water temperature to the outdoor air (Atlanta)

## 5.4 System simulation results of the prototype system

A sub-hourly analysis tool was needed to most accurately account for the competing IHP operating modes, and representative inlet conditions that will be seen simultaneously by the system heat exchangers (HXs) while heating water. This was accomplished linking the HPDM with TRNSYS. With the HPDM/TRNSYS combination, annual energy simulations have been carried out for the typical climates of the USA: Atlanta (mixed-humid), Houston (hot-humid), Phoenix (hot-dry), San Francisco (marine) and Chicago (cold). The HPDM/TRNSYS model was used to calculate estimates of annual performance (using 3-minute time steps) for three systems installed in a 167 m<sup>2</sup> (1800 ft<sup>2</sup>) ZEH, the AS-IHP, the GS-IHP and a baseline system of same functionality and complying with DOE minimum requirements.

### 5.4.1 Baseline system

A standard split-system A/A heat pump with USDOE-minimum required efficiency (SEER 13 and HSPF 7.7<sup>1</sup>) provides space heating and cooling under control of a central thermostat that senses indoor temperature. It also provides dehumidification (DH) when operating in cooling mode, but does not separately control the humidity. A standard electric storage water heater (WH) with USDOE minimum mandated energy factor (EF=0.90) provides domestic hot water needs. Ventilation meeting the requirements of ASHRAE Standard 62.2-2004 (ASHRAE 2004) is provided using a central exhaust fan. A separate stand-alone dehumidifier (DH) is used to meet house dehumidification needs during times when the central heat pump is not running to provide space cooling. A DH efficiency or energy factor (EF<sub>d</sub>) of 1.4 l/kWh (0.0014 m<sup>3</sup>/kWh) was used based on the USDOE proposed minimum requirement for 2012. A whole-house humidifier (H) accessory was included with the heat pump to maintain a minimum 30% relative humidity (RH) during the winter. Hot water from the WH tank was used for the humidifier supply based on manufacturer specifications for application with heat pumps. The type humidifier adapted for the analyses consumes no power other than a negligibly small amount needed to operate the water flow control solenoid valve.

Baseline system control set points used in the TRNSYS simulation were as follows – 21.7°C ±1.4°C and 24.4°C ±1.4°C for first stage space heating and cooling, respectively; 18.9°C ±1.1°C for second stage space heating (electric back up heater); 48.9°C ±2.8°C for WH; 55% RH ±4% for DH; and 34% RH ±4% for H.

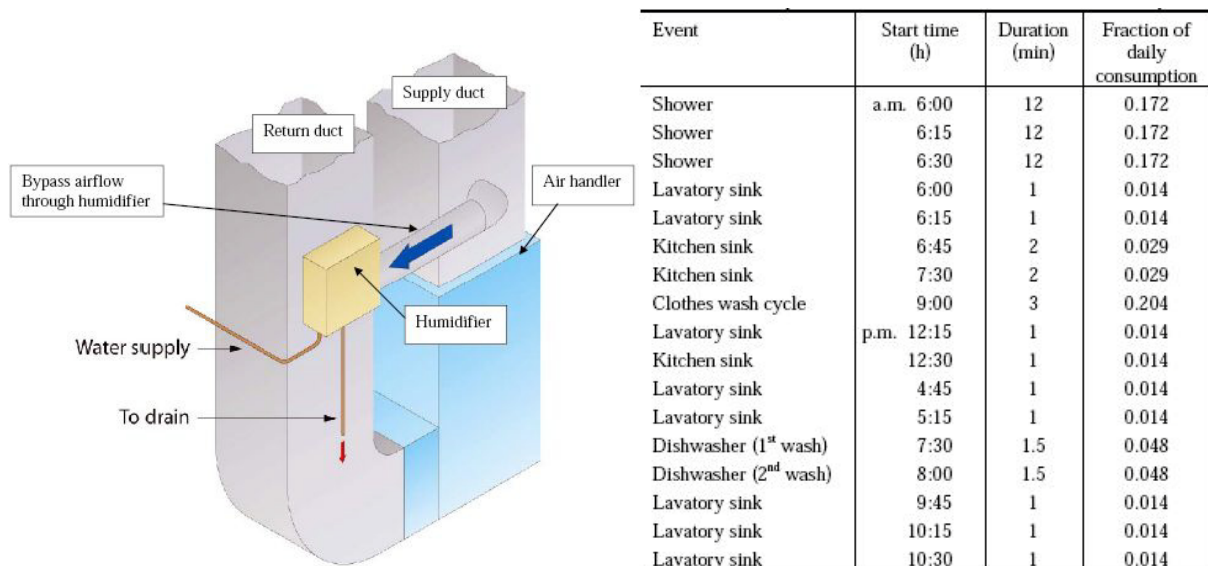


Fig. 46: Integration of humidifier (left) and DHW tapping profile used for the simulation (right)

<sup>1</sup> It has to be considered, that the values are in [(BTU/h)/W]. To compare to European seasonal performance factors the values have to be divided by 3.4134 resulting in an SPF-SH = 2.3 and an SPF-SC = 3.8.

### 5.4.2 GS- and AS-IHP

The air-source IHP, illustrated in Fig. 39, uses one variable-speed (VS) modulating compressor, two VS fans, a single-speed pump, and in total of four HXs (two air-to-refrigerant, one water-to-refrigerant, and one air-to-water) to meet all the HVAC and water heating (WH) loads. A WH tank (same size as for baseline) is included for hot water storage. The same humidifier type as used for the baseline system heat pump was included with the IHP as well. Ventilation (V) air is drawn into the IHP air handler section through a modulating damper as shown.

The set points for 1<sup>st</sup> and 2<sup>nd</sup> stage space heating, space cooling, DH, and H as used for the baseline were also used for the IHPs. For WH, the 1<sup>st</sup> stage (IHP water heating) set point was  $46.1^{\circ}\text{C} \pm 2.8^{\circ}\text{C}$  with a 2<sup>nd</sup> stage set point of  $41.9^{\circ}\text{C} \pm 1.4^{\circ}\text{C}$  to control an electric resistance back-up heating element in the upper portion of the WH tank. The 2<sup>nd</sup> stage WH set point was intentionally set lower than the 1<sup>st</sup> stage set point to maximize the amount of water heating supplied by the IHP.

### 5.4.3 Heat pump model

As first implementation, the HPDM was directly called from TRNSYS. An extensive effort was undertaken to couple the two codes that the outputs of the TRNSYS from modeling the time-dependent ZEH indoor space and water heater conditions would become inputs to the HPDM. In turn, the HPDM output conditions of the indoor air and water leaving the equipment heat exchangers are coupled back to the TRNSYS house and water heater modules to update their operating states. Initially, this was a direct link with the HPDM called at each time step in the appropriate mode of operation. Due to long run times, a second approach was implemented that provided a faster and more robust route.

A map-based approach combined with multi-dimensional interpolation became the basic method applied to facilitate IHP annual performance analyses using the TRNSYS/HPDM linkage. Using the HPDM, performance arrays are generated to encompass the anticipated full range of possible operation. While the number of required calls to obtain close interpolations of IHP performance in all modes was not small, at a few thousand, it is much smaller than the more than 160000 calls needed to call HPDM directly for each simulation time step of 3 minutes. As importantly, once these runs were completed successfully once, the data array could be saved and reused by recall at the outset of successive runs for different climates, or houses, or even control logic strategies. A full set of IHP performance maps is generated at the outset of the TRNSYS simulation run. These performance maps are set up to save all output values (presently numbering 30) that might be needed for linkage to the rest of the TRNSYS equipment and house models.

To specify the heat pump configurations needed for the IHP performance maps five heat pump input data files are used: for space cooling, space heating, space cooling with heat recovery water heating, outdoor source water heating, and ventilation air cooling. Eight parametric input control files, one for each possible mode of IHP operation are used. The parametrics needed for the performance mapping, in addition to compressor speed, are indoor temperature, and relative humidity and outdoor temperature (EWT for GS-IHP) for space cooling modes and outdoor temperature, relative humidity (EWT for GS-IHP) and indoor temperature for space heating. For the water heating modes, the range of possible inlet water temperatures is used in place of outdoor temperature for the combined space cooling mode. For the outdoor source water heating, the inlet water temperature parametric replaces that of the indoor air temperature. In the ventilation air cooling mode, only outdoor temperature and relative humidity are needed.

Full details of the house, controls modeling and the HPDM/TRNSYS linkage approach are given in Murphy, Rice et al. (2007a) and Murphy, Rice et al. (2007b).

#### 5.4.4 Annual energy performance

Tab. 6 provides summary results for the baseline HVAC system for a 167 m<sup>2</sup> ZEH house.

*Tab. 6: Annual site HVAC/WH system energy use and peak with Baseline system*

Location	HP cooling capacity [kW]	HVAC site energy use, [kWh]	HVAC hourly peak demand (W/S/SA)* [kW]
Atlanta	4.40	7230	8.6/4.6/2.1
Houston	4.40	7380	6.1/4.4/2.2
Phoenix	5.28	6518	6.1/3.9/2.1
San Francisco	3.52	4968	5.7/5.6/1.6
Chicago	4.40	10773	9.7/6.1/2.4

\* W – winter maximum; S – summer maximum; SA – summer mid-afternoon (*Tab. 6-Tab. 8*)

Tab. 7 and Tab. 8 provide results for the air-source and ground-source IHPs, respectively, including hourly peak demand in kW for winter and summer (W/S).

*Tab. 7: Estimated annual site HVAC/WH system energy use and peak with air-source IHP*

Location	HP cooling capacity [kW]	HVAC site energy use [kWh]	HVAC hourly peak demand (W/S/SA)*[kW]	Energy savings vs. baseline HVAC [%]
Atlanta	4.40	3349	2.2/1.5/1.2	53.7
Houston	4.40	3418	1.9/1.1/1.1	53.7
Phoenix	5.28	3361	2.1/1.7/1.7	48.4
S. Francisco	3.52	1629	1.8/1.6/0.8	67.2
Chicago	4.40	5865	7.3/1.6/1.0	45.6

For the air-source IHP, the simulation results show between 46-67% energy savings vs. the baseline depending upon location.

For the ground-source IHP, the simulation shows over 50% (52-65%) savings in all locations. Maximum peaks occurred in the winter and generally during 6-8 am (roughly coincident with winter utility peak periods). The water use schedule assumed for the analysis included a significant draw during that time of day for morning showers making electric back-up element activity likely (adding to back-up electric space heating in the colder locales). Maximum summer peaks are somewhat lower and generally occurred during the 6-8 am as well for the same reason.

*Tab. 8: Estimated annual site HVAC/WH system energy use and peak with GS-IHP*

Location	HP cooling capacity [kW]	HVAC site energy use [kWh]	HVAC hourly peak demand (W/S/SA)* [kW]	Energy savings vs. baseline HVAC [%]
Atlanta	4.40	3007	2.0/1.1/1.0	58.4
Houston	4.40	3290	1.8/1.1/1.0	55.4
Phoenix	5.28	2909	1.7/1.2/1.2	55.4
S. Francisco	3.52	1699	1.8/1.6/0.6	65.8
Chicago	4.40	5126	6.9/1.7/0.8	52.4

Summer hourly peaks during the noon-7pm time period (roughly coincident with summer system peak period of most US utilities) were ~1.6-2.4 kW for the baseline system vs. ~0.8-1.7 kW for the AS-IHP and ~0.6-1.2 kW for the GS-IHP.

Fig. 47, Fig. 48 and Fig. 49 give the percental energy savings for the 5 climatic sites and the table in Fig. 49 right presents a comparison of the SPF in the different operation modes.

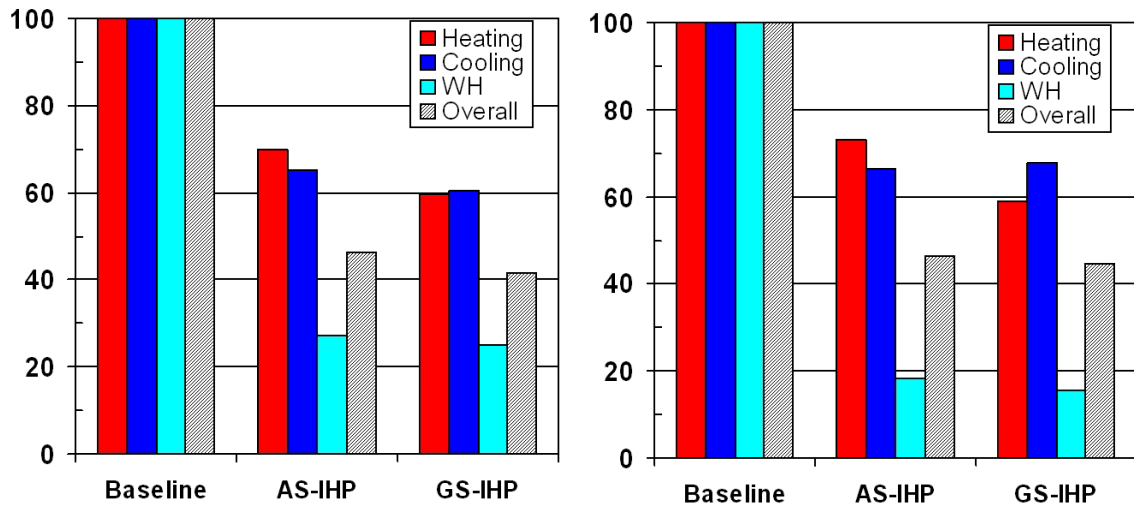


Fig. 47: Simulation results of projected energy savings in different operation modes for Atlanta (left) and Houston (right)

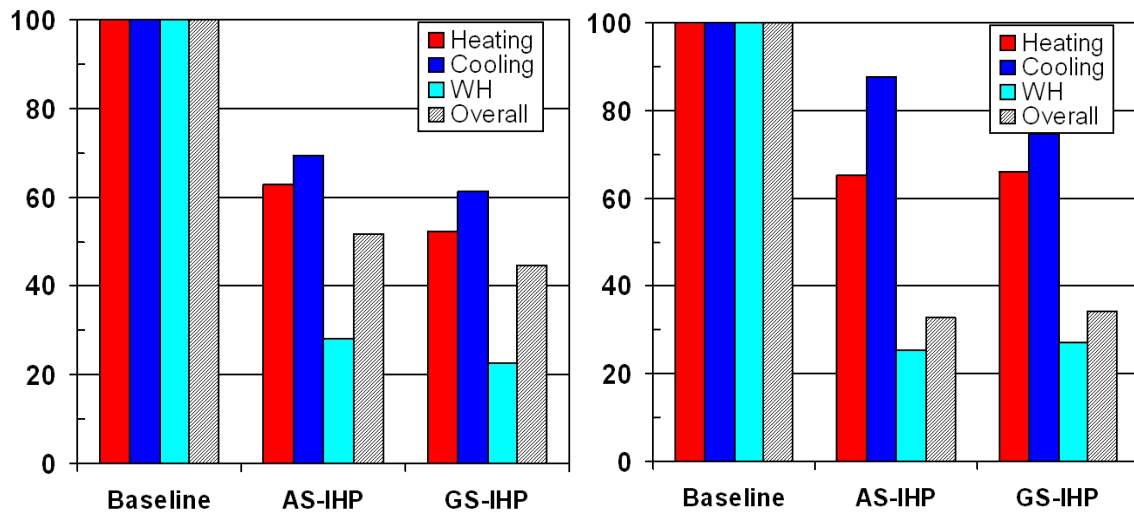
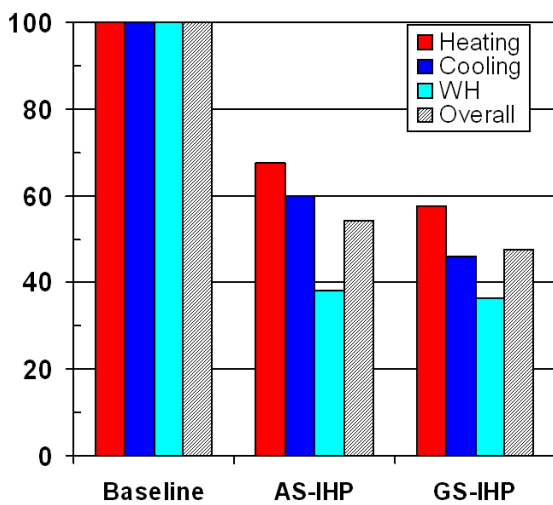


Fig. 48: Simulation results of projected energy savings in different operation modes for Phoenix (left) and San Francisco (right)



Site		Baseline	AS	GS
Atlanta	SH	2.67	3.82	4.48
	SC	3.49	5.34	5.76
	DHW	0.89	3.30	3.57
Houston	SH	2.73	3.73	4.64
	SC	3.48	5.24	5.13
	DHW	0.89	4.84	5.75
Phoenix	SH	2.95	4.70	5.66
	SC	2.94	4.25	4.79
	DHW	0.89	3.56	4.42
San Francisco	SH	3.09	4.75	4.68
	SC	3.38	3.83	4.63
	DHW	0.90	3.55	3.31
Chicago	SH	2.10	3.10	3.65
	SC	3.50	5.85	7.61
	DHW	0.89	2.32	2.44

Fig. 49: Simulation results of Chicago (left) and calculated seasonal performance factors in all five locations

Tab. 7: AS-IHP and GS-IHP performance vs. baseline system in ZEH

Loads (167-m <sup>2</sup> ZEH from TRNSYS)		Equipment				
		Baseline	AS-IHP		GS-IHP	
Source	kWh	Energy use, kWh (I <sup>2</sup> r)	Energy use, kWh (I <sup>2</sup> r)	Energy reduction compared to baseline	Energy use, kWh (I <sup>2</sup> r)	Energy reduction compared to baseline
<b>Atlanta (mixed-humid)</b>						
Space Heating	4775	1789 (51)	1251	30.1%	1066	40.4%
Space Cooling	5735	1643	1073	34.7%	996	39.4%
Water Heating	3032	3402	924 (142)	72.8%	855 (144)	74.9%
Dedicated DH	158	208	82	60.4%	73	64.9%
Ventilation fan	-	189	20	89.6%	17	90.9%
<b>Totals</b>	<b>13701</b>	<b>7230</b>	<b>3349</b>	<b>53.7%</b>	<b>3007</b>	<b>58.4%</b>
Humidifier water	499 kg		618 kg		647 kg	
<b>Houston (hot-humid)</b>						
Space Heating	1766	648	474	26.9%	381	41.1%
Space Cooling	9927	2853	1894	33.6%	1936	32.1%
Water Heating	2505	2816	556 (91)	80.2%	477 (76)	83.1%
Dedicated DH	704	875	482	44.9%	484	44.7%
Ventilation fan	-	189	12	93.7%	11	94.3%
<b>Totals</b>	<b>14902</b>	<b>7380</b>	<b>3418</b>	<b>53.7%</b>	<b>3290</b>	<b>55.4%</b>
Humidifier water	75 kg		87 kg		89 kg	
<b>Phoenix (hot-dry)</b>						
Space Heating	1580	535	336	37.1%	279	47.9%
Space Cooling	9759	3317	2296	30.8%	2038	38.6%
Water Heating	2189	2477	696 (19)	71.9%	560 (1)	77.4%
Dedicated DH	-	-	-	na	-	-
Ventilation fan	-	189	33	82.7%	32	83.1%
<b>Totals</b>	<b>13527</b>	<b>6518</b>	<b>3361</b>	<b>48.4%</b>	<b>2909</b>	<b>55.4%</b>
Humidifier water	170 kg		229 kg		240 kg	
<b>San Francisco (marine)</b>						
Space Heating	2881	932	607	34.8%	616	33.9%
Space Cooling	88	26	23	12.5%	19	25.3%
Water Heating	3387	3767	957 (100)	74.6%	1025 (203)	72.8%
Dedicated DH	42	54	11	80.3%	10	80.6%
Ventilation fan	-	189	32	83.2%	28	85.2%
<b>Totals</b>	<b>6398</b>	<b>4968</b>	<b>1629</b>	<b>67.2%</b>	<b>1699</b>	<b>65.8%</b>
Humidifier water	34 kg		38 kg		29 kg	
<b>Chicago (cold)</b>						
Space Heating	11425	5448 (1415)	3686 (614)	32.3%	3133 (293)	42.5%
Space Cooling	2550	729	436	40.1%	335	54.0%
Water Heating	3807	4286	1644 (327)	61.6%	1568 (371)	63.4%
Dedicated DH	94	121	83	31.9%	75	38.0%
Ventilation fan	-	189	17	91.1%	15	92.2%
<b>Totals</b>	<b>17877</b>	<b>10773</b>	<b>5865</b>	<b>45.6%</b>	<b>5126</b>	<b>52.4%</b>
Humidifier water	1369 kg		1639 kg		1721 kg	

### 5.4.5 Economic analysis

Along with the performance analyses above, a preliminary assessment of the system costs and payback for the IHPs vs. the baseline has been completed as well. Murphy et al. (2007b) provides full details of the cost estimation.

Tab. 9: Estimated installed costs of baseline HVAC/WH system (2006 US dollars)

City	HP cooling capacity [kW]	HP cost	DH cost	WH cost	V cost	H cost	Total cost
Atlanta	4.40	\$3'985-4'590	\$415	\$503	\$305	\$200	\$5408-6013
Houston	4.40	\$3'985-4'590	\$415	\$503	\$305	\$200	\$5408-6013
Phoenix	5.28	\$3'995-4'628	\$415	\$503	\$305	\$200	\$5418-6051
San Francisco	3.52	\$3'974-4'578	\$415	\$503	\$305	\$200	\$5397-6001
Chicago	4.40	\$3'985-4'590	\$415	\$503	\$305	\$200	\$5408-6013

Tab. 9 provides the baseline system costs and Tab. 10 the estimated cost for the AS IHP along with its energy cost savings and estimated simple payback of 5-10 years vs. the baseline.

Tab. 10: Estimated installed costs and payback for air-source IHP (2006 US dollars)

City	Electricity price [\$/kWh]	HP cooling capacity [kW]	Total cost [\$]		Premium over baseline system [\$]		Energy cost savings/Year [\$]	Simple payback over baseline system, [yr]	
			low	high	low	high		low	high
Atlanta	0.0872	4.40	7'582	8'786	2'174	2'773	338	6.4	8.2
Houston	0.108	4.40	7'582	8'786	2'174	2'773	428	5.1	6.5
Phoenix	0.0896	5.28	7'596	8'862	2'178	2'811	283	7.7	9.9
S. Francisco	0.1196	3.52	7'568	8'762	2'171	2'761	399	5.4	6.9
Chicago	0.0844	4.40	7'582	8'786	2'174	2'773	414	5.2	6.7

For the ground-source IHP a vertical bore ground HX (GHX) configuration was assumed. Results are given in Tab. 11. Installed cost in 2006 US\$ of the GHX (including connection to the IHP package) was estimated at ~\$16.40/m (\$5/ft) of bore.

Tab. 11: Estimated installed costs and payback for ground-source IHP (2006 US dollars)

City	Electricity price [\$/kWh]	HP cooling capacity [kW]	Total cost [\$]		Premium over baseline system [\$]		Energy cost savings/year [\$]	Simple payback over baseline system [yr]	
			low	high	low	high		low	high
Atlanta	0.0872	4.40	8'671	9'748	3'263	3'735	368	8.9	10.1
Houston	0.108	4.40	8'671	9'748	3'263	3'735	442	7.4	8.5
Phoenix	0.0896	5.28	9'410	10'549	3'992	4'498	323	12.3	13.9
S. Francisco	0.1196	3.52	8'657	9'724	3'260	3'723	391	8.3	9.5
Chicago	0.0844	4.40	8'511	9'588	3'103	3'575	477	6.5	7.5

Tab. 12 gives the estimated bore lengths for a vertical GHX in each of the five cities as derived from long-term sizing runs using the TRNSYS/HPDM model. Sizing was based on limiting the long-term entering water temperature (EWT) to the IHP from the GHX to a maximum of 35°C during cooling operation in all cities.

For heating operation, the long-term minimum EWT criteria was 5.6°C (using water as the GHX fluid) for all cities except Chicago where the minimum EWT criteria was -1.1°C (using a 20% propylene glycol brine solution).

Tab. 12: Estimated total bore lengths and installed costs for vertical GHXs (2006 US dollars)

City	Total bore length [m]	Installed cost [\$]
Atlanta, Houston, San Francisco	110	1800
Phoenix	154	2525
Chicago	100	1640

## 5.5 Proposed concept design specifications

Based on the research and development done by ORNL to date, design specifications are provided, along with a recommended control strategy. It should be noted that all R&D conducted thus far for the IHP has been aimed at the ZEH. As the marketplace moves toward ZEH-type residences, smaller, more efficient space-conditioning and water-heating systems that can accommodate not only customary loads, but also new active ventilation and dehumidification requirements, will be needed. The relatively large number of current two-story houses with multiple smaller heat pumps might provide a nearer-term market that could induce manufacturers to produce such “futuristic” equipment, especially for “early adopters.” If these trends intersect with international component cost reduction trends observed in variable-speed, high-efficiency equipment, and with the increasing cost, capacity, and emissions pressures associated with the world energy production markets, the residential AS-IHP (Fig. 1) and GS-IHP (Fig. 2), may fill a substantial and valuable niche in the energy-efficiency arsenal. However, to achieve penetration in the current housing market, whose houses differ from the ultimate ZEH goal, modifications to these recommendations to produce a product optimized for the current market will be needed. These modifications may include elimination of some functions and substitution of less expensive components to produce a simpler, less-expensive product for initial market penetration. Work with manufacturing partners towards this latter goal is underway.

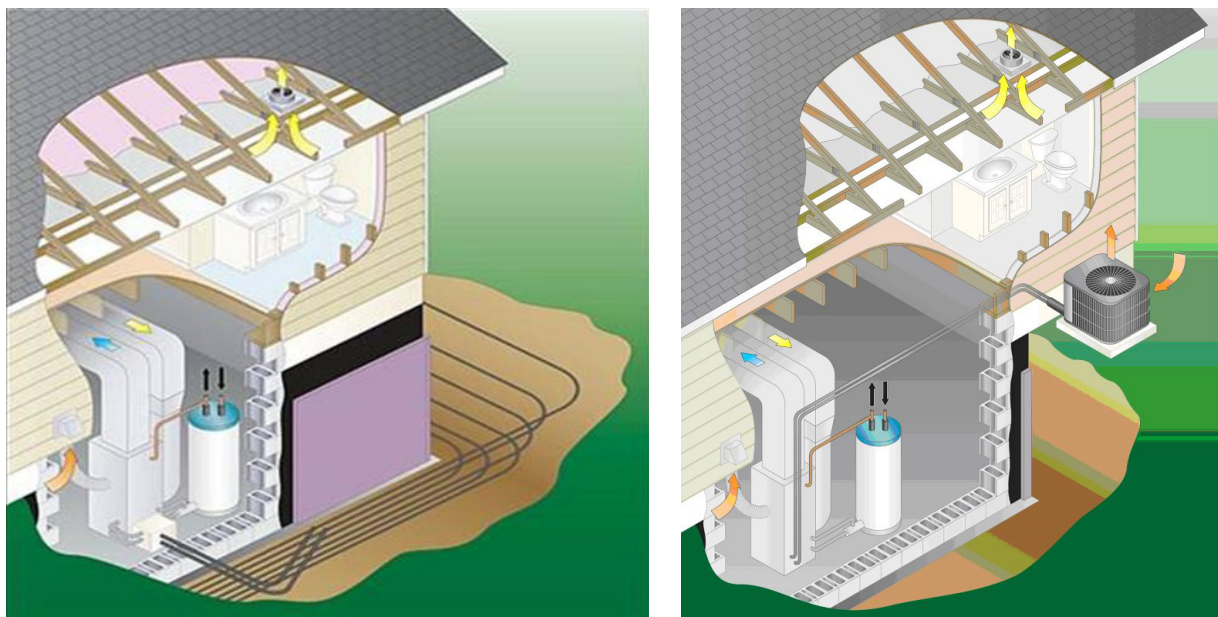


Fig. 50: Conceptual installation of the GS-IHP (left) and AS-IHP in ZEH (right)

Salient features of both IHP types as embodied in this study include a variable speed rotary compressor incorporating a brushless direct current permanent magnet motor which provides all refrigerant compression, a variable speed fan for the indoor section, and a single-speed pump for water heating operation. The AS-IHP includes a variable speed fan for the outdoor section as well, while the GS-IHP includes a multiple-speed ground coil circuit pump. A viable embodiment of the AS-IHP design for a net ZEH application is suggested to be a split-system air-source heat pump consisting of two main sections as illustrated in Fig. 37 left: an indoor section with compressor and indoor air handler (could be split into two sections) and an outdoor air handler section. Provision may be made to accommodate additional operating modes such as an outside air economizer mode, if deemed cost-effective in meeting performance goals. In the following, design specifications of the single components are described.

### **5.5.1 Refrigerant Compressor (C)**

The concept requires a high-efficiency, hermetic, variable-speed motor/compressor. A suggested option is a rotary compressor with an electronically commutated, BDC-drive motor with a permanent magnet rotor. A minimum R-410A compressor-only COP of 3.3 at ARI air-conditioning rating conditions (ARI 1999) at 60 Hz is recommended. The rated capacity at 60 Hz (3600 rpm) is 2.9 kW to obtain the 4.4 kW design cooling capacity at the 79-Hz design cooling frequency with R-410A. The suggested variable speed ranges to approach the energy savings potential in chap. 5.4.4 are at least 2.8 to 1 in SC, 2.0 to 1 in DHW and 3.6 to 1 in SH, e.g. a maximum speed range of 28 to 100 Hz was available in a laboratory prototype with applied speeds of 28 to 79 Hz SC, 45 to 90 Hz in DHW, and 28 to 100 Hz SH. A higher maximum speed in SH mode up to 118 Hz, a 4.2 to 1 speed range, is recommended to obtain better heating season performance, as shown in the earlier analysis for the prototype R-410A system.

### **5.5.2 Indoor Fan (FI)**

The concept requires a high-efficiency, variable-speed motor/fan combination. A suggested option is a centrifugal fan driven directly by an integral electronically commutated motor with pulse-width-modulation (PWM) speed control. The suggested variable speed range is at least 3.5 to 1 with constant airflow control capability.

### **5.5.3 Outdoor Fan (FO)**

The concept requires a high-efficiency, variable-speed motor/fan combination. A suggested option is a multi-bladed propeller fan driven directly by an integral electronically commutated motor with PWM speed control. The suggested variable speed range is at least 2.0 to 1.

### **5.5.4 Refrigerant-to-Water Heat Exchanger (HXRWI)**

The suggested arrangement is counterflow, helical, tube-in-tube with a single refrigerant circuit in the annulus and a single water circuit in a central convoluted water tube. Water-side pressure drop should be no more than 20 kPa at 12 liters/min water flow. The UA heat transfer rating at maximum water heating speed and 7 liter water flow should be not less than 570 W/K to give 4.1 kW of water heating at 8.3°C outdoor ambient temperature. The construction must be double-walled, vented, and approved for potable water use. Suitable provision must be made for either prevention of water-side fouling or access to surfaces subject to such fouling for periodic maintenance cleaning.

### **5.5.5 Water-to-Air Heat Exchanger (HXWA)**

The suggested arrangement is a perpendicular (relative to the air flow) coil using copper tubing with aluminium fins. The minimum recommended UA heat transfer rating for this coil is 43 W/K. Suitable provision must be made for either prevention of water-side fouling or access to surfaces subject to such fouling for periodic maintenance cleaning.

#### **5.5.6 Indoor Refrigerant-to-Air Heat Exchanger (HXRAI)**

The suggested arrangement is a sloped (relative to the air flow) coil using grooved copper tubing with enhanced aluminium fins. The minimum recommended UA heat transfer rating for this coil is 425 W/K at design cooling conditions.

#### **5.5.7 Outdoor Refrigerant-to-Air Heat Exchanger (HXRAO)**

The suggested arrangement is a wrap-around coil using copper tubing with enhanced aluminium fins. The minimum recommended UA heat transfer rating for this coil is 750 W/K at design cooling conditions.

#### **5.5.8 Electrical Resistance Water Heating Elements**

Both lower and upper electrical resistance water heating elements are recommended to have 4.5 kW heating capacity at 230 VAC.

#### **5.5.9 Domestic Water Pump (PI)**

A single-speed potable water pump rated for 45 kPa pressure lift at 12 litres/min for duties up to 95°C. 1000 kPa working pressure is suggested.

#### **5.5.10 Hot Water Storage Tank (WT)**

An insulated potable hot water storage tank with a minimum capacity of ~180 litres is recommended.

#### **5.5.11 Other components**

One or two expansion valves (EVO and EVI) are required for refrigerant flow/expansion control. A reversing valve (RV) is required to shift refrigerant flow direction between cooling and heating mode functions. Two water flow control valves are required to direct water flow either through or around the water heating heat exchanger (HXRWI) and the water-to-air tempering coil (HXWA). The implementation is by means of a two-position bypass valve for the HXRWI (either full through flow or full bypass flow) and a variable position valve for the HXWA (continuous range from full through flow to full bypass flow) to permit control of the temperature of the air exiting this device.

#### **5.5.12 Components GS-IHP**

Most of the components for the GS-IHP are identical as those for the AS-IHP except the outdoor heat exchanger and fan are replaced with a second water/refrigerant heat exchanger (HXRWO) and a multiple speed water/antifreeze circulation pump, respectively. A single equipment package containing all components and to be located in an indoor mechanical room is suggested as illustrated in Fig. 37 right.

#### **4.11.4.1 Ground Coil Interface Refrigerant-to-Water Heat Exchanger (HXRWO)**

A tube-in-tube helical heat exchanger is used, consisting of an inner single-wall fluted tube surrounded by an outer smooth tube. Water (or an antifreeze/water mixture) flows inside the inner wall of the fluted tube while refrigerant passes through the annulus formed. The arrangement is counter-flow for modes in which the device acts as a refrigerant condenser (e.g. SC mode) and co-flow when it acts as a refrigerant evaporator (e.g. SH mode). The minimum recommended UA heat transfer rating for this coil is 750 W/K at design cooling conditions.

#### **4.11.4.2 Ground Coil Loop Pump (PO)**

A multiple-speed (2-3 discrete speeds) or variable-speed circulator pump suitable for operation with water or water/antifreeze solution is required. Suggested design specifications for maximum speed operation are 80 kPa pressure lift at 15 litres/min.

## 5.6 Conclusions and Outlook

Following conclusions and recommendations of a further in-depth analysis are highlighted (Murphy et al. (2007a) and Murphy et al. (2007b))

### 5.6.1 Conclusions

1. The GS-IHP system (using R410A) is estimated to achieve >50% energy savings vs. the baseline system used in the study in all locations including Chicago. These predicted savings are obtained with active humidity control applied throughout the year.
2. For a scenario of a \$1000 system tax credit combined with a favorable time-of-use + demand utility rate structure, simple payback of the IHP systems vs. the baseline system in the ZEH fall to about 1.5 to 3 years for the AS-IHP and 2.5-5 years for the GS-IHP, respectively.
3. Using a Solid Water Sorbent-enhanced horizontal ground heat exchanger requiring no additional trenching beyond that required for water supply or sewer piping, the estimated first cost of the GS-IHP is reduced to about the same as that for the AS-IHP and base scenario simple paybacks are about 4 to 8 years.
4. Desuperheating operation with the GS-IHP and AS-IHP was found not to be beneficial compared to the currently employed alternative water heating approaches. Elimination of the desuperheater allows use of a single-speed water pump reducing the cost, simplifies the controls and results in much lower pump run time.
5. A new approach was developed for the domestic hot water loop of the IHP that reduces the maximum condensing temperatures when simultaneously tempering indoor air and water heating, uses lower temperature water to accomplish indoor air tempering, and simplifies the water tank connections.
6. Modification to the IHP control logic in winter to assign priority to water heating (over space heating) significantly improved overall IHP efficiency and energy savings.

### 5.6.2 Recommendations

1. Implementation and analysis of split condenser operation in the winter heating mode is needed to assess the benefits of simultaneous space heating and water heating operation. The same analysis capability can be used as needed to look further at possible dual condenser operation in cooling mode to reduce condensing temperatures under low speed cooling operation where compressor head pressure capabilities are more limited.
2. Consideration should be given to obtaining further water heating by cooling the compressor with water leaving the indoor water-to-refrigerant heat exchanger. This would boost the water temperatures returning to the DHW tank with compressor shell heat loss without raising condensing temperatures and could provide a beneficial means to cool the compressor motor under the elevated head pressures seen with full condensing water heating.

### 5.6.3 Field monitoring

Field monitoring of the ground-source heat pump will start in summer 2010 in at least 2 research houses. Field tests of the air-source heat pump will follow, starting in the end of 2010. Field test are carried out by the Zero Energy Building Research Alliance (ZEBRAAlliance) which besides the ORNL comprises also a local utility, an architecture office and local home builders (TVA and Schaad).

Besides the evaluation of the field operation of the IHP types other technologies will be tested in the research houses such as different variants of thermal insulation, a interior utility wall which includes all the supply and return lines for water air and electricity as well as a foundation ground heat exchanger.

Fig. 51 gives an overview of the intended field monitoring and the test houses. More details on the test houses and the field test are given on a System Concept sheet.

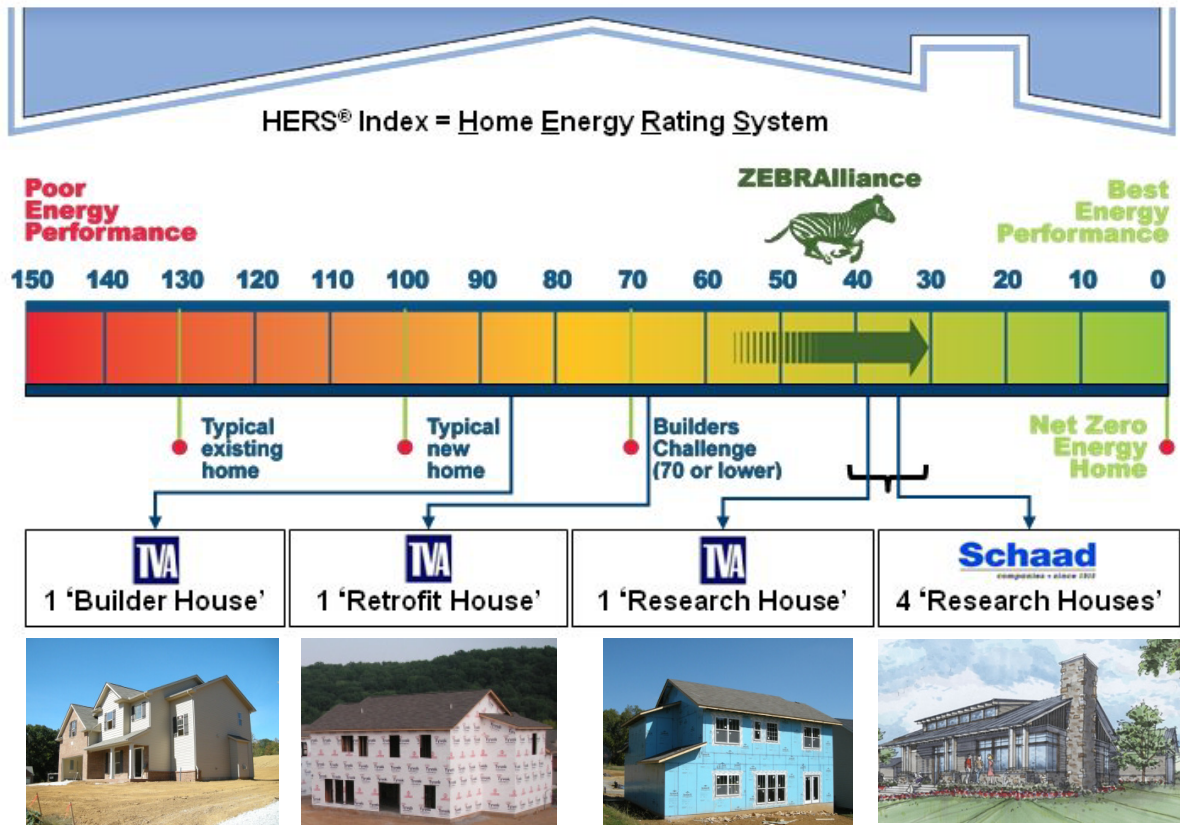


Fig. 51: Overview of intended field tests





The heat pump is connected to a high-temperature (HT) DHW storage tank and a low-temperature (LT) accumulator tank by means of two water loops with pumps and non-return valves. The LT accumulator tank is connected to the space heating system. According to EN378 an *indirect system design* is required for DHW (HT) tank since propane (flammable working fluid) is used as the working fluid. Both tanks have integrated heat exchanger coils in stainless steel (OD/ID 18/15 mm, L 26 m).

The main components for the integrated heat pump unit are:

- *Evaporator* – SWEF brazed PHE B15-10, 0.36 m<sup>2</sup>, height/width 6.5
- *Condenser* – SWEF brazed PHE B15-10, 0.36 m<sup>2</sup>, height/width 6.5
- *Desuperheater* – SWEF brazed PHE B8-10, 0.23 m<sup>2</sup>, height/width 4.3
- *Suction gas heat exchanger* – SWEF brazed PHE, B5-10, 0,12 m<sup>2</sup>, height/width 2.6
- *Compressor* – Danfoss SC15CNX, single-stage, hermetic piston, 2900 rpm, 15.28 cm<sup>3</sup>
- *Expansion valve* – Danfoss TUA R22, thermostatic with internal pressure equalization

The heat pump unit is equipped with a suction gas (internal) heat exchanger which increases the discharge gas temperature from the compressor and with that increases the superheat and the average temperature during heat rejection without increasing the condensation temperature/pressure. This is favourable for a heat pump which supplies heat to a low-energy or passive house where the high-temperature DHW demand typically constitutes 50 to 80% of the total annual heating demand of the house.

Fig. 53 shows, as an example, the temperature changes for the working fluid in the heat pump unit at 0/50 °C evaporation/condensation temperature, 30 K compressor superheating, 2 K pressure loss in the evaporator/condenser and 65% isentropic efficiency for the compressor (Zijdemans, 2007).

Due to the application of the suction gas heat exchanger, the heat quantity rejected in the desuperheater at 75 °C average temperature is about 40% of the condenser capacity at 50 °C. The lower the evaporation temperature and the higher the condensation temperature, the larger is the superheat.

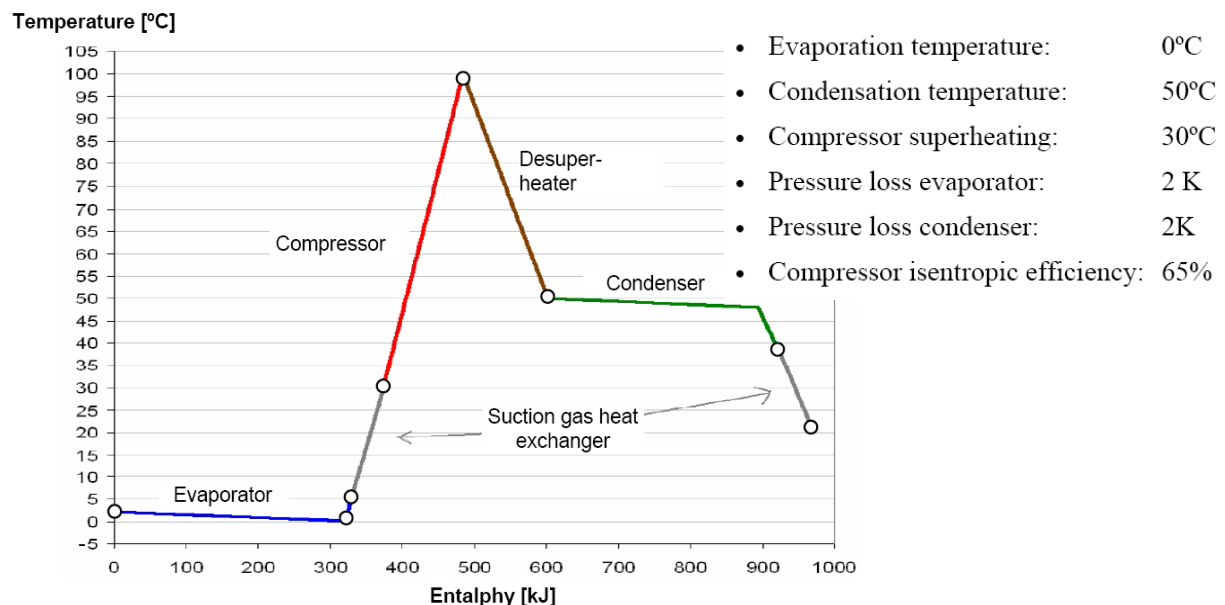


Fig. 53: Sample temperatures of the propane heat pump cycle

## 6.3 Results of prototype component testing

Propane (R290, C<sub>3</sub>H<sub>8</sub>) is being used as working fluid since it is a natural fluid with negligible GWP and excellent thermophysical properties. All necessary components for the heat pump unit are available in the required capacity range from leading manufacturers. Since propane is a highly flammable fluid (AIT<sup>2</sup> 470°C, LEL/UEL<sup>3</sup> 2.1/9.5%) and the total charge for the prototype unit is about 250 g (i.e. > 150 g), the heat pump system has been designed as follows:

- Indirect, closed system design for the heat pump unit with indirect closed water loops for heat rejection to the high-temperature DHW storage tank and the floor heating system
- Installation of the heat pump unit in a gas-tight cabinet (IP 20) which is vented to the ambient and equipped with a leak detector (type NC) – visual alarm
- Only soldered joints for the heat pump unit inside the cabinet, no flare couplings
- Ex-proof low-pressure and high-pressure controllers (IP 44)
- Gas-tight cabinet for the electrical equipment (IP 20)

Fig. 54 shows the heat pump (left), the cabinet for the electrical equipment (middle) and the two storages (right).



Fig. 54: Prototype heat pump, cabinet for the electrical equipment and storage tanks

### 6.3.1 Operating Modes – Operational Strategy

The prototype water-to-water propane heat pump system is designed to operate in three main operating modes (ref. principle sketch, Fig. 52):

- Domestic hot water (DHW) heating only
- Space heating only
- Combined mode – space heating and domestic hot water (DHW) heating

---

<sup>2</sup> AIT – Auto Ignition Temperature

<sup>3</sup> LEL – Lower Explosion Limit, UEL – Upper Explosion Limit

The compressor and the circulation pumps for the HT and LT water loops are controlled by a programmable digital control unit (PLS). Temperature sensors are placed about 300 mm above the bottom in the HT and LT storage tanks. Tab. 13 shows the main control strategies in "hot water mode", "space heating mode" and "combined mode":

Tab. 13: Main control strategies in the different heating modes for the prototype heat pump system.

Heating mode	Compressor operation	HP pump	LT pump	Operation – description
<b>Domestic hot water (DHW) mode</b> – no space heating demand	On	On	Off	When the water temperature in the HT storage tank drops below e.g. 50 °C, the compressor and the circulation pump in the HT water loop start. The compressor and the pump are stopped when the temperature reaches the set-point, e.g. 60 °C. Both the condenser and the desuperheater are active during operation in the hot water mode. During tapping of domestic hot water (DHW) from the 300 litre HT storage tank, the cold city water (5 to 10 °C in Norway) is circulated through the heat exchanger coil in the 300 litre LT storage tank and preheated to about 30 °C, before it is reheated by the heat exchanger coil in the HT tank
<b>Space heating mode</b> – no DHW heating demand	On	Off	On	When the water temperature in the LT storage tank drops below e.g. 30 °C, the compressor and the circulation pump in the LT water loop start. The compressor and the pump are stopped when the temperature reaches the set-point, e.g. 35 °C. Only the condenser is active during operation in the space heating mode since the HT pump is switched off.
<b>Combined heating mode</b> – both space heating and DHW heating demand	On	On	On	The compressor and the pumps for the LT and HT circuits are switched on. Both the condenser and the desuperheater are operative. As in DHW mode, the DHW is preheated in the LT tank by condenser heat.
<b>No heating demand</b>	Off	Off	Off	The entire heat pump unit is switched off

In order to control/limit the maximum discharge temperature from the compressor, the suction gas heat exchanger is equipped with a by-pass and a magnetic valve. When the exhaust gas temperature exceeds the maximum allowable temperature level (approx. 100 °C), the magnetic valve opens.

Since the supply water for the floor heating system is circulated *from the top* of the low-temperature (LT) storage tank, the supply temperature will always be in the required range, even during periods when there is a considerable hot water demand, i.e. at large city water flow rates (5-10 °C) through the heat exchanger coil in the LT storage tank.

### 6.3.2 Instrumentation

The prototype heat pump system has been instrumented as follows (ref. principle sketch, Fig. 52)

- *Heat flow meters* (Kundo/G20 volume flow meter + temperature Pt1000 sensors) for the space heating system (LT tank), preheating of DHW (LT tank) and reheating of DHW (HT tank)
- *Electric power/energy meters* for the compressor only and for compressor and pumps
- *Temperature sensors* (Pt100) for the heat source, heat pump unit (miscellaneous) and ambient air

### 6.3.3 Laboratory Testing

The prototype heat pump system has been tested in the laboratory at the Norwegian University of Science and Technology (NTNU). The test in space heating mode was carried out in accordance with the requirements in the European standard EN 14511, "Air conditioners, Liquid Chilling Packages and Heat Pumps with Electrically Driven Compressors for Space Heating and cooling".

Tab. 14 shows the main results from the laboratory test. Due to limitations in the test rig, the lowest water temperature for the heat source was 8.1 °C and not 5.0 °C as stated by EN 14511 (Zijdemans, 2007).

Tab. 14: Test results of the prototype unit testing according to EN 14511 (Zijdemans, 2007).

Heat source		Heat sink		Heating capacity [W]	COP [-]
Inlet [°C]	Outlet [°C]	Inlet [°C]	Outlet [°C]		
8.1	5.2	30.1	34.8	2281	4.2
8.1	5.3	35.7	40.0	2091	3.9
8.2	5.6	41.0	45.1	2018	3.6
10.3	7.2	30.2	35.0	2330	4.4
10.2	7.2	35.5	40.0	2197	4.1
10.1	7.2	40.6	45.2	2202	3.8
15.1	11.6	29.6	34.9	2578	4.8
15.2	11.7	34.9	40.0	2479	4.4
15.0	11.8	40.1	45.1	2406	4.1

The calculated *Carnot efficiency*,  $\eta_C^4$  for the prototype heat pump unit ranged from approx. 0.30-0.40 and 0.45-0.50 when including and excluding the heat exchanger losses, respectively.

Since the performance of the condenser, desuperheater, suction gas heat exchanger and compressor were in the same order of magnitude as the simulated values, it was concluded that the main reasons for the relatively low COP and low Carnot efficiency were *the poor performance of the evaporator and unstable superheat control for the expansion valve*.

<sup>4</sup> ( $COP = COP_C \cdot \eta_C$ ) where COP is the real Coefficient of Performance of the heat pump,  $COP_C$  is the Coefficient of Performance for a reversed Carnot Cycle (reference heat pump cycle) and  $\eta_C$  is the Carnot efficiency

- The average heat transfer coefficient (U-value) of the evaporator was only 50% of the calculated value, and this is most likely caused by a low average liquid-to-vapour velocity. By using a plate heat exchanger with a smaller cross sectional area and larger thermal length (larger height-to-width ratio), the heat transfer efficiency would have been improved.
- The superheat for the evaporator ranged from about 5 to 16 K, and the instability was due to bad thermal contact between the sensor bulb and the tube wall. By using thermal pasta between the tube and the sensor, and valve is now operating satisfactorily (Zijdemans, 2007).

## 6.4 Heat pump field testing in a low energy house

The prototype water-to-water propane heat pump system has been installed in a pilot house, which has a total floor area 172 m<sup>2</sup>. The residence meets the German passive house standard with regard to air-tightness and U-values for the floor, walls and roof. However, since the windows have a higher U-value than required by the passive house standard, the house can be characterized as a combined low-energy/passive house. Fig. 55 shows a photo and a drawing of the house (Zijdemans, 2007).

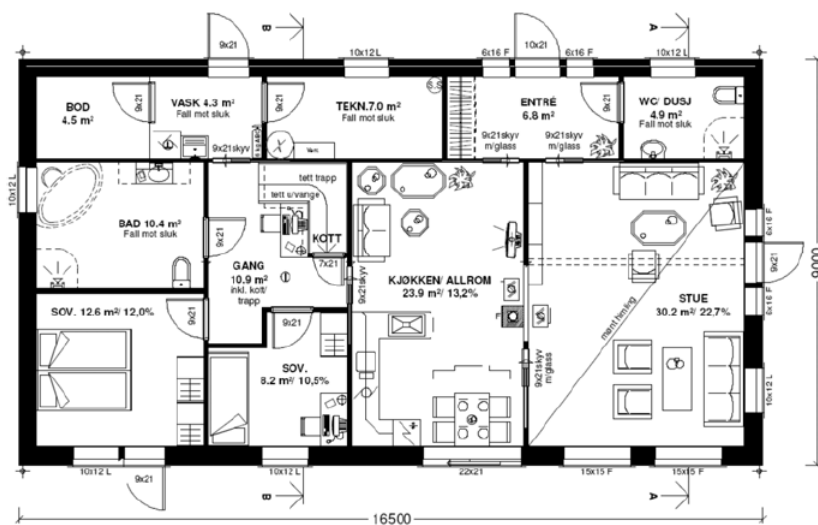


Fig. 55: The 172 m<sup>2</sup> low-energy pilot house in Flekkefjord, Norway (Zijdemans, 2007).

The heat source for the prototype heat pump system is lake water with a temperature that normally fluctuates between 5 and 15 °C during the year (direct heat source system). The calculated thermal power and energy demands for the low-energy/passive house are listed in Tab. 15 (Zijdemans, 2007):

Tab. 15: Calculated thermal power and heating demands for the 172 m<sup>2</sup> pilot house.

Heating demand	Power (W)	Heat (kWh/year)	Specific (kWh/m <sup>2</sup> year)
Space heating	2,400	3,800	20
Hot water heating	500	2,650	15
Total	2,900	6,450	35

The calculated (estimated) total specific energy demand for the house is about 89 kWh/(m<sup>2</sup>year).

Fig. 56 shows the calculated (estimated) net heating demand duration curve for the pilot house, i.e. the thermal power demand for space heating and hot water heating during the entire year. The areas under the curves for “Space heating” and “Total demand” represent the total annual space heating demand and the total annual heating demand for space heating and hot water heating, respectively (Zijdemans, 2007).

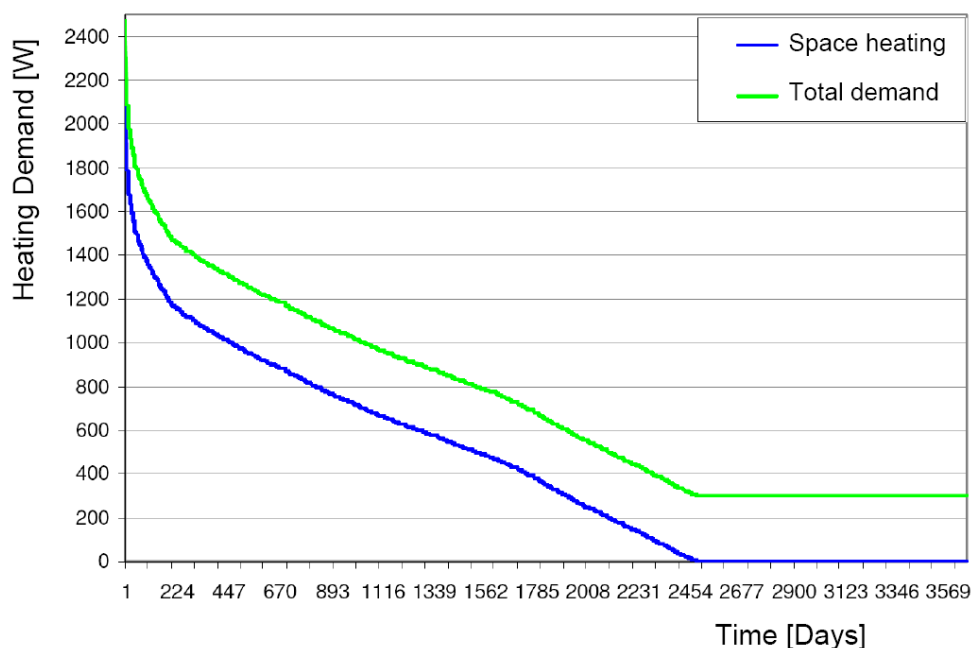


Fig. 56: Estimated heating demand duration curve for the pilot house (Zijdemans, 2007).

The supply water temperature (set-point) for the floor heating system is controlled by a three-way valve. The heat supply to the different rooms is controlled by solenoid valves (on/off) which are controlled by room thermostats.

#### 6.4.1 Field Testing – Measurements and Discussion

The prototype water-to-water propane (R290) heat pump system was installed in the pilot house July 2007, and has been monitored from September 2007 to April 2010 (2.5 years). The measurements have been carried out and prepared by Peter Leendert Zijdemans and David Zijdemans.

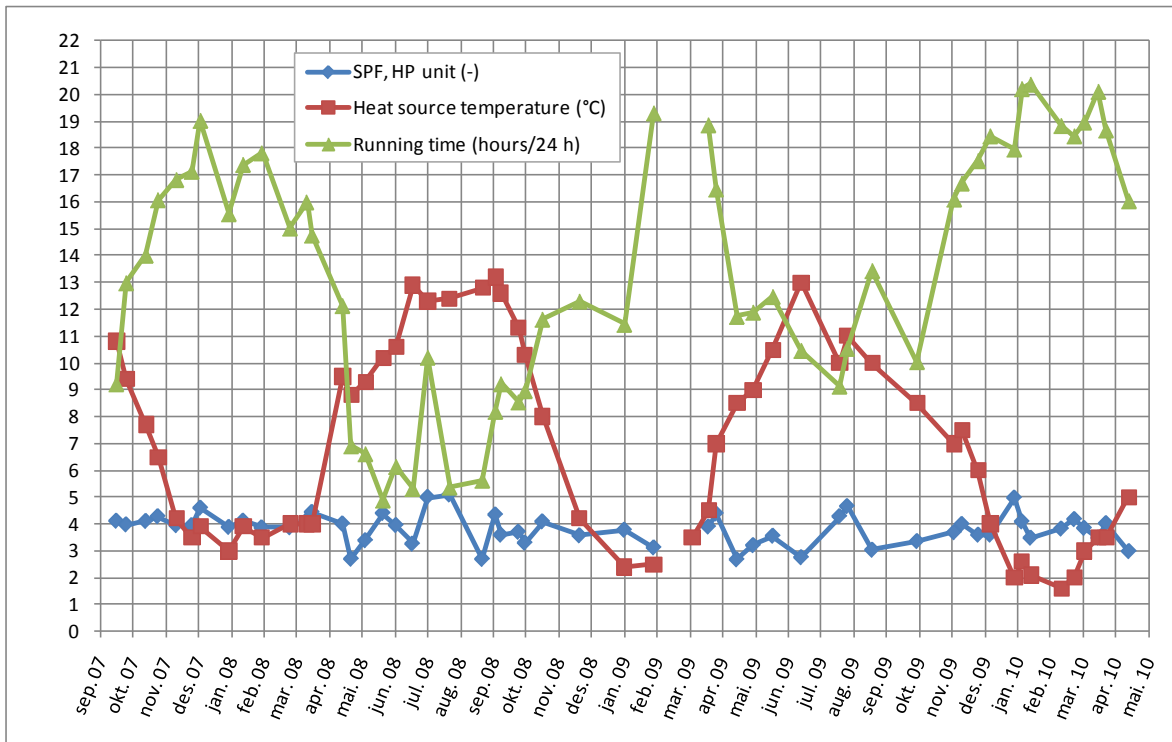


Fig. 57: Measured monthly Seasonal Performance Factor (SPF) for the prototype heat pump (HP) unit, heat source temperature (°C) and running hours for the heat pump (hours/24 hours) (Zijdemans, 2010).

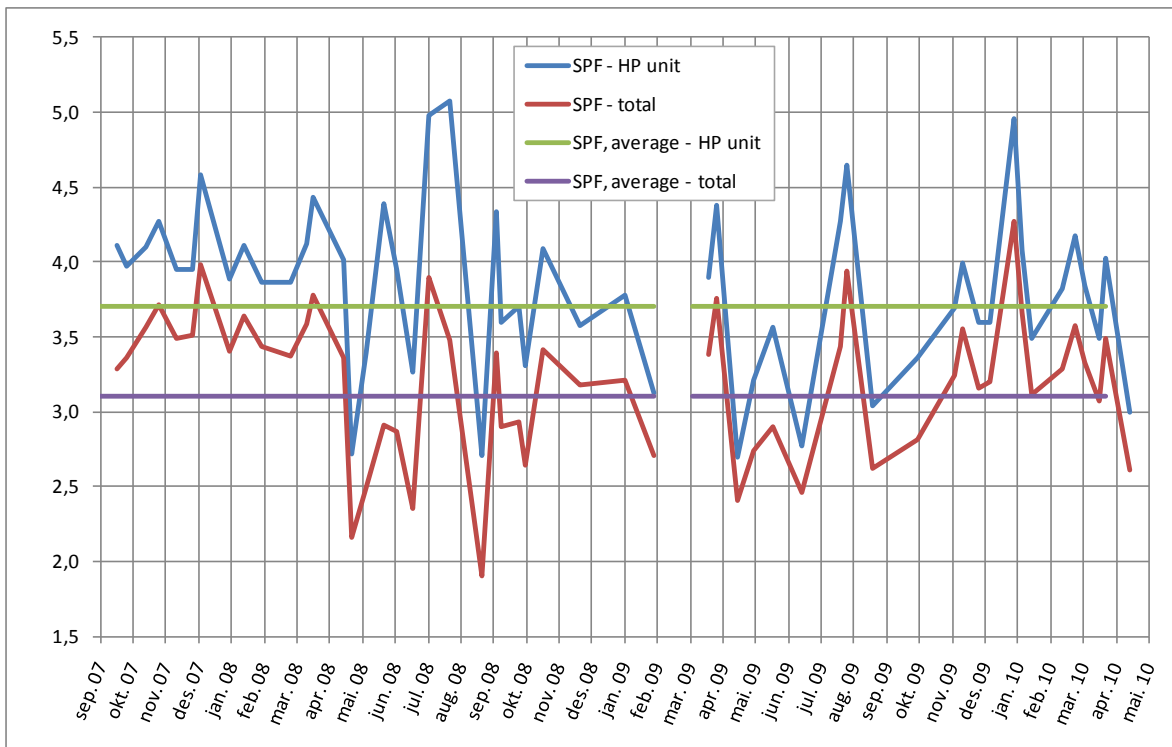


Fig. 58: Measured monthly Seasonal Performance Factor (SPF) and average SPF during the entire measuring period for the prototype heat pump (HP) unit, excl. and incl. input energy to the pumps (Zijdemans, 2010).

Fig. 57 shows the measured monthly Seasonal Performance Factor (SPF) for the prototype heat pump unit, the heat source temperature and running hours while Fig. 58 shows the measured monthly SPF and average SPF during the measuring period excl. and incl. energy input to the pumps. Fig. 59 shows accumulated values for the measured space heating and DHW heating demand (Zijdemans, 2010).

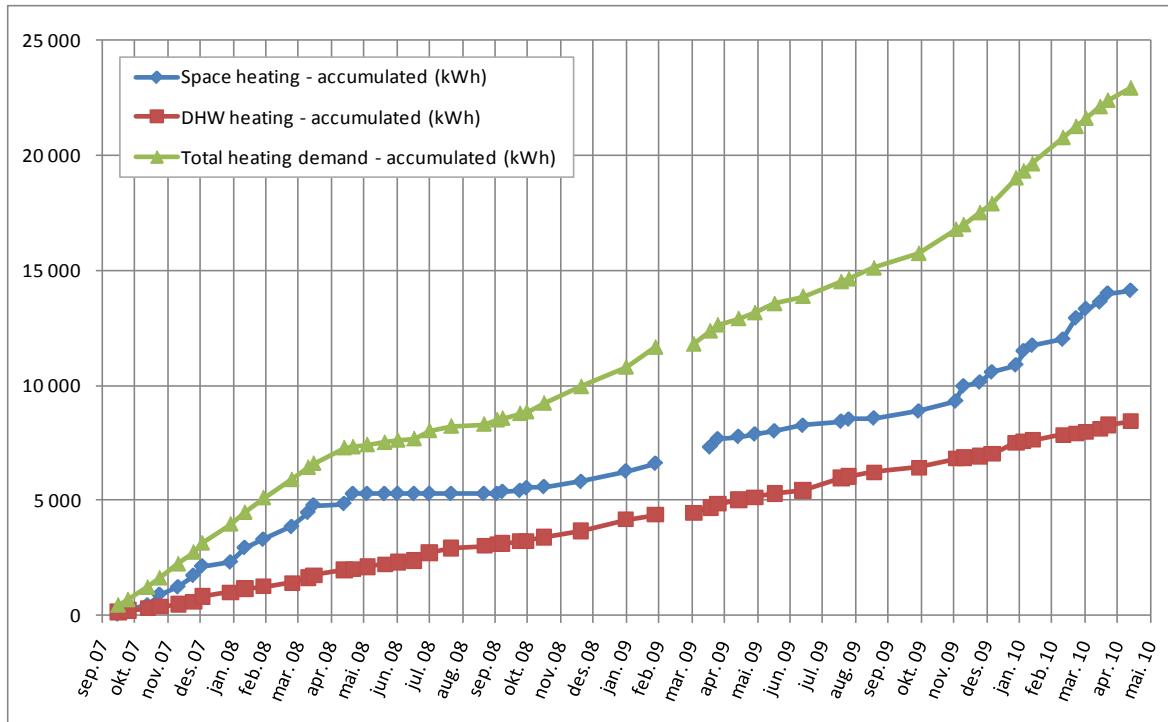


Fig. 59: Measured space heating and DHW heating demand, accumulated values (Zijdemans, 2010).

"SPF – HP unit" refers to the measured Seasonal Performance Factor (SPF) for the heat pump unit including only the driving energy for the compressor, while "SPF – total" refers to the measured SPF for the heat pump system including the total energy input to the compressor and pumps. The heat loss from the LT and HT storage tanks has been included in the calculations of the SPF.

- During February and March 2009 the filter for the lake water inlet was gradually clogged, which resulted in a drop in the water flow rate and finally freezing of the drain pipe (i.e. heat pump halt).
- The average SPF during the entire measuring period for the heat pump unit including only the drive energy to the compressor ("SPF average – HP unit") is **3.7**, while the average SPF including the total energy input to the compressor and pumps ("SPF average – total") is **3.1**. These SPF values correspond to about **70% energy saving compared to an electric heating system**.
- During summer and Christmas the hot water demand is considerably higher than rest of the year due to visitors, which leads to a higher SPF for the heat pump system. In these periods the SPF-total range from about **3.8 to 4.2**, i.e. approx. **74-76% energy saving** compared to an electric heating system.
- The specific heating demand for space heating and hot water heating in the passive house including all energy input as well as heat loss from the hot water tank is approx.

**52 kWh/(m<sup>2</sup>y)**. The heat pump installation reduces the total specific energy use for heating purposes to about **17 kWh/(m<sup>2</sup>y)**.

- During the entire measuring period the DHW heating demand constitutes about **37%** of the total heating demand. This is rather low for a passive house, but the main explanation is that the residence is a relatively large single-family house (172 m<sup>2</sup>) with only two residents.
- The heat exchanger coil in the LT storage tank covers about 60-70% of the total DHW heating demand, whereas the remaining 30-40% is covered by the heat exchanger in the HT storage tank
- Lake water represents an excellent heat source, and the temperature ranges from about 1.5 °C to 13 °C. The lowest temperature is measured during November to April (1.5-4.0 °C).
- The peak load system (electric heaters) has never been used, which clearly demonstrates that the heat pump system was correctly designed for this passive house.

## 7 BUILDING INTEGRATED PV/THERMAL

---

### 7.1 Motivation

A building integrated solar PV/Thermal (BIPV/T) system is the core of two NZEH Pilot houses in the Eastern Canadian province Québec in the frame of a nationwide EQUilibrium™ housing design competition of the governmental institution Canadian Mortgage and Housing Corporation. The EQUilibrium™ Initiative aims at an evaluation of innovative housing concepts with net zero energy consumption throughout Canada for future sustainable buildings. Besides the energy concept, criteria of occupant health and comfort, resource conservation, in particular water, and reduced environmental impacts as well as affordability and repeatability of the concept all over Canada were criteria. Of 70 projects 12 were chosen to be realised and extensively monitored to prove the operational behaviour and evaluate energy performance.

Within IEA HPP Annex 32 two of the winning house concepts located in the Eastern Canadian province Québec were considered in the frame of the Canadian national project, the EcoTerra™ Home in Eastman of the building company Alouette Homes and the Alstonvale Net Zero Energy house in Hudson of Sevag Pogharian Design. Both buildings have similar design features:

The building envelope is optimised for solar passive design featuring a high-quality thermal insulation of a large south-oriented high-quality window area. The inside of the house provides a high thermal mass in order to store solar energy. Both system concepts incorporate a BIPV/T system on the roof of the building in combination with heat pumps.

### 7.2 Building and system concept of the EcoTerra™ Home

This chapter gives the building and system design of the EcoTerra™ home based on information from Noguchi et al. (2008).

The building is a two-storey detached home of a 234 m<sup>2</sup> floor heating area, has two bedrooms both located on the first floor, while the semi-private spaces including the kitchen, dining room, living room and sunspace family room are on the ground floor. Moreover, a basement that serves as a multifunctional space, machine room and garage is located on the north side of the house. By attachment to the façade it acts as a buffer space and reduces the heat loss.



Fig. 60: South view of the EcoTerra™ Home with BIPV/T and family room with concrete floor covered with ceramic tiles

The window areas of 20.9 m<sup>2</sup> south-, 5.2 m<sup>2</sup> east, 6.7 m<sup>2</sup> west and 0.7 m<sup>2</sup> north orientation, respectively, consist of high-quality glazing with triple-layer, low-e coating and argon filling. Large window areas allow the use of daylighting and are an aspect of the occupant's health and comfort. Indoor air temperatures and air quality is increased by the thorough wall insulation and air-tight construction of a natural air exchange lower than 1 h<sup>-1</sup> at 50 Pa. Moreover, a mechanical balanced ventilation system prevents outdoor pollutants while indoor pollutants are continuously exhausted reducing the ventilation losses by up to 75% with a ventilation heat recovery. Ceramic tiles instead of carpets further contribute to less indoor air pollution and to store solar energy gains in the floor. In summer, overhangs and motorised blinds help to prevent an overheating. Trees of the rural setting add further shading of the houses and reduce wind exposure in wintertime.

The core of the building technology is the 3 kW<sub>p</sub> building integrated solar PV/thermal (BIPV/T) system, the heat pump and the thermal storage. BIPV/T compared to stand-alone PV or solar thermal systems has the advantage of simultaneous production of heat and electricity. 22 unisolar amorphous silicon 136 W laminates placed on the 55 m<sup>2</sup> south-facing metal rooftop.

By a roof top ventilation outdoor air is drawn behind the PV-laminate and heats-up while cooling the PV system to achieve a better electric efficiency. The heated air serves various functions inside the houses, primarily for clothes drying whenever the exiting air temperature is above 15°C. If temperature is below this limit, an air-to-water heat exchanger serves to preheat the DHW or the air is ventilated through a hollow floor slab to store the heat in the concrete.

The ÉcoTerra house is heated or cooled by a two-stage geothermal heat pump (nominal COP at B0/W35 of 4.3). In addition to space heating through a ducted forced air system, the heat pump assists water heating with a desuperheater. Fig. 61 depicts the system concept of the EcoTerra™ house.

A further component of the building technology is a waste water heat recovery integrated in the drain. Therein, a heat exchanger coil is placed around the waste water pipe.

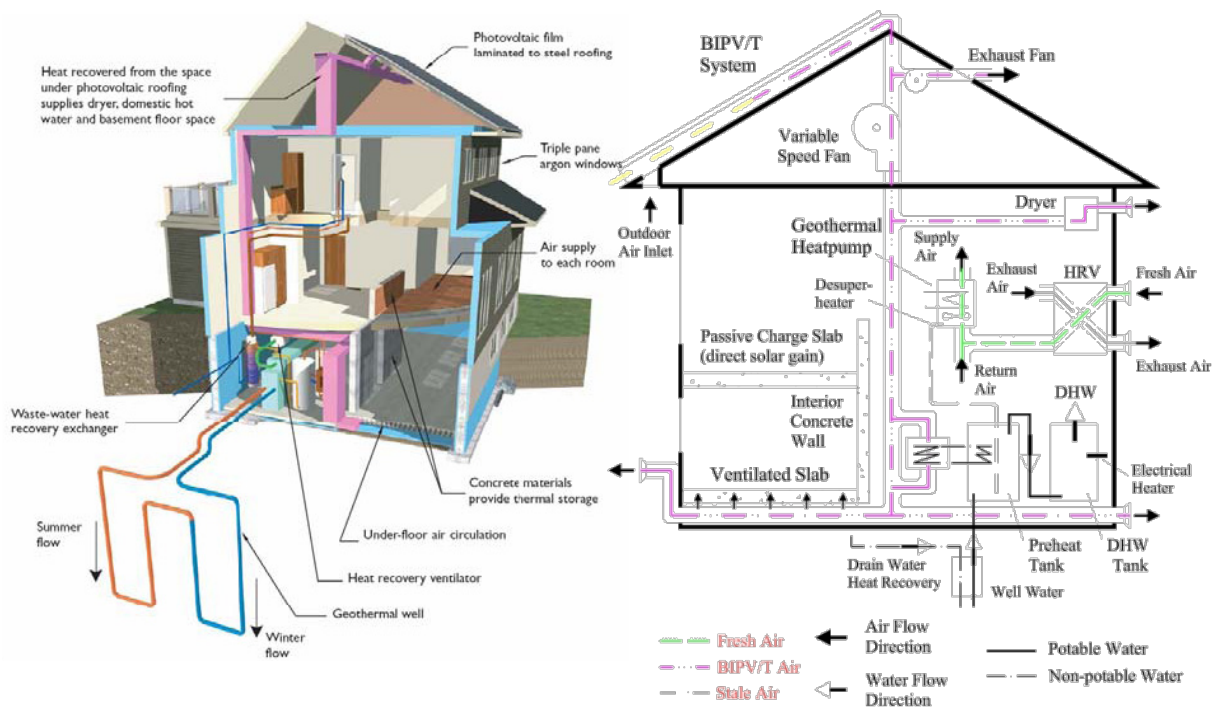


Fig. 61: System concept of the EcoTerra™ Home in Eastman

### 7.3 Simulation and field monitoring of the EcoTerra house

#### 7.3.1 Energy balance

Space heating represents the main part of annual energy consumption, since average temperatures at the construction site Eastman are estimated to -10.4°C in January, 4.6°C in April, 19.4°C in July and 7.1°C in October. The energy needs of the ÉcoTerra house was evaluated with HOT2000, a low-rise residential energy analysis and design software developed by Natural Resources Canada (NRCan) (2008).

The annual gross space heating need of the house was estimated to 21795 kWh without the contributions of passive solar gains and active renewable energies. With consideration of achievable passive solar gains of 9592 kWh/a and internal gains of 3491 kWh/a, the estimated net annual space heating need is reduced to 8712 kWh/a. The DHW energy need was approximated to 3353 kWh/a based on a DHW use of 150 l/d at 55°C.

The annual electrical energy required for interior lighting, appliances and use electrical equipment (e.g. exterior lighting and dryer) was estimated to 3974 kWh/a and 617 kWh for mechanical ventilation. Thus, the total annual energy need of the house before the application of renewable energy technologies has been assessed to 16656 kWh/a.

The annual electricity generation potential of the solar PV system has been evaluated to approximately 3420 kWh for a slope of 30.3° by use of NRCan’s RETScreen (2006) clean energy project analysis tool, which, however, does not take into account the cooling effect of the air flow behind the PV laminates. The BIPV/T system is an on-grid application accompanied with an inverter for the AC/DC conversion. The system allows for redirection of the locally generated electricity surpluses to the grid. The PV thermal heat recovery system of the ÉcoTerra house is estimated to provide 700 kWh/a of 900 kWh/a energy need for clothes drying. From November to March, the hollow core concrete thermal mass in the basement is heated by the warm air from the BIPV/T system. The BIPV/T system is therefore expected to reduce the space heating need by approximately 3800 kWh/a in the heating season. For the other 7 months, the BIPV/T is estimated to supply approximately 1400 kWh/a of the annual DHW needs. The hollow floor slab can be utilized for natural cooling with outdoor night air in summer. Fig. 62 gives an overview of the energy balance of the EcoTerra home and a comparison to other standards.

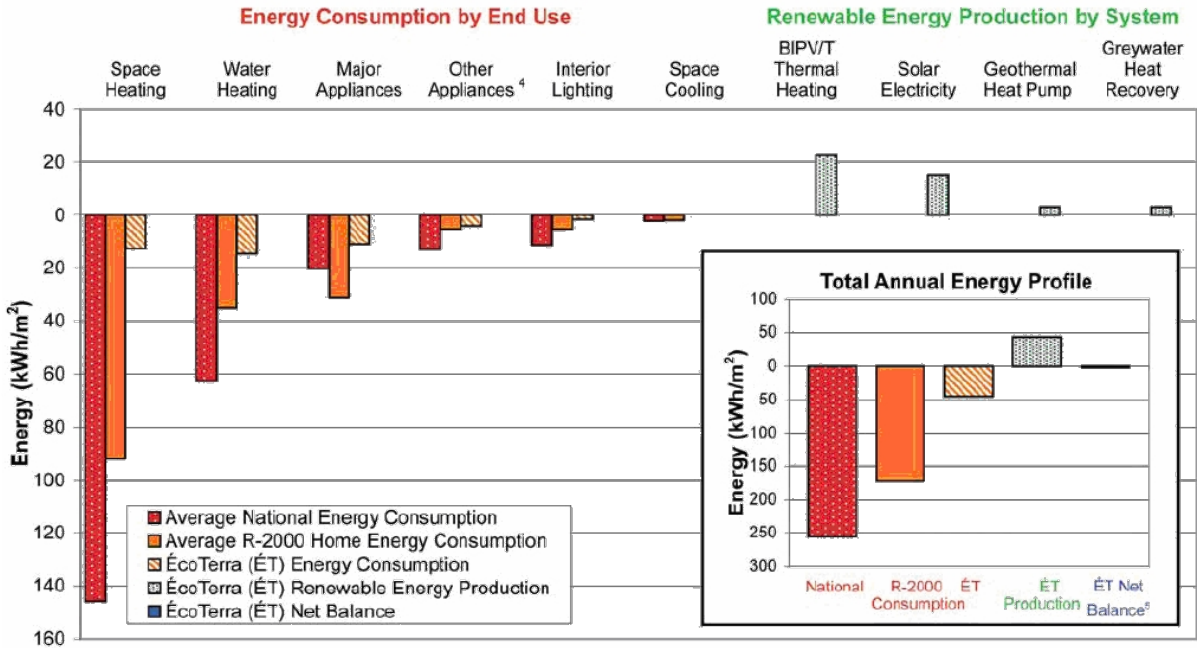


Fig. 62: Simulated energy balance of the EcoTerra™ house compared to state-of-the-art housing and R2000 homes

With consideration of the above-mentioned renewable energy technologies combined with the passive solar techniques applied to the ÉcoTerra house, the annual net space energy consumption could be as low as 1130kWh. The electricity used for DHW could be reduced from 3353 kWh/a to 553 kWh/a by the heat pump desuperheater, BIPV/thermal system and a heat recovery of 21% of the drain-water, but depending on actual water consumption and control strategies the value may become higher. Moreover, in some cases, the savings from different technologies are not expected to be additive; the heat recovery from BIPV/T can preheat water. If the storage volume is adequate, it can be heated further with the desuperheater. The energy consumption of indoor lighting, appliances and exterior use of electrical equipment was decreased from 3974 kWh/a to 3274 kWh/a with the reduced clothes dryer annual energy need. When subtracting the PV electricity generation of 3420 kWh/a from the sum of these figures, the annual energy consumption of the ÉcoTerra house can be re-estimated at 2155 kWh/a. However, if the energy systems are not properly controlled in an integrated manner, this consumption could possibly reach 4000 kWh/a or more.

**7.3.2 Field monitoring results**

Fig. 63 right shows the diurnal air temperature of March 17, 2008 at different positions (see Fig. 63 left) of the BIPV/T at different volume flow rates. The outlet air (position 6) is heated up to about 40 °C.

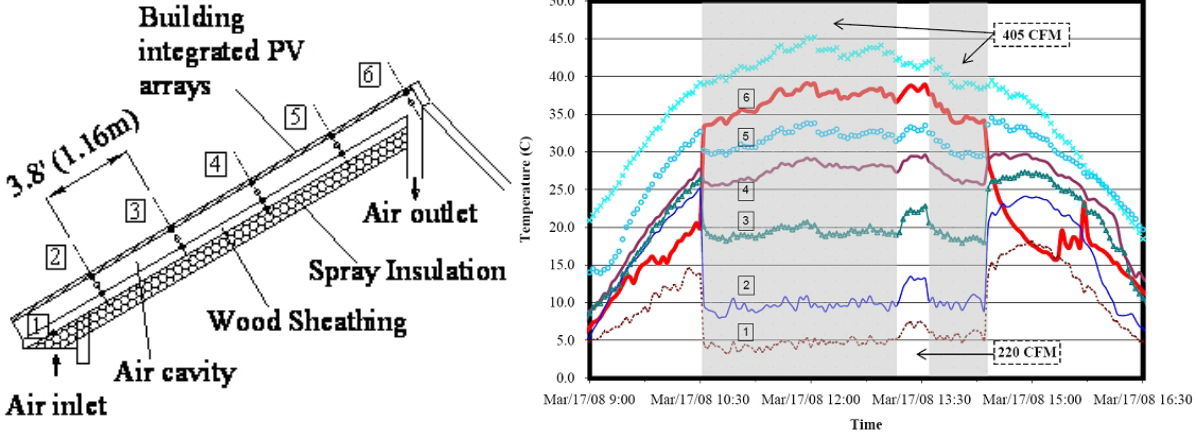


Fig. 63: Diurnal temperatures of the air in BIPV/T on March 17, 2008 with different flows

Fig. 64 shows the energy balance of the PV system. While in February 2008, mainly energy was received from the grid, in May, generated electricity is fed back to the grid during 8 hours of the day, which creates a surplus of generated electricity over the electricity consumption of the houses during that day.

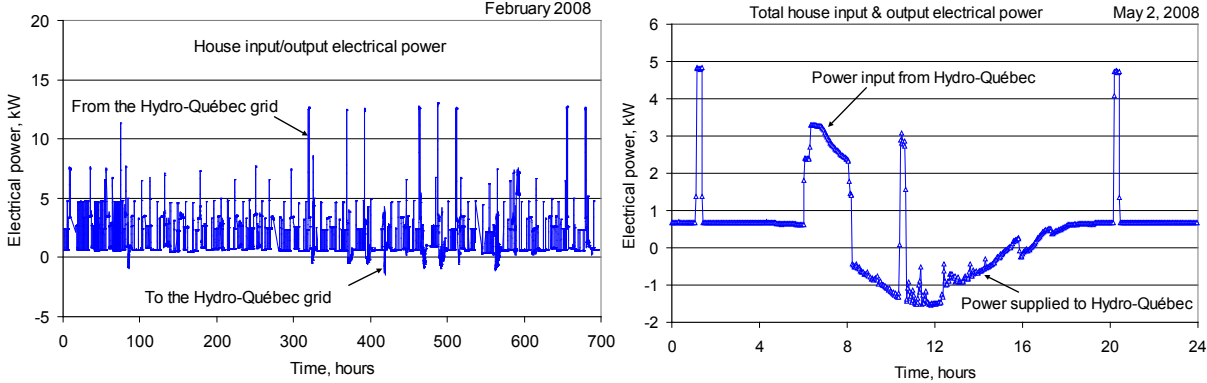


Fig. 64: Electricity contribution to consumption of grid connected PV in Feb. and May 2008

## 7.4 Building and system concept Alstonvale NZEH

The Alstonvale Net Zero Energy house (ANZEH) is the second winning EQUilibrium™ house concept located in Hudson, Québec. Information is based on Candanedo et al. (2008) and Candanedo and Anthienitis (2009).

The building has a floor area of 230 m<sup>2</sup> and a volume of 630 m<sup>3</sup>. The building design is oriented to use as much passive solar gains as possible. Therefore, well-insulated walls of an U value of 0.18 W/(m<sup>2</sup>K), ceiling with U-values of 0.08 W/(m<sup>2</sup>K) and floor insulation of U-values of 0.22 W/(m<sup>2</sup>K) as well as 50m<sup>2</sup> triple-layer argon-filled low-e window area, which constitutes a glazing fraction of 43% of the south façade, are applied. Further window areas are east and west facing, while no windows are integrated in the north façade. Increased thermal mass as capacity for passive thermal storage dampening the temperature fluctuations is provided by 15-cm thick concrete slab floors and a large interior masonry wall.

The ANZEH has a solar chimney connected to the indoor space. This chimney has an east-facing controllable damper, which remains closed during the winter; during the summer, it enhances natural convection, thus removing hot air from the house interior. Other features include the use of energy-efficient appliances and a design that enhances daylighting complemented with low consumption compact fluorescent lamps. Properly-sized overhangs prevent excessive solar heat gains during the summer. Motorised theatre curtains, located behind the main south-facing windows, contribute to controlling solar heat gains, while improving comfort and adding to the aesthetic value. Fig. 60 shows a drawing of the house with the BI-PV/T system on the roof and the state of the built house in Sept. 2009.



*Fig. 65: Design concept and south-oriented view of the Alstonvale Net Zero Energy House*

As in the EcoTerra house the BIPV/T located on the roof constitutes the main energy supply system of the house. However, the energy concept is different, as shown in Fig. 61, since the heated air of the PV/T system is used as heat source for an air-to-water heat pump.

In order to boost the heating of the outlet air temperature of the 8.4 kW<sub>p</sub> PV/T-system a glazed area is located above the PV panels. Of the 8.4 kW<sub>p</sub> of the solar PV panel, 5.5 kW<sub>p</sub> are dedicated to cover the energy need of the house, while ≈1.5 kW are installed for balancing the local transportation need of the building users assuming an electrically driven car, see details in 7.5.1. Moreover, the concept comprises a local food production on the estate in order to get to a net zero energy lifestyle comprising housing, transportation and food.

In a ducting behind the outlet of the PV/T the heated air is led to an air-to-water heat exchanger for direct charging of a 4000 l thermal energy storage (TES) or as heat source for 2 heat pumps. This design required a HX that operates in a wide range of flow and heat transfer rates. The liquid side using a water-glycole mixture needed flow rates between 0.57 l/s and 1.13 l/s; the air flow rates would be between 1700 m<sup>3</sup>/h and over 3400 m<sup>3</sup>/h, where the heat transfer rates would vary from 5 kW to more than 20 kW. Thus, a heat exchanger with much larger heat transfer areas as commonly used in residential applications is required.

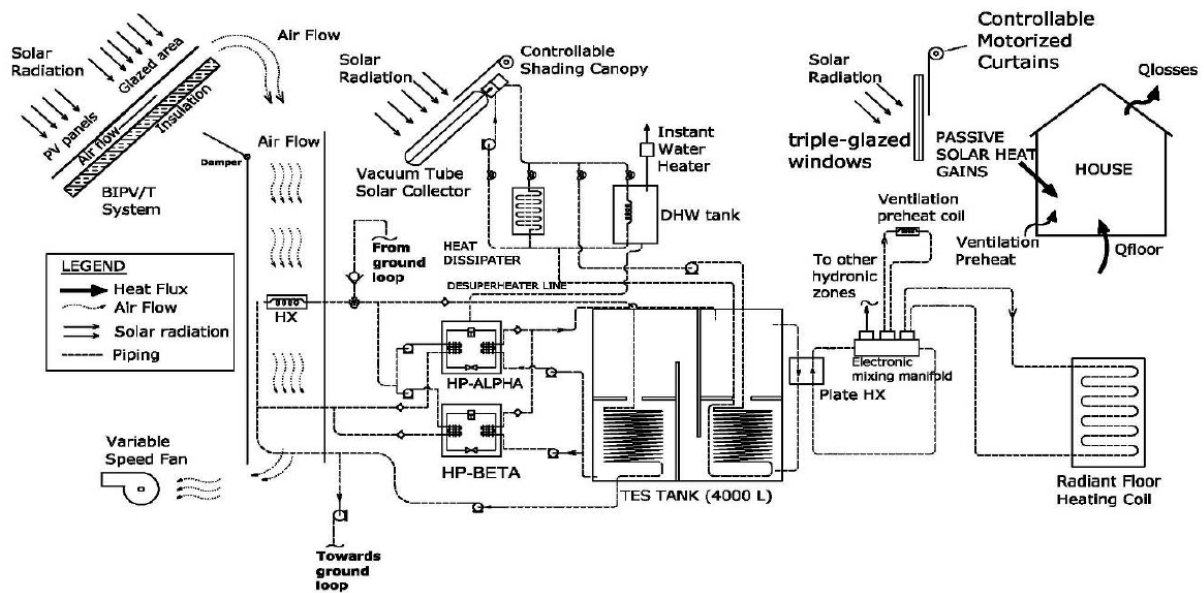


Fig. 66: Building and system concept of the Alstonvale Net Zero Energy home in Hudson (Pogharian et al., 2008)

It was chosen to 8-rows of coils, with 16 passes in total, with dimension of 0.914 m by 1.27 m and a total face area of 1.16 m<sup>2</sup>. Due to a small rated pressure drop on the air side varying between 15 and 42 Pa a bypass duct is not needed. Due to space limitations of the basement mechanical room, the HX will be located in the garage, where also room for smooth duct transitions is available.

For capacity control reasons two heat pumps are integrated. The chosen heat pumps have to deliver the required peak heating load (about 12-13 kW). They also have to operate at part load under varying flow rates and temperatures, with a good COP preferably above 5. It is important to have the lower temperature limit of operation at the source side as low as possible (preferably near or below 0 °C), in order to extend the range of the HP operating conditions, as this will reduce the need for the operation of the back-up system. After evaluating the products available on the local market, it was decided to work with 2 single-stage HPs of a nominal output of 10.6 kW, each operating in parallel under a wide range of conditions. The configuration with two heat pumps offers, for instance, to work with very low flow rates and temperatures by operating only one heat pump and still deliver about 7 kW to the storage.

As back-up system for the case of missing solar irradiation, a ground loop is included as second heat source, since this only required small changes in the piping (the addition of a 3-way valve and a pump), and extended the usefulness of the heat pumps by giving them an additional function. The wide range of temperatures that can be handled by the selected heat pumps facilitates the implementation of this dual-source system.

The chosen storage volume of 4000 l should allow approximately one day of heat storage for a 6 kW heating load (close to the average) at a tank maximum temperature of 55 °C. After circulating through the heat pump(s), the water will be deposited at the top of the tank. This tank will have horizontal baffles and a vertical division to favour and maintain the thermal stratification in the tank, which has been estimated between 5 to 8 °C. Water from the tank could not be circulated directly through the air-to-water HX piping, since a water-glycol mixture is necessary to prevent freezing and bursting of pipes. A coil was added for this heat exchange. A plate heat exchanger allows heat transfer between the radiant floor heating system and the tank.

The tank also has one additional coil permitting heat transfer between the buffer storage and the 400 l DHW tank. Two evacuated tube solar collectors (AP-20), each with about 3 m<sup>2</sup> of gross area and 20 tubes, are used for domestic hot water heating. Furthermore, a waste wa-

ter heat recovery called “Power-pipe” is integrated to preheat the DHW. DHW is produced instantaneously using heated water from the DHW tank. Additionally, heat dissipater to release the excess heat, mainly in the summer months, is installed. In addition, a motorized canopy, which can be extended over the edge of the awnings to improve the shading of the windows in summer, will be used to cover the solar collector.

## 7.5 Simulations of the ANZEH energy system

### 7.5.1 Energy balance

The annual energy consumption and generation is estimated using the programs RETScreen (2006), Mathcad and Matlab. Expected energy consumption of the building technology and appliances as well as generated energy are given in Fig. 67. For aesthetical reason and snow downtime, the PV system in the final design has been increased to 48 panels, and therefore, a surplus of about 1000 kWh of produced electricity is estimated. On the other hand, more PV panels means less heat production due to the reduced glazed area above the PV system, but with a low-e coating of the glazing, this can be partly compensated.

Annual Energy consumption	kWh
Heat pumps	2500
Fan and pumps	800
Domestic hot water	50
ventilation	800
Lighting	350
Domestic appliances	3000
Electric plug in vehicle	1600
<b>Total</b>	<b>9000</b>
<b>Energy generated by the PV</b>	<b>10000</b>
<b>Surplus generation</b>	<b>1000</b>

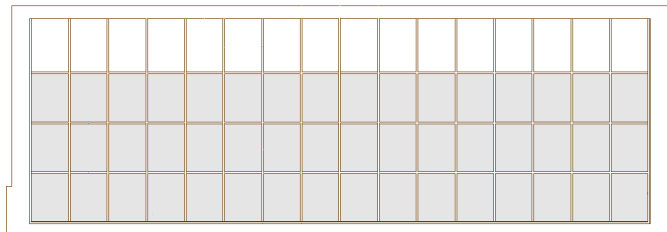


Fig. 67: Estimated energy consumption and generation and final PV/T configuration

As mentioned above, 1.5 kW<sub>P</sub> of PV panels has been included to supply much of the power needed for a plug-in hybrid-electric vehicle. The consumption per charge of a hybrid-electric has been estimated to be 9 kWh, allowing the user to drive for 40 km according to Moore (2005). Assuming that 3.5 charges are required per week, about 1600 kWh are needed per year. A calculation carried out in RETScreen (2006) for Montréal conditions shows that 1.5 kW<sub>P</sub> on a south-facing 45° roof generates approximately 1840 kWh of electricity per year. The integration of car and house offers synergies: the electric drive vehicle (EDV) may be charged by the PV/T system or base load generation. In turn, the EDV may act as an energy storage resource for the house by powering the home’s critical circuits in the event of emergencies. Just as a single EDV can act as an energy storage resource for a single house, conceivably thousands of EDVs can act, collectively, as a significant energy storage resource for the entire electric grid. The ANZEH will explore this concept, known as vehicle-to-grid (V2G).

### 7.5.2 Simulation of control strategies

In order to optimise the system performance the control strategy is essential for the coordination of the ANZEH systems. Therefore, conventional rule based control has been compared to predictive control strategies in Candanedo et al. (2008), which take into account the forecast of the solar irradiation of the next day to determine the control parameter, in the case described below, the set point of the storage temperature. The two control strategies compared are

- (A) keeping the tank fully charged (i.e., the minimum temperature at the bottom was kept at ≈49 °C, which is the maximum tabulated temperature of the heat pumps sink side) by using the BIPV/T air; and
- (B) keeping the tank at a temperature which is a function of the solar radiation expected for the next day (the tank temperature set point could be either 35, 40, 45 or ≈49 °C).

Strategy (A) guarantees that heat is always available. (B), however, should save electrical energy since unnecessary charging the tank is avoid and the COP of the heat pumps will be higher for lower sink side (storage tank) temperatures. The available heat in the BIPV/T air depends only on the air temperature, since the air flow rate was kept constant at 755 l/s for the study. Both control strategies follow the pattern:

- When BIPV/T air temperature is greater or equal to 46°C (near the technical operational limit of the heat pumps), the HX is used directly;
- Between 10 and 46 °C, both GSW036 heat pumps are used simultaneously.
- Between 3 and 10 °C, since there is less heat available, only one GSW3036 heat pump is turned on (a different criterion could be established for deciding between the operation of either one or two heat pumps);and,
- If the BIPV/T air temperature is below 3°C, no heat is provided to the thermal storage reservoir unless the temperature at the bottom of the tank is below 30 °C (i.e. the tank is discharged).
- If this occurs, the backup system (i.e., one heat pump with the ground source loop) is turned on.

The expected solar radiation for any given day is also used, in both control strategies, as an input of a simple anticipatory control scheme for controlling the position of the blinds/curtains. Regulating solar heat gains helps to control indoor temperature fluctuations of the house in order to avoid overheating. If despite these measures, the operative temperature of the house still exceeds 25°C (a possible problem during the shoulder seasons) fresh-air supply is increased. The operative temperature set point was kept at 21°C, with a tolerance of 2 K; no mechanical cooling was used. For these simulations, no linkage was made between the DHW and the reservoir, although in practice it will exist. A typical meteorological year (TMY2 file) for Montréal was used.

Tab. 16: Comparison of control strategies for the ANZEH building technology

	Oct		Nov		Dec		Jan		Feb		Mar		Apr	
	A	B	A	B	A	B	A	B	A	B	A	B	A	B
Heat from ground loop	0	0	486	547	1580	1796	1546	1796	344	221	84	301	1	41
Heat directly from PV/T HX	0	0	0	0	16	0	0	0	0	0	0	0	0	2
Heat from PV/T (1 HP)	124	73	432	331	326	300	218	197	232	671	209	192	279	242
Heat from PV/T (2 HPs)	158	127	634	596	850	654	928	631	1221	815	899	607	450	344
Heat supplied to reservoir	282	200	1552	1474	2772	2750	2692	2624	1797	1707	1192	1100	730	629
Heat supplied for space	134	235	1420	1421	2729	2730	2565	2583	1659	1661	1036	1039	572	571
% PV/T	100	100	66	63	40	35	50	32	78	87	93	73	100	93
HPs electrical consumption	89	54	361	344	544	597	443	597	443	399	227	255	227	156

As a simplification, these simulations do not include the interaction with the solar collector for DHW. Table 1 shows simulation results for the heating season for both control strategies. Savings are obtained by controlling the charge status of the tank (Strategy B). Concerning the control above described Strategy B is not optimal and there is room for improvement. In addition, the ground loop source is used more often with this strategy. It is desirable to increase the usage of the heat exchanger for the direct recovery of heat, and to incorporate the solar radiation available at the current day in the calculation of the reservoir temperature set point. Other predictive control strategies have been explored and reported in Candanedo et al. (2009).

## 7.6 Conclusions

The Canadian contribution comprises two winning housing concepts realised within the EQUilibrium initiative as P&D for innovative sustainable housing in Canada, the EcoTerra™ Home and the Alstonvale Net Zero Energy house (ANZEH), both located in the Québec province in Eastern Canada.

Besides a high-quality building envelope applying a thorough thermal insulation of the

envelope, large south-oriented triple glazed window areas with low-e coating and sufficient thermal mass by inside concrete wall and floor construction elements, both houses incorporate a roof integrated PV/T system as core component for the design of the building technology. The EcoTerra house makes direct use of the heat for the PV/T for clothes drying, DHW preheating and storing the heat in a hollow floor slab, while the ANZEH uses the heat, depending on the temperature, as heat source of two heat pumps. A ground loop, the main heat source for the EcoTerra house, only serves as back-up in the ANZEH. Both houses are or will be extensively field-monitored. First results of the EcoTerra home have been given, but further results could not be covered in the time frame of IEA HPP Annex 32



## 8 CONCLUSIONS

---

Due to changed loads in low energy houses compared with conventional houses, the building technology should be adapted to the specific need. In recent years, development of integrated system solutions for low energy houses has started, including a heat pump as core component of the integration.

Benefits of integrated systems in low energy houses were the motivation to continue the development of integrated heat pumps solutions for low energy houses in the frame of IEA HPP Annex 32, mainly focussing on two aspects which are not found very often in available developments:

- the addition of further functionalities, in particular passive space cooling and dehumidification
- the use of natural refrigerants

Dehumidification is a crucial building service in different areas of the world. Therefore, a dehumidification function has been integrated in a prototype, which thereby can cover all building needs with one unit. Moreover, dehumidification can be efficiently operated with simultaneous DHW generation. Compared to standard minimum requirement technologies, significant simulated energy savings in the range of the 50% target for Net Zero energy houses have been reached. System payback times range between 5-15 years, but can be lowered depending on the market conditions.

CO<sub>2</sub> heat pumps can be favourable as heat pumps water heaters. Nevertheless, integrated solutions with CO<sub>2</sub> for space heating and DHW show promising results, as well, in particular with high DHW fractions, which may occur in ultra-low energy houses. However, development potentials are seen both on the component level and concerning the system integration.

It is still difficult to get components for CO<sub>2</sub> heat pumps, in particular compressors for the small capacity range. Moreover, small compressors shall be further developed regarding the performance data, which is essential for a good system performance. Ejector technology could further enhance the performance.

While most of the prototypes developed in the frame of the IEA HPP Annex 32 are system prototypes, two Canadian projects in the frame of the EQUILIBRIUM™ Pilot and Demonstration project extend the prototypes to technology integrated in the building envelope. By including roof integrated solar PV/Thermal panels in the system concept, the building envelope serves as energy source for the system technology. Thereby, functionality of the building envelope is extended, which may add to the complexity, but offers further opportunities for cost savings by multifunctional building and system components.

Some of the developed prototypes are currently field monitored or field monitoring is in preparation. However, field results could not be covered in the time frame of the IEA HPP Annex 32.



## 9 ACKNOWLEDGEMENT

---

The operating agent as editor of this report is very grateful for the valuable contributions of all participants of the IEA HPP Annex 32 and for the constructive discussion and co-operation. It has to be emphasised that the Annex 32 is a co-operative research project and results are taken from national contributions.

The operating agent would like to thank the Swiss Office of Energy (SFOE) for funding and supporting the project, in particular the research programme manager Prof. Dr. Thomas Kopp for advising in the Annex 32 project and the Swiss national project within the Annex 32.



## 10 REFERENCES

---

- ANSI/ASHRAE Standard 62.2-2004: Ventilation and Acceptable Indoor Air Quality in Low-Rise Residential Buildings, American Society of Heating, Refrigerating, and Air-Conditioning Engineers, 2004, US
- Baxter, V.D. (2005). HVAC Equipment Design Options for Near-Zero-Energy Homes – A Stage 2 Scoping Assessment. ORNL/TM-2005/194. November, US
- Baxter, V.D. (2008) System assessment and field monitoring, US country report IEA HPP Annex 32 Task 2, ORNL, May, US
- BFE (2008). Bundesamt für Energie (Hrsg.). Wärmepumpen - Planung, Optimierung, Betrieb, Wartung, Faktor Verlag, January, CH
- Candanedo, J. and Athenitis, A. (2009) Application of Predictive Control Strategies in a Net Zero Energy Solar House, PLEA2009 - 26th Conference on Passive and Low Energy Architecture, Quebec City, Canada, 22-24 June 2009, CA
- Candanedo, J., Minea, V. and Athenitis, A. (2008) Low energy houses in Canada: National Initiatives and achievements, Concordia University, Montreal, Canada, Workshop IEA HP Conference 2008, Zurich, May 19, CA
- Candanedo, José A., O'Neill, B., Athienitis, Andreas K., Pogharian S. (2008). Major aspects of the energy system design of the Alstonvale Net Zero Energy House, Montreal, CA
- DIN 1946-2 (1994) Raumluftechnik Gesundheitstechnische Anforderungen (VDI Lüftungsregeln), Beuth-Verlag, Berlin, DE
- EN 14511-3:2007 Air conditioners, liquid chilling packages and heat pump with electrically driven compressors for space heating and cooling – Part 3: Test methods, CEN, Brussels, EU
- EN 378:2008 Refrigerating systems and heat pumps. Safety and environmental requirements, CEN, Brussels. EU
- Gabotherm (2006). Technical Information Gabofloor Fußbodenheizung gabo TAC, Fa. Gabotherm, Stand Juli 2006
- Heimrath R., Haller M. (2007). Project Report A2 of Subtask A: The Reference Heating System, the Template Solar System - A Report of IEA SHC Task 32: Advanced Storage Concepts for Solar and Low Energy Buildings
- Heinz, A., Rieberer, R. (2010). System assessment and field monitoring, Country report Austria IEA HPP Annex 32 Task 2 and Task 3, Graz, March, AT
- Hjerkinn, T. (2007). Analysis of Heat pump water Heater system for Low-Energy Block of Flats (in Norwegian with English summary), Master thesis at the Norwegian University of Science and Technology (NTNU), Dept. of Energy and process Eng. EPT-M-2007-24, NO
- Jordan U., Vajen K. (2001). Realistisches Trinkwasser-Zapfprofil für bis zu 60 Wohneinheiten, OTTI '01, Tagungsbericht, 11. Symposium Thermische Solarenergie, 9.-11.5. 2001, Staffelstein.
- Justo Alonso, M., Stene, J. (2010). IEA Heat Pump Programme Annex 32 – Economical Heating and Cooling Systems for Low-Energy Houses - Umbrella Report, System Solutions, Design Guidelines, Prototype System and Field Testing – NORWAY, Final country report Norway IEA HPP Annex 32, SINTEF Technical report TR A6966, Trondheim, May, NO
- Kasuda, T., Archenbach, P.R. (1965). Earth Temperature and Thermal Diffusivity at Selected Stations in the United States, ASHRAE Transactions, Vol. 71, Part 1, 1965

- Klein, S.A. (2007). Engineering Equation Solver, Academic Commercial V7.934-3D, F-Chart, Madison, US
- KULI (2009). KULI Energy Management Simulations Software, Magna Powertrain, Engineering Center GmbH&Co KG, Austria, [www.kuli.at](http://www.kuli.at)
- Mauthner R. (2008). Ejektor für Kompressionskälteanlagen; Seminararbeit Wärmetechnik und Wärmewirtschaft am Institut für Wärmetechnik, Technische Universität Graz
- Meteonorm (2005). Meteonorm, V 5.1, Fabrikstraße 14, CH-3012, Bern, Schweiz, 2005, [www.meteonorm.com](http://www.meteonorm.com)
- Moore, B. (2005). The Promise of Plug-in Hybrids., [http://www.evworld.com/modules/win\\_printdoc.cfm?section=article&docnum=897&doctitle=The%20Promise%252](http://www.evworld.com/modules/win_printdoc.cfm?section=article&docnum=897&doctitle=The%20Promise%252). Retrieved on March 2008
- Murphy, R. W., C. K. Rice, V. D. Baxter, and W. G. Craddick (2007a). Air Source Integrated Heat Pump for Near Zero Energy Houses: Technology Status Report, ORNL/TM-2007/112, July, US
- Murphy, R. W., C. K. Rice, V. D. Baxter, and W. G. Craddick (2007b). Ground Source Integrated Heat Pump for Near Zero Energy Houses: Technology Status Report, ORNL/TM-2007/177, September, US
- Pogharian, S., Ayoub, J., Candanedo, José A., Athienitis, Andreas K. (2008). Getting to a net zero energy lifestyle in Canada, The alstonvale net zero energy house, 23rd European PV Solar Energy Conference 2008, Valencia, September, CA
- RETScreen (2006). RETScreen International, Natural Resources Canada, retrieved on 10 April 2008, CA, download available on <http://www.retscreen.net>
- HOT2000 (2008) HOT2000 Sustainable Building and Communities, Natural Resources Canada, retrieved on 10 April 2008, CA, download available at [http://www.sbc.nrcan.gc.ca/software\\_and\\_tools/hot2000\\_e.asp](http://www.sbc.nrcan.gc.ca/software_and_tools/hot2000_e.asp)
- Noguchi, M. Athienitis A., Delisle, V., Ayoub J., Berneche B. (2008). Net Zero Energy Homes of the Future: A Case Study of the ÉcoTerraTM House in Canada, Renewable Energy Congress, Glasgow, Scotland, July 19-25
- Rice, C. K and W. L. Jackson (2002). DOE/ORNL Heat Pump Design Model on the Web, Mark VI Version October, USA, download at <http://www.ornl.gov/~wj/hpdm/MarkVI.html>.
- Skaugen, G. (2002) Investigation of Transcritical CO<sub>2</sub> Vapour Compression Systems by simulation and Laboratory Experiments Doctoral Thesis at the Norwegian University of Science and Technology (NTNU), Dept of Energy and Process Eng., 2002-141. ISBN 82-471-5536-2, NO
- Solar Energy Laboratory (Univ of WI), TRANSSOLAR Energietechnik, CSTB – Centre Scientifique et Technique du Bâtiment, and TESS – Thermal Energy System Specialists (2007). TRNSYS 16: a TRAnsient SYstem Simulation program, Version 16.01.0000, US
- SEL (2005), TRNSYS 16, A Transient System Simulation Program, V 16.0.0.38, Solar Energy Lab, University of Wisconsin – Madison, USA, 2005
- Stene J. (2004), Residential CO<sub>2</sub> Heat Pump System for Combined Space Heating and Hot Water Heating; Doctoral thesis at the Norwegian University of Science and Technology, Department of Energy and Process Engineering, ISBN 82-471-6316-0, NO
- Stene, J. (2006) Residential CO<sub>2</sub> heat pumps for combined space heating and Hot water heating – System design, test procedures and calculation of SPF, Report No. TR A6102, SINTEF Energy Research, NO

- Stene, J. (2007) IEA HPP Annex 32 - Economical Heating and Cooling Systems, State-of-the-Art Report Norway, SINTEF Technical Report TR – A6506-07, Sintef Energy Research, Trondheim, April, NO
- Stene, J. (2008) IEA HPP Annex 32 – 1) Analysis of CO<sub>2</sub> heat pump system for low-energy and passive houses, 2) Field testing of an integrated propane heat pump system in a passive house, SINTEF Technical report TR A6676, Trondheim, May, NO
- TESS – Thermal Energy System Specialists (2004), Type 556 - Horizontal Ground-Coupled Heat Exchanger, Solar Energy Lab, University of Wisconsin, USA
- Vaillant (2002), Vaillant Digital – Planung und Technik, Schulungsunterlagen der Fa. Vaillant, Stand 10/2002
- Vohra, A., Murphy, R.W., Rice, C.K., Baxter, V.D., Craddick, W.G. (2007) Integrated Heat Pump System Technology Development for Near Zero Energy Home (ZEH) Applications, IEA HPP Annex 32 Workshop, Kyoto, Dec. 2007, US, download at [http://www.annex32.net/pdf/presentations/Annex32\\_workshop\\_Kyoto\\_Baxter.pdf](http://www.annex32.net/pdf/presentations/Annex32_workshop_Kyoto_Baxter.pdf)
- Zijdemans, D. (2007) Analysis of Heat pump system for a passive house (in Norwegian with English summary), Master thesis at the Norwegian University of Science and Technology (NTNU), Dept. of Energy and process Engineering, EPT-M-2007-62, NO
- Zijdemans, D. (2008) Data from field measurements in the pilot house, communication with J. Stene, NO



**Heat Pump Centre**

c/o RISE - Research Institutes of Sweden

PO Box 857

SE-501 15 BORÅS

Sweden

Tel: +46 10 516 5512

E-mail: [hpc@heatpumpcentre.org](mailto:hpc@heatpumpcentre.org)

[www.heatpumpingtechnologies.org](http://www.heatpumpingtechnologies.org)

Report no. HPT-AN32-4